

Tesis Doctoral

Reactores trickle bed con operación periódica: aplicación al tratamiento de contaminantes en medio acuoso

Ayude, María Alejandra

2006

Este documento forma parte de la colección de tesis doctorales y de maestría de la Biblioteca Central Dr. Luis Federico Leloir, disponible en digital.bl.fcen.uba.ar. Su utilización debe ser acompañada por la cita bibliográfica con reconocimiento de la fuente.

This document is part of the doctoral theses collection of the Central Library Dr. Luis Federico Leloir, available in digital.bl.fcen.uba.ar. It should be used accompanied by the corresponding citation acknowledging the source.

Cita tipo APA:

Ayude, María Alejandra. (2006). Reactores trickle bed con operación periódica: aplicación al tratamiento de contaminantes en medio acuoso. Facultad de Ciencias Exactas y Naturales. Universidad de Buenos Aires.

Cita tipo Chicago:

Ayude, María Alejandra. "Reactores trickle bed con operación periódica: aplicación al tratamiento de contaminantes en medio acuoso". Facultad de Ciencias Exactas y Naturales. Universidad de Buenos Aires. 2006.

EXACTAS UBA

Facultad de Ciencias Exactas y Naturales



UBA

Universidad de Buenos Aires

**UNIVERSIDAD DE BUENOS AIRES
FACULTAD DE CIENCIAS EXACTAS Y NATURALES
DEPARTAMENTO DE INDUSTRIAS**

**REACTORES TRICKLE BED CON OPERACION
PERIODICA: APLICACION AL TRATAMIENTO
DE CONTAMINANTES EN MEDIO ACUOSO**

**PERIODIC OPERATION OF TRICKLE-BED
REACTORS: EFFECT ON CATALYTIC WET
OXIDATION OF ORGANIC POLLUTANTS**

MARÍA ALEJANDRA AYUDE

TESIS DOCTORAL

**PARA OPTAR AL TITULO DE DOCTOR DE LA
UNIVERSIDAD DE BUENOSA AIRES**

DIRECTORAS:

Dra. MIRYAN CELESTE CASSANELLO FERNANDEZ

Dra. PATRICIA MÓNICA HAURE

- 2006 -

AGRADECIMIENTOS

En primer lugar, quiero agradecer muy especialmente a mis directoras, Dras. Miryan Cassanello y Patricia Haure por su paciencia, apoyo, cariño, y predisposición permanente e incondicional a aclarar mis dudas; también al Dr. Osvaldo Martínez por su valiosa colaboración en el desarrollo de esta tesis a través de sus acertadas observaciones críticas.

Mis más sinceros agradecimientos a los miembros de la División Catalizadores y Superficies (UNMdP) por el día a día y a los miembros del PINMATE por su cálida hospitalidad. A Paola Massa y Alejandra Muzen por su ayuda desinteresada y a Sol Fraguío y Javier González, por los almuerzos compartidos.

Mi reconocimiento al Consejo Nacional de Investigaciones Científicas (CONICET), a la Fundación Antorchas, a la Agencia Nacional de Promoción Científica y Tecnológica (ANPCyT), a la Universidad de Buenos Aires y a la Universidad Nacional de Mar del Plata por su apoyo económico.

Agradezco por último a mi familia, mis amigas, en especial a Vera y a Margarita, quienes con sus cordiales hospedajes hicieron más que amenas mis estadías en la ciudad de Bs. As., y a Facundo por su inquebrantable paciencia y comprensión durante el tiempo que le dediqué al desarrollo y a la redacción de esta tesis.

RESUMEN

Los reactores de lecho mojado, conocidos como reactores “trickle bed” (RTB), se emplean ampliamente en diversas industrias, petroquímica, química, bioquímica y para tratamiento de efluentes, siendo particularmente recomendados para la oxidación catalítica de contaminantes orgánicos, en particular de fenol, dada la baja relación de volumen de líquido a volumen de sólido que minimiza reacciones secundarias en fase homogénea. Dichos reactores, tradicionalmente, se operan en estado estacionario en condiciones en las cuales las resistencias externas al transporte de materia suelen ser significativas. La operación periódica constituye una alternativa para mejorar la performance del reactor sin necesidad de cambios de diseño significativos. El sistema opera continuamente en estado no estacionario incrementando la velocidad de transporte de materia hacia la superficie externa del catalizador. La modulación de flujo líquido afecta los fenómenos fluidodinámicos y de transporte y su interacción con la reacción química y genera acumulación en el interior de la partícula. A pesar de los numerosos resultados alentadores reportados, esta tecnología no se emplea aún a nivel industrial esencialmente por la falta de una metodología rigurosa de diseño. En este contexto, el presente trabajo aborda un estudio sistemático de la influencia de emplear modulación del caudal de líquido sobre una reacción catalítica en un RTB, a partir de: i) la formulación y resolución de un modelo exhaustivo a escala de pastilla catalítica, que provea los elementos necesarios para comprender la compleja interacción entre la dinámica de la reacción química y la transferencia de materia intrapartícula, y como la misma se ve afectada por la modulación del líquido que circula alrededor; ii) la determinación de la influencia de la modulación del flujo de líquido sobre los perfiles axiales y temporales de retención o “holdup” de líquido en una columna rellena con circulación de gas y líquido en cocorriente descendente (maqueta fría de un RTB). Se desarrolla una herramienta matemática para predecir condiciones de operación óptimas cuando el flujo de líquido es modulado, logrando establecer argumentos sólidos para decidir *a priori* si una estrategia de operación periódica mejorará o no la performance de un RTB. Asimismo, se obtiene información fluidodinámica relevante para describir el comportamiento del RTB bajo modulación de caudal de líquido, que resulta imprescindible para definir parámetros claves de diseño, los cuales se requieren para el modelo desarrollado a escala de pastilla catalítica.

ABSTRACT

Trickle bed reactors (TBR) are among the most widely commercially employed three phase fixed-bed reactors for applications in the petrochemical, chemical, biochemical and waste treatment processes. They are also suitable for the catalytic oxidation of dissolved organic contaminants, particularly to eliminate phenol from aqueous solutions, due to the low liquid to solid ratio that prevents undesirable secondary reactions. Traditionally, TBRs are operated at steady state conditions in the trickle flow regime, a regime with low gas-liquid interaction where the reaction rate is frequently controlled by external mass transfer resistances. Periodic operation refers to a mode of process that can be implemented with very low investment, in which the system is forced to run continuously in a transient mode. Arising from the competition between the phases in supplying reactants to the catalyst, the possibility of performance enhancement exists. In spite of numerous works reporting the improvements arising from periodic operation of TBRs, a cycling strategy is still not been applied commercially mainly due to the lack of an established methodology of design. Hence, rigorous experimental and modeling efforts are still necessary to understand the phenomena underlying periodic operation before commercial implementation. In this context, the present work has the aim of i) providing a mathematical tool for interpreting experimental results and predicting optimal operating conditions for liquid flow modulation. Modeling allows fundamentally based arguments to decide whether a cyclic strategy would provide process intensification; ii) finding a suitable way to describe the hydrodynamic behavior of a TBR under liquid flow modulation, to be incorporated into the model at particle scale. A mathematical tool aiding the establishment of optimal operating conditions for periodic operation is developed, which allows proposing fundamentally based arguments to decide *a priori* if a cycling strategy would be favorable to improve TBR performance for a given reaction system. Likewise, relevant hydrodynamic information to describe TBR behavior under liquid flow modulation is obtained. This information allows determination of key design parameters, required to improve the model proposed at the particle scale and to extend it to the integral reactor.

CONTENTS

INTRODUCCIÓN	1
INTRODUCTION.....	5
I. STATE OF THE ART.....	8
I.1. TRICKLE BED REACTORS	8
I.1.1. HYDRODINAMICS	10
I.1.1.1. FLOW REGIMES	11
I.1.1.2. LIQUID HOLDUP	12
I.1.1.3. WETTING EFFICIENCY	15
I.1.2. MASS TRANSFER	17
I.1.2.1. GAS- LIQUID MASS TRANSFER.....	17
I.1.2.2. LIQUID - SOLID MASS TRANSFER	19
I.1.2.3. INTRAPARTICLE MASS TRANSFER.....	20
I.1.2.4. CATALYST DESIGN.....	20
I.1.3. REACTION SYSTEM.....	21
I.1.3.1. LIMITING REACTANT	21
I.1.3.2. OVERALL EFFECTIVENESS FACTOR	22
I.1.4. PERIODIC OPERATION OF TBRs.	23
I.1.4.1. DEFINITION.....	23
I.1.4.2. EXPERIMENTAL STUDIES IN REACTION SYSTEMS.....	25
I.1.4.3. EXPERIMENTAL HYDRODYNAMICS STUDIES.....	29
I.1.4.4. MODELING STUDIES.....	31
II. MODELING LIQUID FLOW MODULATION AT THE PARTICLE SCALE.....	34
II.1. MODEL DEVELOPMENT	34
II.1.1. EFECTIVENNESS FACTOR AND ENHANCEMENT DUE TO PERIODIC OPERATION.....	37
II.1.2. PARAMETERS EVALUATION	38
II.2. SIMULATED DYNAMIC PROFILES	39
II.3. FACTORS AFFECTING THE REACTION OUTPUT	43
II.3.1. MASS TRANSFER	43

II.3.2. WETTING EFFICIENCY	44
II.3.3. RATIO OF REACTANT CONCENTRATION	46
II.3.4. CYCLING PARAMETERS	50
II.3. PREDICTION OF EXPERIMENTAL TRENDS FOR CWAO	52
II.3.1. CATALYTIC OXIDATION OF ALCOHOLS	53
II.3.2. CATALYTIC PHENOL OXIDATION.....	57
III. EXTENSION OF THE MODEL TO CATALYST WITH NON-UNIFORM ACTIVE SITES DISTRIBUTION	60
III.1. MODEL DEVELOPMENT	60
III.1.1. EFFECTIVENESS FACTOR AND ENHANCEMENT DUE TO PERIODIC OPERATION.....	64
III.1.2. SIMULATION PARAMETERS.....	65
III.2. SIMULATED DYNAMIC PROFILES.....	66
III.3. FACTORS AFFECTING THE REACTION OUTPUT	69
III.3.1. CYCLING PARAMETERS.....	69
III.3.2. INTERNAL MASS TRANSFER AND ACCUMULATION EFFECTS.....	72
III.3. FINAL REMARKS	75
IV. HYDRODYNAMICS OF PERIODIC OPERATION IN TBRS.....	77
IV.1. EXPERIMENTAL	77
IV.1.1. CONDUCTANCE TECHNIQUE.....	80
IV.1.2. TRACING TECHNIQUE.....	82
IV.2. RESULTS	85
IV.2.1. STEADY STATE EXPERIMENTS	85
IV.2.2. CYCLING EXPERIMENTS	89
IV.2.2.1. CONDUCTANCE PROBES CALIBRATION.....	96
IV.2.2.2 INSTANTANEOUS LIQUID HOLDUPS UNDER CYCLING	100
IV.2.2.3. CORRELATION OF LIQUID HOLDUP UNDER PERIODIC OPERATION	121
V. CONCLUSIONS	130
APPENDIX A	136

A.1- DIMENSIONAL MASS BALANCES	136
A.2- FINITE DIFFERENCE APPROACH.....	138
A.3- MODEL VERIFICATION.....	140
APPENDIX B	142
APPENDIX C	143
C.1. RTD EXPERIMENTS	143
C.2. STEADY STATE EXPERIMENTS	144
C.3. CYCLING EXPERIMENTS	145
APPENDIX D	148
NOTATION	149
REFERENCES.....	152
CURRICULUM VITAE.....	162
IV. HYDRODYNAMICS OF PERIODIC OPERATION IN TBRS.....	77
IV.1. EXPERIMENTAL	77
IV.1.1. CONDUCTANCE TECHNIQUE.....	80
IV.1.2. TRACING TECHNIQUE	82
IV.2. RESULTS	85
IV.2.1. STEADY STATE EXPERIMENTS	85
IV.2.2. CYCLING EXPERIMENTS	89
IV.2.2.1. CONDUCTANCE PROBES CALIBRATION	96
IV.2.2.2 INSTANTANEOUS LIQUID HOLDUPS UNDER CYCLING	100
IV.2.2.2.1. EFFECT OF CYCLE PERIOD AND SPLIT	111
IV.2.2.2.2. EFFECT OF THE GAS VELOCITY	118
IV.2.2.2.3. EFFECT OF THE MEAN LIQUID VELOCITY.....	119
IV.2.2.3. CORRELATION OF LIQUID HOLDUP UNDER PERIODIC OPERATION	121
V. CONCLUSIONS	130

APPENDIX A	136
A.1- DIMENSIONAL MASS BALANCES	136
A.2- FINITE DIFFERENCE APPROACH.....	138
A.3- MODEL VERIFICATION.....	140
APPENDIX B	142
APPENDIX C	143
C.1. RTD EXPERIMENTS	143
C.2. STEADY STATE EXPERIMENTS	144
C.3. CYCLING EXPERIMENTS	145
APPENDIX D	148
NOTATION	149
REFERENCES	152
CURRICULUM VITAE	162

INTRODUCCIÓN

Las reacciones catalíticas heterogéneas, que involucran frecuentemente la conversión de reactivos presentes en fase líquida y gaseosa empleando un catalizador sólido, constituyen la base de un gran número de procesos químicos, petroquímicos y de tratamiento de efluentes (Dudukovic et al., 2002). En particular, la oxidación completa (a dióxido de carbono y agua) de los compuestos orgánicos presentes en las aguas residuales, empleando catalizadores heterogéneos y oxígeno molecular como oxidante, ha cobrado particular interés en los últimos años. La posibilidad de operar en condiciones de trabajo relativamente moderadas al utilizar catalizadores heterogéneos, hace que este proceso (frecuentemente llamado “Catalytic Wet Air Oxidation”, CWAO) sea uno de los más atractivos para el tratamiento de efluentes acuosos. Los reactores de lecho mojado, conocidos como reactores “trickle bed” (RTB), son los más apropiados para estos procesos, siendo particularmente recomendados para la oxidación de soluciones de fenol. La baja relación de volumen de líquido a volumen de sólido, típica de estos reactores, minimiza la polimerización en fase homogénea de este contaminante.

Tradicionalmente, los reactores Trickle Bed se operan en estado estacionario en un régimen de baja interacción entre las fases, conocido como régimen de flujo Trickle. En esas condiciones, la velocidad de reacción frecuentemente está controlada por las resistencias externas al transporte de materia. La operación periódica constituye una alternativa para mejorar la performance del reactor sin necesidad de cambios de diseño significativos. Por medio de esta técnica, el sistema es forzado a operar continuamente en estado no estacionario, alternando el caudal de líquido entre dos niveles predeterminados mientras que el gas fluye en forma constante. De esta forma, se incrementa la velocidad de transporte de materia hacia la superficie externa del catalizador y los perfiles de concentración de reactivos en el interior de la pastilla también se modifican. En general, para un sistema isotérmico, la modulación de flujo líquido afectará los procesos fluidodinámicos y de transporte en el exterior de la pastilla catalítica, pero también el transporte de materia, reacción química y acumulación en el interior de la partícula se verán modificados. La interacción entre estos fenómenos externos e internos es muy compleja. Por ello, a pesar de los resultados alentadores obtenidos por diferentes investigadores

(Castellari and Haure, 1995, Kadhilkar et al., 1999) esta tecnología no ha sido aún aplicada a nivel industrial. Es imprescindible continuar con estudios (tanto experimentales como teóricos) que permitan comprender los fenómenos relacionados con la modulación del flujo líquido como paso previo a su uso comercial.

Otra forma de mejorar la operación de un sistema catalítico en general y en particular de un RTB, es mediante el adecuado diseño del catalizador, tanto en su forma geométrica como a través de una adecuada distribución del material catalítico. Las alternativas de distribución del material catalítico en el interior de una partícula en un RTB que opera en estado estacionario han sido extensamente estudiadas (Gavriilidis et al., 1993). Sin embargo, el impacto de emplear operación periódica cuando se utilizan catalizadores con una distribución de los sitios activos definida no ha sido examinado en forma sistemática ni a través de modelos.

Como se mencionara anteriormente, es necesario estudiar en profundidad el impacto que la modulación del caudal de líquido produce en los procesos fluidodinámicos y de transporte en el exterior de la pastilla catalítica. Si bien se han propuestos distintas correlaciones empíricas para evaluar los parámetros hidrodinámicos en un RTB en estado estacionario, no existe información para la operación periódica. A partir de experimentos dinámicos se deben establecer las correlaciones específicas para operación periódica. (Lange et al., 2004).

En la mayoría de las contribuciones disponibles en la literatura, se proponen sólo explicaciones cualitativas de resultados experimentales. La interacción entre los efectos hidrodinámicos, de transporte, cinéticos y de acumulación que tiene lugar en un RTB bajo operación periódica es muy complicada. En consecuencia, no existe aún un modelo exhaustivo que describa el comportamiento del reactor integral considerando todos los factores y, que haya sido verificado experimentalmente.

En este contexto, el objetivo del presente trabajo es llevar a cabo un estudio sistemático de la influencia de emplear modulación del flujo de líquido sobre una reacción catalítica en un RTB, a partir de:

- ✓ la formulación y resolución de un modelo exhaustivo a escala de pastilla catalítica, que provea los elementos necesarios para comprender la compleja interacción entre la dinámica de la reacción química y la transferencia de

materia intrapartícula, y como la misma se ve afectada por la modulación del líquido que circula alrededor

- ✓ la determinación de la influencia de la modulación del flujo de líquido sobre los perfiles axiales y temporales de retención o “holdup” de líquido en una columna rellena con circulación de gas y líquido en cocorriente descendente (maqueta fría de un RTB).

Mediante el desarrollo de estos objetivos, se ha logrado:

- ✓ Desarrollar una herramienta matemática para predecir condiciones de operación óptimas cuando el flujo de líquido es modulado. El modelado facilitará la construcción de argumentos sólidos para decidir *a priori* si una estrategia de operación periódica mejorará o no la performance de un RTB.
- ✓ Analizar la respuesta de una única pastilla con diferentes distribuciones de sitios activos a variaciones temporales de las condiciones externas.
- ✓ Hallar una correlación adecuada para describir el comportamiento hidrodinámico del RTB bajo modulación de flujo líquido, para incorporarla luego al modelo desarrollado a escala de pastilla catalítica.

A modo de resumen, el Capítulo I presenta una introducción general de las características de los reactores Trickle Bed, junto con una revisión de los antecedentes existentes en la literatura en operación periódica.

El Capítulo II tiene el propósito de modelar la variación temporal de una pastilla catalítica sometida alternativamente a diferentes caudales de líquido. En particular se analiza la estrategia de interrupción periódica de la circulación de líquido (modalidad ON-OFF). Se tienen en cuenta los distintos factores que influyen sobre el proceso catalítico, transferencia de masa externa e intrapartícula, mojado parcial del catalizador, acumulación de los reactivos involucrados para el caso de una partícula isotérmica. Se estudia el sistema isotérmico, dado que facilita el aislamiento de los distintos efectos que determinan la velocidad de la reacción alcanzada.

Los resultados a escala de pastilla contribuyen al análisis riguroso del impacto de la operación periódica en el interior de la pastilla y viceversa. Los parámetros hidrodinámicos obtenidos experimentalmente serán incorporados en el modelo. Luego, el modelo completo, junto con el desarrollo de éste a escala de reactor, servirá como base para el diseño del reactor integral. Esto se realizará en trabajos futuros.

En el Capítulo III, el modelo propuesto se extiende a fin de llevar a cabo un análisis de las ventajas de emplear una distribución no-uniforme de sitios activos en el catalizador heterogéneo. Se analiza el impacto sobre el curso de la reacción trifásica de la configuración interna de los sitios activos del catalizador cuando se emplea modulación del flujo de líquido. Para el análisis, se consideran pastillas catalíticas uniformes y egg-shell, con diferentes distribuciones de sitios activos con núcleo permeable o impermeable.

En el Capítulo IV se presentan resultados de experimentos llevados a cabo en un sistema sin reacción de dimensiones de escala piloto tendientes a determinar la variación axial y temporal de la retención (“holdup”) de líquido en RTB con operación periódica. Los ensayos se llevan a cabo utilizando un sistema no-reactivo sobre un lecho de partículas esféricas de $\gamma\text{-Al}_2\text{O}_3$. Se emplea una columna rellena con partículas porosas comúnmente utilizadas como soporte de catalizadores (partículas esféricas de $\gamma\text{-Al}_2\text{O}_3$ de 3mm de diámetro). Se analizan las variaciones temporales de holdup en distintas posiciones axiales del reactor y se propone una correlación empírica que permitirá estimar la variación temporal de holdup de líquido en dichas posiciones, a fin de poder incluir en el futuro esta información en un modelo del reactor integral.

Por último, en el Cap. V se resumen las conclusiones más importantes que surgen de esta tesis y se indica el rumbo a seguir para establecer una metodología sistemática de diseño y escalado de RTB con operación periódica.

INTRODUCTION

Three-phase reactions, in which gas and liquid reactants are converted into desired products using solid catalysts, provide the basis for a large number of chemical, petrochemical, biochemical waste treatment and polymer processes (Dudukovic et al., 2002). Trickle beds reactors (TBR) are among the most widely commercially employed three phase reactors for these applications. They are also suitable for the catalytic oxidation of dissolved organic contaminants.

Traditionally, trickle-bed reactors are operated at steady state conditions in the trickle flow regime, for which the interaction between the phases is low. Under those conditions, overall reaction rate is frequently controlled by external mass transfer resistances. Periodic operation refers to a mode of process in which the system is forced to run continuously in a transient mode. When cycling is imposed to a TBR, the bed is periodically flushed with liquid, while the gas phase is fed continuously. Arising from the competition between the phases in supplying reactants to the catalyst, the possibility of performance enhancement or detriment by working under unsteady-state conditions exists in these reactors.

In the last decade, the improvements in terms of production capacity and/or conversion that can be attained in reactor performance if fluid flow rates are modulated have been highlighted (Castellari and Haure, 1995; Kadhilkar et al., 1999). Furthermore, this technique can be implemented with very low investment. Nevertheless, a cycling strategy has still not been applied commercially mainly due to a lack of an established methodology, and partly also by apprehensions about operation and control of industrial reactors under transient conditions. Hence, rigorous experimental and modeling efforts are still necessary to understand the phenomena underlying periodic operation before commercial implementation.

In most contributions presented in the literature, only qualitative explanations of experimental results have been presented. However, outcomes have not been contrasted with a model of TBR operating under liquid flow modulation. Therefore, a mathematical tool to decide *a priori* whether a cyclic procedure will provide process intensification would be extremely valuable.

Another alternative to enhance the performance of catalytic systems, including TBRs, is the design of tailored catalyst. The impact of non-uniform activity catalysts on reactor performance under steady state operation had been extensively studied (Gavriilidis et al., 1993). However, no work has analyzed the impact of catalytic distribution on periodic operation.

The comprehension of the underlying hydrodynamics plays an important role in the understanding of fundamental physical characteristics of trickle-bed reactors. Studies on hydrodynamic parameters have been accomplished under steady state operation. Numerous correlations have been proposed. However, the effect of non steady state operation on liquid hold-up, mass transfer coefficients and wetting efficiency has been scarcely investigated. With the objective of simulating reactor performance when a cycling strategy is used, dynamical experiments for the development of specific correlations for periodically operated TBRs are required (Lange et al., 2004).

The factors governing the reaction rate in periodic operation present different dynamical responses to the liquid flow perturbation and interactions become quite complex. Thus, modeling is still a challenge.

In this context, the aims of the present work are to:

- ✓ provide a mathematical tool for predicting optimal operating conditions when liquid flow is modulated. Modeling allows fundamentally based solid arguments to decide whether a cyclic procedure would provide process intensification.
- ✓ analyze the response of a single particle with different catalyst distribution to temporal modifications of the external conditions.
- ✓ find a suitable way to describe the hydrodynamic behavior of a TBR under liquid flow modulation, to be incorporated to the model at particle scale.

In development of these objectives, the work has succeeded in:

- ✓ Developing a mathematical tool to determine operating conditions that will lead to significant improvements of reactor performance by using an ON-OFF strategy of liquid flow modulation. The model aids in building fundamentally based arguments to decide *a priori* if a periodic operation strategy will improve the TBR performance.

- ✓ Examine comparatively the outcome of the catalytic reaction at the particle scale while using catalysts with different distributions of active sites under external liquid flow modulation.
- ✓ Get further insights in the transient behavior of the liquid holdup at different axial positions in the bed, developing a correlation to approximately account for the time dependence of the liquid holdup in a TBR with an ON-OFF strategy of liquid flow modulation.

In brief, Chapter I presents a general introduction to TBRs, accompanied by a review of the most relevant papers presented in the literature on periodic operation of TBRs.

Chapter II has the purpose of modeling the time course of the reaction rate for a catalyst particle that is immersed in an alternating ON-OFF liquid flow. Partial external wetting, intraparticle dynamics and changing external conditions are considered.

Results at the single particle cannot be compared with experimental outcomes of an integral reactor. However, this approach is still valuable since it allows decoupling essential factor affecting the system to observe its response to temporal variations of several parameters. Thus, qualitative trends predicted by the model are compared to experimental results.

In Chapter III, the model is extended to account for the analysis of the impact of internal particle configuration on liquid flow modulation. Uniform and egg shell particles, with different widths of active layer and permeable or impermeable core, are also considered in the analysis.

Chapter IV reports on cycling experiments performed using a non-reacting system, consisting of a packed bed of inert $\gamma\text{-Al}_2\text{O}_3$ spherical particles contacted with air and water flows. Experiments were conducted at different gas and liquid flows and cycling parameters. An empirical correlation to estimate the liquid holdup time variation at different reactor axial positions in a periodically operated trickle bed reactor is proposed.

Finally, Chapter V presents the most relevant conclusions that arise from this thesis.

I. STATE OF THE ART

I.1. TRICKLE BED REACTORS

Fixed bed catalytic reactors in which gas and liquid phases flow concurrently downwards are known as Trickle Bed Reactors (TBRs). These reactors are particularly important in the petroleum industry where they are used primarily for hydro-treating, hydro-desulfurization and hydro-denitrogenation; other commercial applications are found in the petrochemical industry, involving mainly hydrogenation and oxidation of organic compounds. TBRs are also employed in wastewater treatment and chemical and biochemical processes. (Dudukovic et al., 2002; Gianetto and Specchia, 1992; Martínez et al., 1994).

TBRs provide flexibility and simplicity of operation, as well as high throughputs and low energy consumption. These reactors are usually operated at high temperatures, to overcome kinetics and/or thermodynamics restraints. High pressures are then required to improve gas solubility and mass transfer rates. Particles are relatively large to avoid excessive pressure drop. Then, the catalyst load is usually high, since particles are not fully used due to internal transport limitations.

Drawbacks are related mainly to difficulties in achieving good fluid phase distribution. Poor performance or even hot spots and sintering of the catalyst may be occasioned by excessive channeling. In addition, heat and mass transfer rates are generally lower than in systems with suspended solids, like slurry reactors or three-phase fluidized beds. The hydrodynamic of TBRs is intricate and significantly affects reactor performance, since it modifies the mass and heat transport characteristics.

The major aspects that determine reactor performance are depicted in Fig. 1.1 (Martinez et al, 1994). Interactions between factors are also indicated in the figure. Comprehensive reviews, which recall the numerous worldwide contributions on the different aspects illustrated in Fig. 1.1 are available (*e.g.*, Nigam and Larachi, 2005; Dudukovic et al., 2002; Al-Dahhan et al., 1997; Saroha and Nigam, 1996; Martínez et al., 1994; Gianetto and Specchia, 1992).

The performance of a gas-liquid-solid reacting system is quite complex and depends on several factors, which are closely related in between: transport and hydrodynamic processes that occur outside the particle and transport processes and chemical reaction that take place inside the particle. Furthermore, catalyst characteristics (size, geometry, active sites distribution) can also influence the reactor behavior. Successful modeling relies on the ability to understand and quantify the transport-kinetic interactions on a particle scale, interfacial transport on particle and reactor scales, flow pattern of each phase and phase contacting pattern, and how these change with variations in reactor scale and operating conditions (Dudukovic et al., 2002).

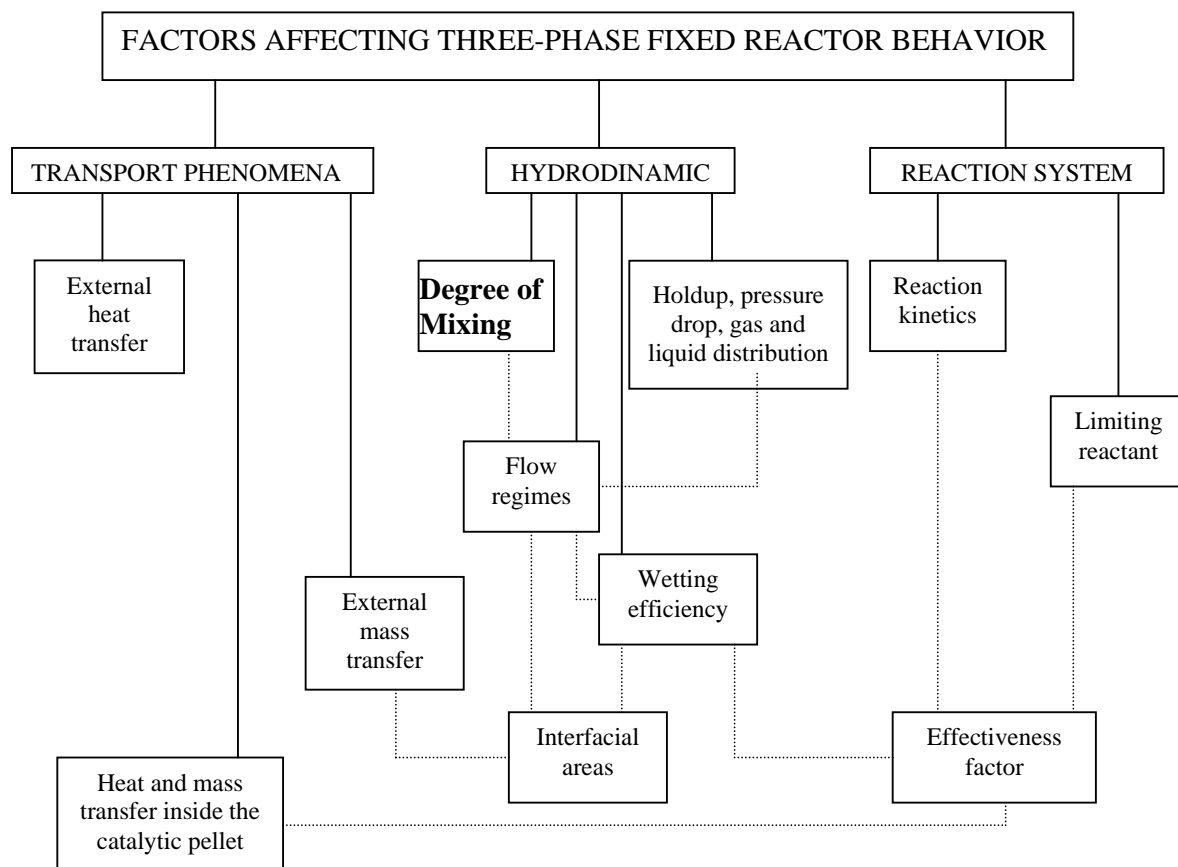


Figure I.1: Factors affecting three-phase fixed reactor behavior. (Martínez et al. 1994)

Traditionally, TBRs are operated at steady-state conditions. The most common flow regime employed is the trickle flow regime, for which interactions between the phases are low and mass transport is frequently rate controlling. Thus, an integrated approach (catalyst selection, reactor design, process configuration) could be used to improve reactor performance. Process Intensification (PI) is the strategy of making significant reductions in the size of a chemical plant in order to achieve a given production objective (Nigam and Larachi, 2005). Process Intensification of a trickle-bed reactor can be obtained by liquid flow modulation, provided that the mass transfer characteristics of the limiting reactant are improved. Flow maldistribution that could arise, and the formation of hot spots, must be prevented or at least controlled (Nigam and Larachi, 2005).

Recent studies have demonstrated reactor performance improvements over the optimal steady state when the liquid flow is periodically interrupted while the gas phase is fed continuously, *i.e.*, ON-OFF strategy of liquid flow modulation (Silveston and Hanika, 2002). Heat and products are removed from the catalyst mainly during the ON cycle while in the OFF portion of the cycle, the bed partially drains. The overall mass transport rate of the gaseous reactant to the catalyst is increased and reaction proceeds between the reactants in the flowing gas and those in the liquid that remains in the bed.

In the next sections, efforts will be focused to review those factors most related to the aim of this work. Particularly, available information for periodic operation of TBRs will be presented for the parameters that have been studied and/or used for the modeling.

I.1.1. HYDRODINAMICS

The hydrodynamic parameters (liquid holdup, wetting efficiency, liquid distribution, pressure drop) directly influence the conversion and selectivity that could be achieved in a TBR. The relative amount of liquid present in the bed (or liquid holdup) and the way in which that liquid circulates through the bed (related to the liquid distribution and the wetting efficiency) depend on several factors, such as liquid and gas flow rates, physical properties of the fluids, catalyst characteristics, operating pressure and temperature, etc. Hydrodynamic parameters required for reactor design and scale-up are usually estimated using correlations developed from experiments in cold mock-ups. It should be mentioned

that correlations proposed for estimating key hydrodynamic parameters have been developed under steady-state conditions. Hence, available correlations would only be strictly valid for steady-state operation.

I.1.1.1. FLOW REGIMES

Different flow regimes can be observed in a TBR depending on the gas and liquid flow rates, the physical properties of the fluids and the geometrical characteristics of the reactor and the packing (Saroja and Nigam, 1996; Charpentier and Favier, 1975). Several flow regime maps and correlations in terms of physical properties are available, although data does not always agree.

At low liquid and gas flow rates, the liquid flows in laminar films or in small rivulets, with low hydrodynamic interaction between the phases. This *trickle flow* regime often gives rise to axial dispersion, maldistribution, and incomplete external catalyst wetting of the solid.

An increase in the liquid and the gas flow rates leads to the *pulsing flow* regime, characterized by the formation of alternate slugs (liquid-rich and gas-rich slugs) traveling along the reactor. Pulses continuously renew the liquid in stagnant zones up to a point where its stagnant nature disappears, which improves reactor performance (Boelhouwer, 2001). The pressure drop increases remarkably and shows a fluctuating behavior. This regime is generally characterized by higher mass transfer coefficients and more uniform liquid distribution through the packing than the trickle flow regime (Tsochatzidis and Karabelas, 1995). However, pulsing flow is also associated with high operating costs.

A further increase in the liquid flow rate, at relatively low gas flow rates, can induce the appearance of a *bubbling flow*, where the liquid is the continuous phase and the gas is carried along the reactor as bubbles. On the other hand, at high gas flow rates and very low liquid flow rates, the *spray flow* regime exists, where the gas is the continuous phase and the liquid flows as isolated drops dispersed in the gas stream.

Generally, laboratory reactors are operated under trickle or pulsing flow regimes. Most industrial trickle-bed reactors operate in the trickling flow regime, near the transition to pulsing flow in order to ensure complete wetting of the packing (Burghardt *et al.* 1999).

I.1.1.2. LIQUID HOLDUP

The liquid holdup is a measure, although approximate and incomplete, of the effectiveness of contacting between the liquid and solid catalyst. It is defined as the fractional volume of the liquid inside a reactor (Satterfield, 1975). The liquid holdup is also an important parameter commonly used to characterize the hydrodynamics of three phase reactors. It affects the degree of catalyst wetting and liquid film thickness; thus, liquid holdup depends on operating conditions, fluid physical properties as well as packing bed characteristics (Martinez et al, 1994).

For a bed consisting of porous particles, the liquid holdup includes internal and external contributions. If the internal pores are completely filled with liquid, as usually happens due to capillarity effects, then the internal holdup (that is the liquid held in pores of the catalyst) can be simply calculated from the bed and particle void fractions. The external holdup can be separated into static and dynamic holdup. Static holdup comprises the fluid trapped between particles. It is independent of gas and liquid flow rates, while it increases with decreasing particle sizes and increasing surface tension (Murugesan and Sivakumar, 2005). Dynamic holdup determines the residence time of the liquid phase and it is also an important parameter for safety considerations when a strong exothermic reaction is taking place (Gabarain et al., 1997).

Liquid holdup can be evaluated by volumetric, gravimetric, radiometric and tracer techniques (Martínez et al., 1994).

The volumetric technique, or drainage method, has been widely used for estimating the dynamic liquid holdup because of its simplicity. The liquid held in the reactor after interrupting abruptly the fluids circulation is associated to the total liquid holdup. The dynamic liquid holdup is calculated from the liquid that drains from the column. The liquid that remains inside corresponds to the static holdup. However, the drainage technique has been criticized because data is measured at zero liquid flow rate, which has no sense for reactor design purposes (Martínez et al., 1994). Urrutia et al. (1996) suggested that the dynamic liquid holdup should be calculated by extrapolation of the linear region in a representation of the liquid drained from the reactor vs $t^{-1/2}$, where t is the time. Values obtained are generally larger than those reported using the drainage method. The authors claimed that this methodology helps reconciliation between liquid holdup results obtained

by dynamic and drainage methods. It should be mentioned that their study was conducted at zero gas flow rate.

The gravimetric technique relies in weighting the liquid that remains in the reactor after interrupting abruptly the fluids circulation. Gravimetric and volumetric techniques, though simple and widely applied, only provide average values of the liquid holdup over the entire bed length (Nemec, 2002).

Radiometric and tracer techniques have also been extensively used. Radiometric methods lead to more local values, since they are based on the change in the transmitted photon counts arising from the different amount of liquid and gas intercepting the beam. With the same fundamental principle, tomographic methods have been applied to get local values of liquid holdups and liquid distribution in TBRs (Lutran et al., 1991; Marchot et al., 1999). Naturally, the information obtained is very complete. However, implementation is expensive and safety considerations are required.

Tracer techniques have been used particularly to examine characteristics of the liquid circulation, the so-called macromixing (Wen and Fan, 1975; Nauman and Buffham, 1983). By postulating flow models to describe the liquid circulation, the flow model parameters and the liquid holdup have been obtained simultaneously from stimulus-response techniques (Nauman and Buffham, 1983; Cassanello, 1992). Residence time distribution (RTD) curves, using pulse or step perturbations, are analyzed by fitting in the time or in the frequency domains or from the corresponding moments. Large spread in the measured signal is observed when certain fluid portions have very long residence times (Westertep et al., 1984). This effect is reduced when the relative fraction of the dynamic holdup increases, for instance at higher liquid flow rates. Moreover, great care should be taken when working with porous packings, since part of the tracer could be adsorbed in the particles, resulting in long tails. Gianetto et al. (1986) highlighted that this technique may give poor results if the tracer concentration in the tail of the response curve is not determined with accuracy.

Approximate values of liquid holdups within packed beds have also been obtained by conductimetric methods (Muzen and Cassanello, 2005; Burns et al., 2000; Basic and Dudukovic, 1995; Tzochatzidis et al., 1992; Prost and Le Goff, 1964). The response of the conductance probe used is contrasted to the liquid holdup measured by one of the traditional procedures. The conductimetric method can be carried out without interfering with the flow

by using flushed electrodes or electrodes that resemble the packing. It allows characterization of the liquid flow pattern in packed beds through accurate instantaneous measurements. Tsochatzidis et al. (1992) examined radial and axial liquid distributions at various bed heights using local and ring conductance probes, respectively.

Several correlations were developed for the estimation of the total, dynamic holdups. However, most of them are restricted to a limited range of application in terms of packing dimension, bed voidage and physical properties of the fluids (Dudukovic et al. 2002). The correlations used in this thesis to contrast their predictions with steady state experiments of liquid holdup, as well as for the static liquid holdup, are listed in Table I.1. The operating conditions used in the present work are within the range at which these correlations were determined.

Table I.1 Liquid holdup correlations for trickling flow in packed beds

References	Correlation
Lange et al. (1978)	$\varepsilon_l = 0.16.(1 - \varepsilon_s) \left(\frac{D_c}{2.R} \right)^{0.33} .Re_l^{0.14}$ <p>method: tracer</p>
Mills and Dudukovic (1984)	$\frac{\varepsilon_l}{\varepsilon} = 2.02.Re_l^{0.34} .Ga_l^{-0.197}$ <p>method: tracer.</p>
Stegmüller (1986)	$\varepsilon_l = 26.3.Re_l^{0.58} .Ga_l^{-0.56}$ <p>method: tracer</p>
Larachi et al. (1991)	$\frac{\varepsilon_l}{\varepsilon_b} = 1 - 10^\Gamma; \quad \Gamma = 1.22.We_l^{0.15} .\chi_g^{-0.15} .Re_l^{-0.2}$ <p>method: tracer</p>
Static holdup	
Saez and Carbonell (1985)	$\varepsilon_s = \frac{1}{20 + 0.9.E\ddot{o}^*}; \quad E\ddot{o}^* = E\ddot{o}.\varepsilon_b^2.(1 - \varepsilon_b)^2$ <p>method: drainage,</p>

Murugesan and Sivakumar (2005)	$\varepsilon_s = 0.036 \left[E\ddot{o}' \left(\frac{\sigma_w}{\sigma_l} \right)^{1.5} \right]^{-0.23}$	$E\ddot{o}' = E\ddot{o} \left(\frac{2}{3} \phi_s \cdot \frac{\varepsilon_b}{(1 - \varepsilon_b)} \right)^2$
	method: gravimetric	

Additionally, the general correlation developed by Iliuta et al. (1999c) is also considered, to take advantage of its wide range of validity, since it was developed based on an extensive database of liquid holdup measurements in TBRs, using a combination of Artificial Neural Network and Dimensional Analysis. A user friendly excel datasheet is available at <http://www.gch.ulaval.ca/~larachi> for the estimation of liquid holdup.

To estimate the static liquid holdup, the widely accepted correlation of Saez and Carbonell (1985) was used. A recent review of the most important correlations developed for estimation of the static holdup in fixed beds can be found in Murugesan and Sivakumar (2005).

I.1.1.3. WETTING EFFICIENCY

Partial wetting of the particles, which leads to more direct contact between the gas and the catalyst, is a unique feature of TBRs. It has to be considered for the design and scale up of TBRs, especially within the trickle flow regime.

For moderately exothermic reactions (where drying inside the pellet is prevented), the particles are completely filled with liquid due to capillarity, while the external surface of the particles may be covered with liquid only partially (Figure I.2) (Satterfield, 1975). External partial wetting is usually characterized by the wetting efficiency (f), defined as the fraction of the external area of the catalyst effectively wetted by liquid.

External wetting efficiency is generally estimated by measuring the reaction rate of well known reactions and formulating appropriate reactor models. In addition, the dynamic tracer technique and the dissolution and/or dye adsorption techniques have also been used (Martinez et al., 1994). A complete description of the methods employed for the evaluation of the wetting efficiency can be found in Pironti et al. (1999).

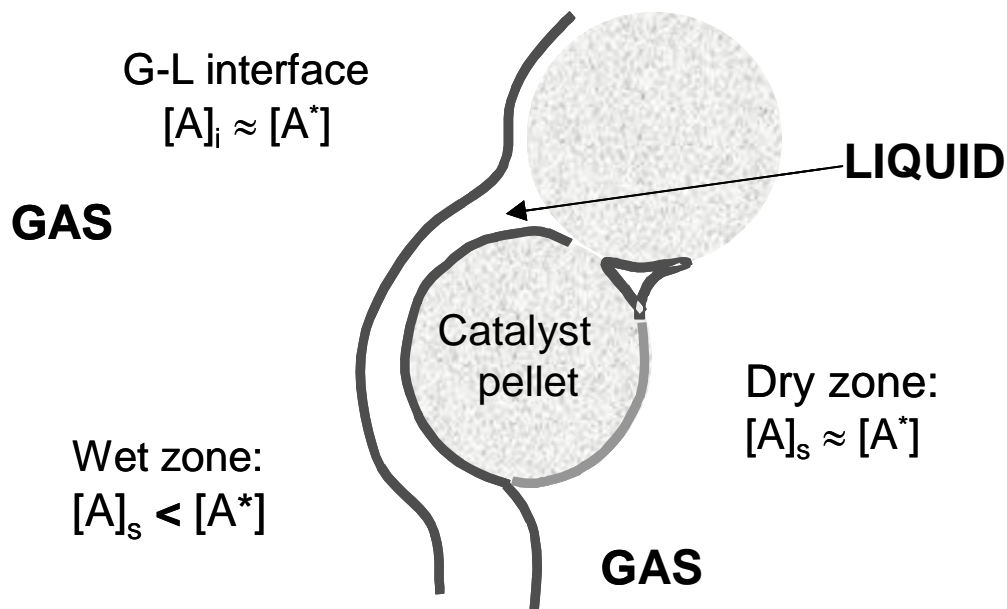


Figure I.2: Schematic representation of a partially wetted catalyst pellet.

Several empirical correlations for determining the wetting efficiency have been developed. Data available in the literature is scattered due to the complexity of the liquid hydrodynamics. Larachi et al. (2001) developed a methodology to estimate the wetting efficiency in TBRs using an extensive database and combined approaches, relying on artificial neural network and dimensional analysis. The wetting efficiency was found to be a function of a combined two phase flow Reynolds number and liquid Stokes, Froude and Galileo numbers.

Herskowitz (1981) proposed a simple correlation developed for gas-limited reactions controlled by external mass transfer. The wetting efficiency was determined by comparison between experimental and calculated rates for the hydrogenation of α -methylstyrene over a palladium catalyst. The expression proposed to estimate the external wetting efficiency, f , is:

$$f = 1.3013 + 0.0739 \ln (u_1) \quad (\text{I-1})$$

valid for $0.0002 < u_l < 0.01$ m/s.

Since correlations are strictly valid within the specific range of operating conditions for which they have been developed, the performance of experiments under actual conditions is always recommended. However, due to its simple dependence with the liquid superficial velocity, Eq. (I-1) has been considered to estimate the wetting efficiency for aiding the model presented in this thesis.

I.1.2. MASS TRANSFER

When a reaction between a gas reactant A and a non volatile liquid reactant B takes place within a completely wet porous catalyst, the following steps can be identified (Ramachandran & Chaudhari, 1983)

- transport of A from bulk gas phase to the gas liquid interface
- transport of A from gas liquid interface to the bulk liquid
- transport of A and B from bulk liquid phase to the catalyst surface
- intraparticle diffusion of the reactants inside the catalyst pores
- adsorption of the reactants in the active sites of the catalyst
- surface reaction of A and B to yield products

Mass transfer between phases and within the catalyst can largely affect three-phase processes typically carried out in TBRs. So, in order to model and analyze the behavior of a TBR, it is necessary to take into account these steps and estimate the governing parameters.

I.1.2.1. GAS- LIQUID MASS TRANSFER

The importance of gas-liquid mass transfer on reactor performance depends upon the nature of the reaction system and the flow conditions in the reactor. Numerous contributions have dealt with experimental evaluation of gas-liquid mass transfer coefficients in TBRs, pursuing development of adequate correlations to estimate this key transport parameter. Most of the available information is restricted to steady state operation under different flow regimes. Even though a great number of correlations were proposed, most of them fail to

adequately represent actual results. The lack of success can be attributed to the scattered experimental data (Dudukovic et al., 2002).

An extensive review of the available literature information on gas-liquid mass transfer in TBRs, and updated improved correlations to estimate the mass transfer coefficients and interfacial areas can be found in Larachi et al. (2003). Correlations to evaluate gas-liquid mass transfer coefficients in trickle beds by means of a combination of dimensional analysis and artificial neural networks were proposed based on a large databank by Iliuta et al. (1999a). The interfacial area, the volumetric liquid-side mass transfer coefficients and the volumetric gas-side mass transfer coefficients, were expressed as a function of several dimensionless groups. Then, the impact of fluid velocities, densities, viscosities, diffusivities, surface tension, gravitational acceleration, particle size and shape, bed diameter and porosity was taken into account.

Nevertheless, to incorporate a relationship to relate mass transfer coefficients at different liquid velocities, it is practical to use a simple expression. The correlation proposed by Goto & Smith (1975) has been frequently used to evaluate the gas-liquid mass transport coefficient for the steady state operation of TBRs. The authors measured the absorption and desorption of O₂ in water in a column packed with 0.0541-0.291 cm catalyst particles, for superficial gas velocities within the range 0.2–0.8 cm/s and superficial liquid velocities of 0.05–0.5 cm/s. The following equation was suggested:

$$\frac{k_1 \cdot a_{gl}}{D} = \alpha_1 \cdot \left(\frac{\zeta_1 \cdot u_1}{\mu_1} \right)^n \cdot \left(\frac{\mu_1}{\zeta_1 \cdot D} \right)^{0.5} \quad (\text{I-2})$$

where α_1 and n are constants related to the geometry of the particles and surface area.

The correlation proposed by Goto & Smith (1975) is used in this thesis for aiding the modeling section, since it depends almost exclusively on the liquid superficial velocity. Hence, a simple relation can be established to associate conditions during cycling with a reference steady state.

I.1.2.2. LIQUID - SOLID MASS TRANSFER

The importance of liquid-solid mass transfer on reactor performance depends, once again, upon the nature of the reaction system and the flow conditions in the reactor.

Liquid solid mass transfer measurements in TBRs are generally obtained by determining the dissolution of a soluble packing or by an electrochemical method (Boelhouwer, 2001).

Electrochemical techniques give the instantaneous mass transfer coefficient by measuring the limiting current under diffusion limited transport conditions at a relatively high voltage. Then, the current is independent of the potential at the working electrode and it is a direct measure of the diffusive flux (Rao and Drinkenburg, 1985). This method can be used to get mass transport coefficients under dynamic conditions. Maucci et al. (2001) measured simultaneously and locally liquid-solid mass transfer coefficients in liquid and liquid solid systems. These authors proposed a model based on the surface renewal model, which predicts the instantaneous liquid solid mass transfer between a particle and a liquid from the instantaneous liquid velocity in the presence or absence of particles.

The available literature and updated correlations has also been reviewed by Larachi et al. (2003). Once again, even if these correlations are recommended for evaluating mass transfer coefficients, we seek for a simple relationship, particularly based on the liquid superficial velocity, to be used for aiding the modeling of the periodic operation of TBRs.

Goto & Smith (1975) obtained the liquid solid mass transfer coefficient by measuring the dissolution rate of β -naphthol into water in a TBR packed with 0.0541-0.241 cm catalyst particles, for superficial gas velocities within the range 0.2–0.8 cm/s and superficial liquid velocities of 0.05–0.5 cm/s:

$$\frac{k_s \cdot a_p}{D} = \alpha_1 \cdot \left(\frac{\zeta_1 \cdot u_1}{\mu_1} \right)^n \cdot \left(\frac{\mu_1}{\zeta_1 \cdot D} \right)^{1/3} \quad (\text{I-3})$$

where α_1 and n are constants related to the geometry of the particles and surface area.

Hence, due to its simplicity, Goto & Smith (1975) correlation is considered in this thesis to relate the liquid-solid mass transfer coefficients under periodic and steady state operation of TBRs.

I.1.2.3. INTRAPARTICLE MASS TRANSFER

When an isothermal reaction occurs simultaneously with mass transfer within a porous structure, a concentration gradient is established due to the intraparticle mass transfer resistances, and thus, interior surfaces are exposed to lower reactant concentrations than the external surface. So, the average reaction rate for a catalyst particle under isothermal conditions will always be less than it would be if there were no mass transfer limitations (Satterfield, 1981). An effective diffusion coefficient, usually estimated from the molecular diffusivity of the substance, the particle porosity and tortuosity of the porous structure, is used to characterize the internal mass transport (Lemcoff et al., 1988). Internal transport effects are taken into account through the effectiveness factor, which relates the actual reaction rate to the maximum possible reaction rate if all active sites were in contact with of the same reactant concentration as the one at the outside surface of the particle (Satterfield, 1981).

The general theoretical approach to evaluate the effectiveness factor is to develop the mathematical equations for simultaneous mass transfer and chemical reaction within the catalyst particle (Aris, 1975; Ramachandran and Chaudhari, 1983). Analytical solutions for the internal effectiveness factor as a function of the Thiele modulus are available for isothermal conditions and different reaction orders, catalyst geometries and uniform active sites distribution (Satterfield, 1975).

I.1.2.4. CATALYST DESIGN

To overcome the effect of internal mass transfer resistances, tailoring of the heterogeneous catalyst to conveniently distribute the active element for minimizing transport resistances has been proposed and largely used. The improvement attained in

catalyst performance by suitably distributing the active element in the inert support has been studied both theoretically and experimentally (Gavriilidis et al. 1993; Lekhal et al., 2001). The most frequent arrangement is the so-called “egg-shell”, in which a thin layer of catalytic material is placed in the external surface of a spherical particle.

Several works reported the use of non uniformly active catalysts in TBRs under steady state (Mills et al. 1984; An et al. 2001) and with liquid flow modulation (Gabarain et al. 1997; Houserová et al. 2002; Banchero et al. 2004).

The use of models to evaluate the impact of catalytic active phase distribution on TBRs performance can reduce significantly the experimental work required for designing the catalyst. Gavriilidis et al. (1993) presented a well recognized approach to account for the non uniform distribution of the active element in a catalyst under steady state operation of fixed bed reactors. Also, several authors have modeled the steady state behavior of TBRs loaded with egg-shell catalyst (Beaudry et al. 1987; Harold et al. 1987).

I.1.3. REACTION SYSTEM

The reaction system should be taken into account to evaluate the behavior of a TBR by appropriate models. Kinetic information of the reaction involved is required. Simple generic and lumped schemes can be proposed to formulate the models, provided they capture the essence of the studied reaction. Moreover, simple schemes allow interpreting underlying hydrodynamic and mass transfer effects, which could be hidden if studied by more complex kinetic expressions. The reaction system determines the degree of incidence of mass transfer and hydrodynamics on the reaction rate.

I.1.3.1. LIMITING REACTANT

For a gas-liquid-solid catalyzed system with negligible external mass transport limitations, the limiting reactant can be determined by a criterion proposed by (Khadilkar et al, 1996). The internal diffusion fluxes of the two reactants are compared, defining the following parameter:

$$\gamma = D_B C_{B0} / b D_A C_A^* \quad (\text{I-4})$$

where D is the effective diffusion coefficient of the corresponding reactant within the catalyst particle, C_A^* is saturation gas reactant concentration in the liquid phase, C_{B0} is the initial liquid reactant concentration and b is the stoichiometric coefficient.

The parameter γ is indicative of the relative availability of the species at the reaction site. When $\gamma \gg 1$, the reaction is gas-reactant limited; hence, favoring the access of the gas reactant to the active sites will improve the reaction rate. Conversely, the reaction is liquid-limited if $\gamma < 1$.

The overall reaction rate in a partially wetted pellet can be higher or lower than that achieved for a completely wet particle, depending on the limiting reactant. If the limiting reactant is in the liquid phase and it is non-volatile, a higher mass transport to the catalyst is obtained at higher wetting efficiency. Then, for liquid limited reactions, complete wetting is desired, which is generally achieved in fixed bed reactors with cocurrent upflow operation or in TBRs at high liquid velocities or with catalyst diluted with fines. For a gas-limited reaction, higher reaction rates can be obtained for low wetting efficiencies, where the gas can access the particle directly from the surface; hence, TBRs with moderate and low liquid velocities will present higher reaction rates (Beaudry et al., 1987; Iliuta et al., 1999b)

I.1.3.2. OVERALL EFFECTIVENESS FACTOR

The concept of overall effectiveness factor was first introduced by Sylvester et al. (1975) to simplify the calculation of the reaction rate in three-phase systems. It is defined as the actual rate of reaction divided by the rate obtained by neglecting all the transport resistances. Therefore, the overall effectiveness factor also represents the efficiency of the reactor.

Ramachandran and Smith (1979) evaluated the overall effectiveness factors for a completely wet particle and power law kinetics. This factor depends on the generalized Thiele modulus and a dimensionless parameter that characterizes the external mass transfer

and also represents the ratio of maximum possible rate of mass transfer to the maximum rate of chemical reaction.

As mentioned in the section I.1.1.3, the external surface of the catalyst particles may not be completely covered with liquid in TBRs. If external wetting of the catalyst is incomplete, conventional catalytic effectiveness factors are no longer valid since the reactants concentration is not the same all over the external surface. Excellent approximations have been proposed to estimate the effectiveness factor of partially wetted particles. Lemcoff et al. (1988) have reviewed them and discussed their application in the modeling of TBRs.

Approximations depend on the internal wetting, which may be lower than one for highly exothermic reactions. For isothermal or nearly isothermal conditions, internal wetting is generally assumed due to capillarity forces. Hence, since the model that is formulated and solved in this thesis considers isothermal conditions, only approximations for the case of complete internal wetting are discussed.

Either for gas limited reactions (Ramachandran and Smith, 1979; Tan and Smith, 1980) or for liquid limited reactions (Mears, 1974; Dudukovic, 1977), the overall effectiveness factor of a porous particle with complete internal wetting and partial external wetting, η_{pew} , can be estimated considering the external wetting efficiency, as a weight factor. The overall effectiveness factor is calculated as the sum of the one obtained with complete external wetting, η_{ew} , and nil external wetting, η_{ed} , weighted by the external wetting efficiency (f):

$$\eta_{pew} = f \cdot \eta_{ew} + (1-f) \cdot \eta_{ed} \quad (I-5)$$

I.1.4. PERIODIC OPERATION OF TBRs.

I.1.4.1. DEFINITION.

Periodic operation refers to a type of process in which the system is forced to operate continuously in a transient mode. This Process Intensification technique seems to be

a promising tool to improve the performance of TBRs, especially when the mass transfer of a key reactant is rate controlling or, at least, affects significantly the reaction rate.

Modulations pursuing performance enhancements in TBRs have been mainly of two types: feed composition modulation and liquid flow modulation (Silveston and Hanika, 2002). In this work, the second approach is particularly studied. Since hydrodynamics and heat and mass transport coefficients in TBRs depend on the liquid velocity, its modulation can largely affect the reactor performance.

Liquid flow modulation can be simply accomplished by switching periodically the liquid flow rate between zero and a given value, strategy generally known as ON-OFF cycling. In addition, the liquid flow can be switched between a low (non zero) and a high value, known as BASE-PEAK cycling. Normally, the gas flow rate is kept constant over the entire period. Then, periods of high gas reactant access to the catalyst surface (during the dry cycle) alternate with periods of gas reactant scarcity (during the wet cycles) due to strong mass transfer limitations.

Two parameters define liquid flow modulation: the period, P , which is the total time spent between two predetermined levels and the split, s , defined as the ratio between the time spent in the upper level to the period. Figure I.3 shows a typical liquid flow modulation input profile.

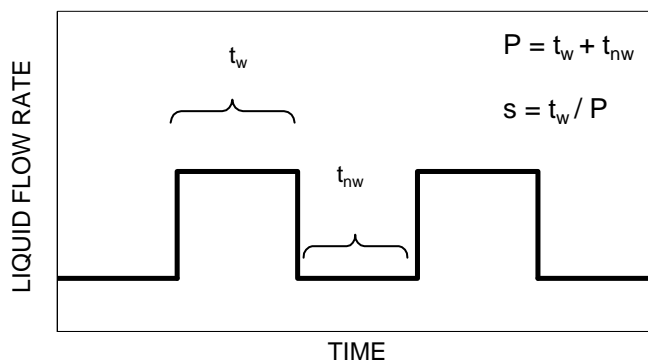


Figure I.3: Cycling mode of operation.

The European Consortium for cycling operation (CYCLOP) has formally defined two types of periodic liquid pulsation (Sicardi et al. 2002):

- The SLOW MODE cycling in which the period is long enough to warrant that “all” the reactor length might work for some time at the minimum and some time at the maximum liquid velocity used. This time is comparable to the liquid residence time in the reactor, which is in the order of some minutes in a TBR.

- The FAST MODE cycling in which part of the reactor works at the minimum and part at the maximum liquid velocity, generating a shock wave.

A clear distinction between fast and slow mode of induced pulsing is the existence of at least one pulse in the packed bed. More specifically, in the fast mode the cycle period should be smaller than the liquid residence time. (Giakoumakis et al., 2005)

Periodic operation in commercial TBRs has not been implemented due to (i) scarce knowledge of key transport and hydrodynamic parameters, and kinetic information, in processes under dynamic conditions, (ii) lack of an established methodology of design and scale-up and (iii) apprehensions about operation and control of large-scale continuous reactors under transient conditions (Khadilkar et al., 1999).

I.1.4.2. EXPERIMENTAL STUDIES IN REACTION SYSTEMS

The application of periodic operation to TBRs was early suggested by Gupta (1985). The work by Haure et al. (1989) represents one of the first experimental studies of periodic operation of a TBR. A growing number of contributions concerning liquid flow modulation in TBRs at laboratory or pilot scale have been presented in the last fifteen years. Some of them are summarized in Table I.2.

The enhancement (ϵ) in reactor performance that can be obtained through cycling is defined as the ratio between the conversion attained with liquid flow modulation and the corresponding steady state conversion at an equivalent mean liquid flow rate. Many contributions have put in evidenced that, for certain sets of parameters, the enhancement can be greater than one even under isothermal conditions (Lange et al., 1994; Khadilkar et al., 1999; Muzen et al., 2005). Thus, reactor performance can be improved by periodic operation even for isothermal or moderately exothermic/endothermic reactions. However,

enhancements less than one had also been experimentally found (Houserová et al., 2003; Muzen et al., 2005; Massa et al., 2005).

The existence of optimal cycling parameters (cycle period and split) for a given reaction system has been experimentally noticed in many opportunities (Banchero et al., 2004; Urseanu et al., 2004; Fraguío et al., 2004; Tukac et al., 2003; Hanika et al., 2003; Khadilkar et al., 1999; Gabarain et al., 1997; Castellari and Haure, 1995). Particularly, a maximum value of ε can exist for a particular split at a given period and *viceversa*.

Table I.2: Experimental contributions aimed at studying the influence of periodic operation in TBRs.

REFERENCE	REACTION SYSTEM	CONDITIONS	PERIOD SPLIT	OBSERVATIONS IN CYCLING
Lange et al. (1994)	α -MS hydrogenation	Gas limited Isothermal	60–600 s 0.2–0.5	Maxima in ε vs P data and in ε vs s data
Lee et al. (1995)	SO ₂ oxidation	Gas limited Non Isothermal	30–60 min 0.01–0.1	Maximum in ε vs s data, related to the time needed to wash the H ₂ SO ₄
Castellari et al. (1995)	α -MS hydrogenation	Gas limited Non Isothermal	0–40 min 0.3–0.5	Maximum in ε vs P data. Optimum period depends on the split
Stradiotto et al. (1999)	Crotonaldehyde hydrogenation	Liquid limited Isothermal	300–1200 s 0.1 y 0.5	$\varepsilon > 1$ only for low liquid flows
Khadilkar et al. (1999)	α -MS hydrogenation	Gas and Liquid limited Non Isothermal	5 – 500 s 0.1–0.6	Maximum in ε vs P data
Turco et al. (2001)	α -MS hydrogenation	BASE-PEAK Gas limited Isothermal	10 min 0.2–0.3	The longer the low liquid flow cycle is, the better is ε .

Houserová et al. (2002)	α -MS hydrogenation cyclohexene hydrogenation	Gas limited Isothermal	0.3–10 min 0.3–0.9	Maxima in ϵ vs P data and in ϵ vs s data Effect of cycling on selectivity
Tukac et al. (2003)	Phenol oxidation	Gas limited Non Isothermal	40–300 s 0.3–0.7	Maxima in ϵ vs P data and in ϵ vs s data
Urseanu et al. (2004)	α -MS hydrogenation	Gas limited Non Isothermal	60–900 s 0.25	Maximum in ϵ vs P data Pilot plant reactor
Fraguio et al. (2004)	Ethanol oxidation	Gas limited Isothermal	9–1000 s 1/3, 2/3	Maximum in ϵ vs P data. Influence of the “past history” of liquid flow in ϵ . Improved selectivity towards final product.
Banchero et al. (2004)	α -MS hydrogenation	Gas limited Isothermal	3–120 s 0.33–0.67	Maxima in ϵ vs P data and in ϵ vs s data
Massa et al. (2005)	Phenol oxidation	Gas limited Isothermal	3–6–10 min 0.16–0.5	Maxima in ϵ vs P data and in ϵ vs s data. Improves selectivity towards final product.
Liu et al. (2005)	2-ethylanthra- quinones hydrogenation	Gas limited Isothermal	20–480 s 0.2–0.6	Maxima in ϵ vs P data and in ϵ vs s data. Improves selectivity towards intermediate product

Many of the studies reported in the open literature were restricted to gaseous reactant limited conditions, where periodic operation can lead to significant increase in production capacity and conversion compared to steady state operation due to favoured direct access of gaseous reactant to the catalyst sites. For liquid limiting reactions, steady state operation is superior to an ON-OFF strategy of periodic operation (Nigam and Larachi, 2005). BASE-PEAK strategies have been suggested in this case to improve liquid distribution and liquid reactant mass transfer and allow quenching of large rises in temperature (Dudukovic et al, 2002; Boelhouwer, 2001).

One promising application of TBRs is the removal of organic compounds present in wastewaters (Kolaczowski et al. 1999). TBRs can allow capacity demands, high pressure and temperature operation conditions, using sufficiently active catalysts with long term stability (Tukac et al, 2003). Their high catalyst load prevents undesirable homogeneous reactions, favoring the mineralization of organic compounds.

Recent studies indicate that, under suitable conditions, Catalytic Wet Air Oxidation (CWAO) reactions can benefit if they are carried out in TBRs with ON-OFF liquid flow modulation. Tukac et al. (2003) studied the oxidation of phenol in aqueous solutions on active carbon extruded catalyst in a laboratory TBR with ON-OFF cycling. Liquid flow modulation modified reactor throughput and hydrodynamics through changes in the liquid holdup, wetting efficiency, pressure drop and temperature. For a given set of operating conditions, phenol conversion was found to be 10% higher than that measured at steady state conditions. Optimal results were obtained for a period comparable to the liquid mean residence time in the reactor. This time was estimated from dynamic holdup experiments. The liquid feed cycle period had a strong effect on the dynamic holdup.

Muzen et al. (2005) reported the catalytic oxidation of alcohols over a Pt/ γ -Al₂O₃ (1% w/w) catalyst in a TBR with ON-OFF liquid flow modulation, using ethanol and benzyl alcohol as model reactants. At the different cycling conditions examined, the authors found that cycling can lead to positive and detrimental effects on conversions, depending on the reactant used. Long cycle periods generally have a negative influence on the enhancement in conversion attained by using liquid flow modulation. For certain conditions, the enhancement vs. cycle period curve showed a maximum.

Massa et al. (2005) reported an experimental study of the oxidation of phenol in aqueous solutions over a CuO/ γ -Al₂O₃ catalyst carried out in a Trickle Bed Reactor with

slow ON-OFF cycling. In the range of operating conditions studied, it was observed that liquid flow modulation has a mild effect on phenol conversion but it does affect product distribution, favoring the mineralization process. When the liquid flow was halted, the intermediate products remain inside the catalyst and were further oxidized to final products. The residence time of the intermediates and the average oxygen concentrations inside the catalytic pellet, under liquid flow modulation, were higher than those attained in steady state operation.

I.1.4.3. EXPERIMENTAL HYDRODYNAMICS STUDIES

Important reactor design parameters, like pressure drop, liquid holdup and wetting efficiency, are affected by the external surface coverage of the catalyst or spreading of liquid over the particles. So, if a liquid flow modulation is imposed, these parameters will be different as the liquid flow increases or decreases. The impact of liquid flow modulation on hydrodynamic factors needs to be addressed in detail. So far, only a few contributions accounting for the influence of liquid flow modulation on the hydrodynamics of a TBR have been reported. Furthermore, the effect of non steady state operation on liquid hold-up, mass transfer coefficients and wetting efficiency have not been directly investigated.

Boelhouwer (2001) investigated different liquid flow modulation strategies in TBRs. The reactor column had an inner diameter of 0.11 m. The bed length was 1.20 and 1.04 m, while the packing used was 3 or 6 mm glass spheres, respectively. Ring conductance electrodes were used to measure the instantaneous cross sectionally average liquid holdup.

The author observed that when the usual square wave cycling is applied, continuity shock waves are formed in the column. It was found that the shock waves decay along the column. Hence, the author argues that the decay process limits the frequency of the cycled liquid feed that induces pulsing flow to rather low values since, at relatively high frequencies, total collapse of the shock waves occurs.

By the induction of natural pulses inside the shock waves, the integral mass and heat transfer rates during the liquid flush is improved. This strategy is called the slow mode of liquid-induced pulsing flow. It appears as an optimized mode of periodic operation, since shorter flushes can therefore be applied.

The fast mode of liquid-induced pulsing flow is considered by Boelhouwer (2001) as an extension of natural pulsing flow. The author suggests that this feed mode of operation is the only fast mode of cycling possible since pulses are stable. An additional advantage of liquid-induced pulsing flow is the possibility of tuning the pulse frequency. For natural and liquid-induced pulsing flow, the relationship between the gas flow rate and the available length for pulse formation is identical.

Borremans et al. (2004) studied the influence of cycling on the liquid distribution in a packed column (I.D. 30 cm) by means of a liquid collector divided in nine compartments and four local heat transfer probes. The 0.3-m-diameter column was packed with 3-mm glass beds up to a total height of 1.3 m. For cycle periods between 20 and 40 s and symmetrical splits, periodic operation at high frequencies was not found to improve significantly the liquid distribution through the bed.

The liquid distribution under natural and pulsing flow conditions was also studied by Xiao et al (2001) but modulating the gas flow rate. These authors showed that the radial liquid distribution is more uniform under the forced pulsing flow than in the natural pulsing flow regime. The liquid is distributed fairly uniformly in radial direction, except for a narrow zone adjacent to the column wall. This was attributed to the hydrophobic characteristics of the column wall. The radial distribution improved along the bed.

Giakoumakis et al. (2005) studied ON-OFF liquid flow modulation in a trickle bed reactor for split 0.5 and frequencies from 0.05 to 10Hz. Axial propagation and attenuation of induced pulses were investigated from instantaneous cross sectionally averaged holdup measurements at various locations along the packed bed. The column used had an inner diameter of 0.14 m and 1.24 m height. The packing material was unpolished-glass-spheres of 6 mm diameter. Under the conditions studied and for fixed mean liquid and gas velocities, the time averaged holdup and the pulse celerity, defined as the distance between two probes divided by the time required for the pulse to cross that distance, were found to be practically constant along the bed. Additionally, these authors concluded that pressure drop and time averaged holdups are apparently not affected by the liquid feeding frequency.

Lange et al. (2004) pointed out the need of accurate quantitative information not only about the liquid holdup corresponding to the minimum and maximum liquid velocities used, but for the entire range of periodic operation to successfully model the hydrodynamics of periodically operated TBRs.

Results presented in the literature only cover a narrow range of experimental conditions. To thoroughly understand the hydrodynamic behavior of TBRs under liquid flow modulation, more experimental results would still be required.

I.1.4.4. MODELING STUDIES

In spite of the important amount of information supporting the development of rating rules for cyclic operation of TBRs, an established model accounting for the underlying transient phenomena to thoroughly describe the reactor behavior is still lacking (Khadilkar et al., 2005). Furthermore, many models rely in assumptions that may hide important effects of liquid modulation.

Even if the formulation of a model finally pursues the prediction of a reaction output at the reactor scale, models can also be very important to get further insights in the complex interaction of the underlying phenomena, particularly for such intricate systems. For instance, although thermal effects will be very important in many systems, the large influence of the temperature on the reaction rate will veil the effect of hydrodynamic and mass transport interactions with the reaction system. To better represent the reactor behavior, it is important to completely understand the system. In addition, some applications, such as CWAO of organic pollutants in diluted aqueous solutions may undergo with mild increase in temperature and cycling can still contribute to improve these processes.

The factors governing the reaction rate while cycling the liquid flow present different dynamic responses to the liquid flow perturbation and interactions become quite complex. The behavior of an isothermal particle placed inside a TBR in which liquid flow modulation is imposed, is affected at two different levels: from mass transport and hydrodynamic processes that occur outside the particle and from mass transport, chemical reaction and accumulation that take place inside the particle. The interaction of these effects in an integral TBR is complicated; thus, several authors had presented models considering only some of the events that affect reactor performance. Hydrodynamic processes require to be studied at the reactor level, taking into account the bed as a whole, even using a non-

reacting system. On the other hand, for simplicity, processes occurring in the interior of the particle can be studied within a single particle.

Lange et al. (1999, 2004), Stegasov et al. (1994) and Liu et al. (2005) developed similar models that accounted extensively for hydrodynamic considerations, but simplified the internal phenomena. With this generalization, changes in reaction rate and accumulation inside the particle cannot be evaluated. This approach is difficult to justify because diffusion is important and transients in the particles will be large in the flow interruption mode of operation. Therefore, these models are able only to partially simulate the influence of liquid flow modulation on reactor performance, since they disregard the transient phenomena occurring inside the particles.

A comprehensive model to account for liquid flow modulation in TBRs has been recently proposed by Khadilkar et al. (2005). The model was formulated at the reactor scale and also considers dynamics within the particles with only a few simplifications. The catalyst behavior was represented by a combination of three classes: totally wet particles, totally dry particles and half wet particles. Mass transfer was described using the Maxwell-Stefan approach (Taylor and Krishna, 1993) to represent multicomponent systems frequently appearing in three-phase catalytic reactors and to avoid the usual assumption of equilibrium at the interfaces.

Alternatively, other studies have focused their attention on the internal phenomena occurring in a single particle and considering specific external wetting and mass transport conditions. Boelhouwer (2001) represented the catalyst as a vertical slab containing pores of 10^{-4} m length. Dynamic mass balances were solved considering internal diffusion for the case of wash-coated catalyst particles with an impermeable core. Mass transfer between the dry and wet zones was not considered. The suggested model accounted for mass transport and accumulation inside the pores, but for a particular situation since the egg-shell catalyst assumed has an impermeable core. The model has been applied mainly to simulate fast BASE-PEAK modulation; reactor enhancement was not evaluated. It was found that the rate of internal diffusion largely determines the optimal cycle period.

Dietrich et al. (2005) evaluated three dynamic particle scale models based on different assumptions with respect to intraparticle concentration profiles and a periodically fluctuating external wetting efficiency. The analysis was applied to a BASE-PEAK liquid flow modulation. In the first case, diffusional mass transfer inside the particle is allowed in

both x and y direction, so 2D concentration profiles are calculated. The second case corresponds to the model developed by Boelhouwer (2001). In the third case, intraparticle profiles are neglected and an average concentration is employed. These authors concluded that the extent of mass transfer limitations and the time dependency of the surface wetting are critical to choose an appropriate dynamic model for a partially wetted particle.

A detailed model at the particle scale was proposed by Kouris et al. (1998) to study the behaviour of a catalytic particle within a TBR in the pulsing-flow regime, where regions enriched in gas and liquid rapidly pass through the reactor. Two approaches were considered: (i) a particle completely covered by liquid during the liquid pulse and completely covered by gas during the gas slug; (ii) a particle covered by liquid in the upper section and by gas in the lower section during the liquid pulse, and the reverse during the gas slug. The authors concluded that catalyst performance can be enhanced in the pulsing-flow regime and that the enhancement depends on the pulse frequency. They also found that, as the period tends to zero, the particle is unable to follow the rapid changes in wetting and reaches a pseudo-stationary state. The analyzed results were restricted to conditions characteristics of the natural pulsing flow, which can be assimilated to a fast cyclic operation of a TBR.

Finally, egg-shell type catalysts with non-uniform active phase distribution are used in TBRs with liquid flow modulation. Many models aimed at describing periodic operation of TBRs packed with egg shell catalysts, neglecting the influence of the dynamics within the particle. However, even if a few recent models have started to consider the possibility of reactant storage in the particle, no systematic comparison of the behavior of particles with different active phase distributions under liquid flow modulation is available.

The model developed in this thesis has the purpose of analyzing in a simple but rigorous way the impact of liquid flow modulation on internal particle behavior, without neglecting completely variations in the key hydrodynamic and mass transfer parameters. Additionally, it searches for a mean to judge if trends established to relate the performances of uniform and egg-shell catalysts during steady state are still valid when liquid flow modulation is imposed.

II. MODELING LIQUID FLOW MODULATION AT THE PARTICLE SCALE

The results presented in the previous chapter demonstrate that a comprehensive study of unsteady-state operation of trickle beds over a wide range of parameters and operating conditions is not yet available. But there is agreement on the fact that, under proper conditions, periodic flow interruption can generate higher conversions than those found under steady-state operation. In most contributions, only qualitative explanations of experimental data are presented. On the other hand, models presented in the literature do not interpret exhaustively the complex interactions between external and internal parameters present during cycling.

The aim of this chapter is to develop a dynamic model to represent the events occurring when a porous catalyst particle is exposed to ON-OFF liquid flow modulation. The effect of changing external conditions and intraparticle dynamics is evaluated for a catalyst particle with uniform concentration of active sites.

Although results at the particle scale cannot be compared with experimental outcomes of an integral reactor, this approach is a useful tool to analyze the impact of liquid flow modulation on internal particle behavior. Thus, qualitative trends predicted by the model are compared with experimental results.

II.1. MODEL DEVELOPMENT

A single reaction between a gaseous reactant (A) and a non-volatile liquid reactant (B) within a porous solid catalyst is considered. The active sites are uniformly distributed in the particle. The kinetic is assumed to be first-order with respect to A and zero-order with respect to B. The last assumption can be justified considering that B is in large excess, as in some oxidation and hydrogenation reactions. Besides, this rate expression allows for an easier verification of model results for steady state and cycling operation if no depletion of B occurs. The usefulness and limitations of this kinetic expression have been pointed out by Harold and Ng (1987) for steady state operation and can be extended to our study.

Isothermal conditions are assumed, to focus the analysis on the mass transport and accumulation effects. Non steady state mass balances for the gas and liquid reactants are formulated and solved for a spherical particle. Behavior during ON-OFF operation is described as a square-wave cycling. This hypothesis is valid mainly for intermediate to slow liquid flow modulation. For fast liquid flow modulation, the square-wave assumption may not represent properly the system, as will be discussed II.3.3. Total internal wetting is assumed during the whole cycle period. The catalyst particle can be completely or partially wet during the ON cycle. Once the liquid flow stops, the particle is immediately exposed to the gaseous reactant. This approach is valid if the time required to drain the bed is smaller than the extent of the dry cycle. Then, mass transport resistances are considered negligible. This last assumption is supported by the significantly higher values of mass transfer coefficients in the gas phase (Tan and Smith, 1981), which would mostly determine the external resistances during the dry period of the cycle.

Taking into account these assumptions, dimensional mass balances, boundary and initial conditions are written for both reactants (see Appendix A). Defining convenient dimensionless parameters, the dimensionless differential mass balances for both reactants inside the catalyst become:

$$\frac{\partial \alpha_A}{\partial \tau} = \frac{\partial^2 \alpha_A}{\partial \rho^2} + \frac{2}{\rho} \cdot \frac{\partial \alpha_A}{\partial \rho} + \frac{\cot \theta}{\rho^2} \cdot \frac{\partial \alpha_A}{\partial \theta} + \frac{1}{\rho^2} \cdot \frac{\partial^2 \alpha_A}{\partial \theta^2} - \phi^2 \cdot \alpha_A \cdot H(\alpha_B) \quad (\text{II-1a})$$

$$\frac{\partial \alpha_B}{\partial \tau} = \delta \cdot \left(\frac{\partial^2 \alpha_B}{\partial \rho^2} + \frac{2}{\rho} \cdot \frac{\partial \alpha_B}{\partial \rho} + \frac{\cot \theta}{\rho^2} \cdot \frac{\partial \alpha_B}{\partial \theta} + \frac{1}{\rho^2} \cdot \frac{\partial^2 \alpha_B}{\partial \theta^2} \right) - \phi^2 \cdot \xi \cdot \alpha_A \cdot H(\alpha_B) \quad (\text{II-1b})$$

where $H(\alpha_B)$ is the Heaviside function.

The model is solved in spherical coordinates considering radial and angular variations in the θ direction. Symmetry in the angle Φ is considered. The wetting efficiency, f , is introduced into the model with respect to a critical value of the angle, θ_f , as $2f = 1 - \cos(\theta_f)$ as proposed by Kouris et al. (1998), for a scheme see Appendix A. The relationship assumes that the wetting efficiency represents the fraction of the sphere area covered by liquid and corresponds to the area of the spherical cup.

Initial and boundary conditions postulated for the wet period of the cycling are:

$$\tau = 0 \quad \alpha_i = 1 \quad i = A, B \quad (\text{II-2a})$$

$$\rho = 0 \quad \frac{\partial}{\partial \rho} \alpha_i = \text{finite} \quad \text{if } 0 \leq \theta < \frac{\pi}{2} \text{ and } \frac{\pi}{2} < \theta \leq \pi \quad i = A, B \quad (\text{II-2b})$$

$$\frac{\partial}{\partial \rho} \alpha_i = 0 \quad \text{if } \theta = \frac{\pi}{2} \quad i = A, B \quad (\text{II-2c})$$

$$\rho = 1 \quad \frac{\partial}{\partial \rho} \alpha_A = \text{Bi}_{\text{gl},A} \cdot (1 - \alpha_A) \quad \frac{\partial}{\partial \rho} \alpha_B = \text{Bi}_{\text{ls},B} \cdot (1 - \alpha_B) \quad \text{if } \theta \leq \theta_f \quad (\text{II-2d})$$

$$\alpha_A = 1 \quad \frac{\partial}{\partial \rho} \alpha_B = 0 \quad \text{if } \theta > \theta_f \quad (\text{II-2e})$$

$$\theta = 0 \text{ or } \theta = \pi \quad \frac{\partial}{\partial \theta} \alpha_i = 0 \quad i = A, B \quad (\text{II-2f})$$

where the defined dimensionless parameters are:

$$\rho = \frac{r}{R} \quad \alpha_A = \frac{C_A}{C_A^*} \quad \alpha_B = \frac{C_B}{C_{B0}} \quad \tau = \frac{t \cdot D_A}{\varepsilon_p \cdot R^2} \quad \delta = \frac{D_B}{D_A} \quad \xi = \frac{b C_A^*}{C_{B0}} \quad \phi^2 = \frac{k \cdot R^2}{D_A}$$

$$\text{Bi}_{\text{gl},A} = \frac{\left(\frac{1}{\text{kl}_A \cdot a_{\text{gl}}} + \frac{1}{\text{ks}_A \cdot a_p} \right)^{-1} \cdot R^2}{3 \cdot D_A} \quad \text{Bi}_{\text{ls},B} = \frac{\text{ks}_B \cdot a_p \cdot R^2}{3 \cdot D_B}$$

For the dry period, the boundary conditions are the same, except Eq.(II-2d-e), which become:

$$\rho = 1 \quad \alpha_A = 1 \quad \frac{\partial}{\partial \rho} \alpha_B = 0 \quad \forall \theta \quad (\text{II-2g})$$

Boundary conditions for solving the equations system under steady-state are (II-2b) to (II-2f).

Model is solved by explicit finite differences. Details of the numerical method are presented in Appendix A. Steady state results obtained with the model are in agreement with generally accepted approximations for three-phase systems. Comparisons have been included in Appendix A.

II.1.1. EFFECTIVENESS FACTOR AND ENHANCEMENT DUE TO PERIODIC OPERATION.

Reactants radial and angular profiles can be evaluated with the model for any moment during the cycle. Then, an instantaneous effectiveness factor can be obtained by integrating in the radial and angular directions:

$$\eta_i = \frac{3}{2} \int_0^1 \int_0^{2\pi} \rho^2 \cdot \sin \theta \cdot \alpha_A(\rho, \theta) \cdot H(\alpha_B(\rho, \theta)) \cdot d\rho \cdot d\theta \quad i = \text{mean, w, nw} \quad (\text{II-3})$$

From the instantaneous overall efficiencies during the wet (η_w) and dry (η_{nw}) cycles, a global overall effectiveness factor for the cycle invariant state, η_{cyc} , can be calculated as:

$$\eta_{cyc} = \frac{\int_0^{\tau_w} \eta_w \cdot d\tau + \int_0^{\tau_{nw}} \eta_{nw} \cdot d\tau}{\tau_w + \tau_{nw}} \quad (\text{II-4})$$

where τ_w and τ_{nw} are the times for which the liquid is ON and OFF, respectively.

An enhancement factor (ε) due to periodic operation can thus be defined based on the steady-state overall effectiveness factor evaluated at the mean liquid velocity (η_{mean}) as:

$$\varepsilon = \eta_{\text{cyc}}/\eta_{\text{mean}} \quad (\text{II-5})$$

II.1.2. PARAMETERS EVALUATION

To compare results, the relationship between the liquid velocity for the reference steady state operation ($u_{1,\text{mean}}$) and during the ON cycle of periodic operation ($u_{1,w}$) is taken into account as:

$$u_{1,w} = u_{1,\text{mean}} \cdot (1/s) \quad (\text{II-6})$$

Accordingly, mass transfer coefficients for the wet cycle would depend on the split as:

$$kl_w = kl_{\text{mean}} \cdot (1/s)^{\gamma_1} \quad (\text{II-7a})$$

$$ks_w = ks_{\text{mean}} \cdot (1/s)^{\gamma_2} \quad (\text{II-7b})$$

The exponents, γ_1 and γ_2 , indicate the influence of the liquid velocity on each mass transfer coefficient and their value depend on the flow regime and on the correlation used to estimate them. Considering trickle flow around the particle, the correlation proposed by Goto and Smith (1975) can be used, with $\gamma_1 = 0.41$ and $\gamma_2 = 0.56$.

Correspondingly, the relationship between the wetting efficiency for steady state and during the wet cycle must be established. Taking into account the correlation proposed by Herskowitz (1981) described in Section I.1.1.3, Eq. I-1 developed for steady state operation has been considered:

$$f_w = f_{\text{mean}} + 0.0739 \cdot \ln(1/s) \quad (\text{II-8})$$

The relationship is valid for liquid velocities lower than 0.01 m/s; for larger liquid velocities, complete external wetting can be assumed.

Finally, Table II.1 summarizes the values assigned to the parameters used in the simulations. The range is selected to analyze limit conditions and taking into account those that have been used for experimental investigations reported in the literature (see Table I.2).

Table II.1: Set of conditions used in simulation.

Parameters	Range
P	90 – 1200 s (0.048 – 0.64)
s	0.1 - 1
$Bi_{gl,mean}$	1 - 100
$Bi_{ls,mean}$	1 - 100
f_{mean}	0.4 - 1
ϕ	5 - 20
δ	0.5 - 1
ξ	0.05 - 0.2

II.2. SIMULATED DYNAMIC PROFILES

Lets first analyze the situation in which the particle is completely wet at steady state conditions and during the wet cycle ($f_w = f_{mean} = 1$). Gas and liquid reactant profiles inside the catalyst for the ON and OFF cycles develop with time, as surface conditions are changed. Invariant concentration profiles at the end of ON and OFF cycles are achieved after 10 to 30 cycles, depending on operating conditions. Figure II.1 represents typical gas and liquid reactant profiles for a given set of parameters. During the wet cycle, when both phases flow continuously, the gas reactant concentration at the catalyst surface is lower than the bulk value due to the gas-liquid mass transfer resistance. The internal profile of component A is established quickly in comparison to B, which is in large excess and can accumulate during this period. The liquid-solid mass transfer resistance considered in this

case is small, leading to a liquid reactant concentration at the catalyst surface close to the liquid bulk concentration.

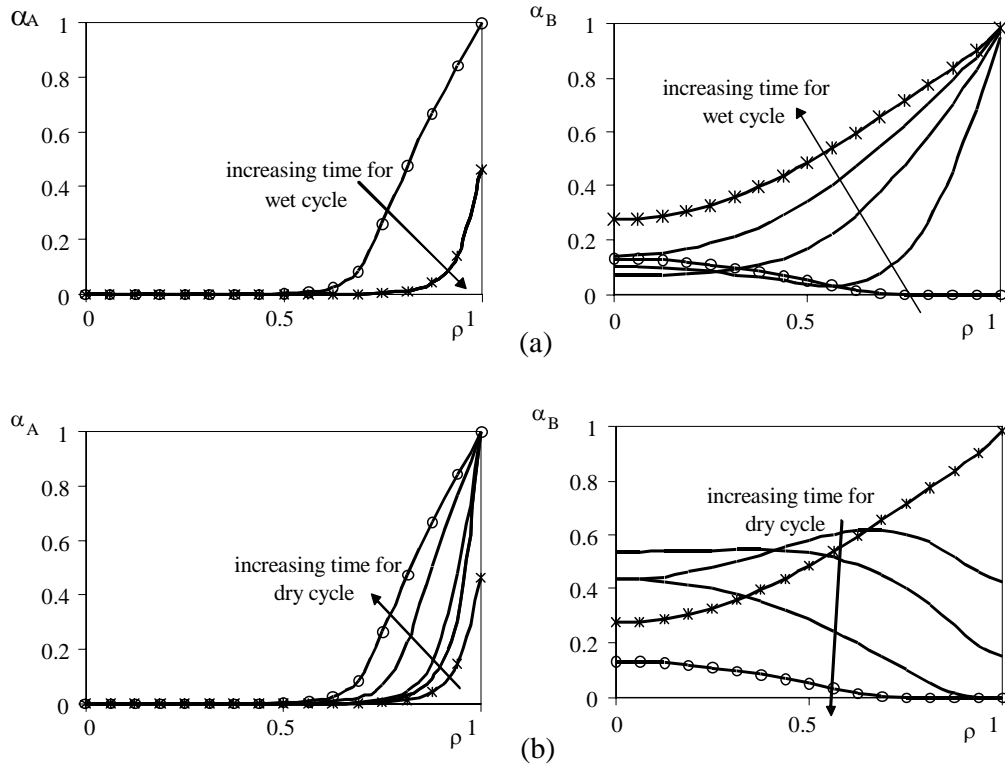


Figure II.1: Time evolution of reactant concentrations inside the catalytic pellet during the (a) wet and (b) dry cycles. Cycle period = 0.64; $s = 0.3$, $\phi = 20$; $Bi_{glS,A, \text{mean}} = 10$; $Bi_{lsB, \text{mean}} = 100$; $\delta = 0.5$; $\xi = 0.05$; $f_{\text{mean}} = f_w = 1$. ($\text{---}\circ\text{---}$) end of dry cycle, ($\text{---}\times\text{---}$) end of wet cycle.

During the dry period of the cycle, the surface concentration of A immediately equals the saturation value. The accumulated liquid reactant B, which is not fed during this period, starts to be thoroughly consumed at a higher rate in the outer layer of the catalyst. An inversion in the radial profile of B occurs. If the dry period is long, a risk of complete consumption of B at certain regions of the catalyst exists. This situation is appreciated in Figure II.1b, where concentration of B has reached values close to zero for $\rho > 0.8$ at the

end of the dry period. When B is completely consumed in the outer layer, A can penetrate further inside the catalyst. For an even lower split, B could be totally consumed in the whole particle and the reaction will stop during the dry period. The gaseous reactant will then reach high concentrations still in the center of the catalyst at the end of the dry cycle. As expected, calculated dynamic concentration profiles are less steep for smaller values of ϕ (not shown).

From reactant profiles, mean liquid reactant concentrations were obtained and instantaneous overall effectiveness factors were calculated as indicated in Eq. II-3. Their cyclic time evolutions during two complete cycles are shown in Figure II.2, for different cycling parameters.

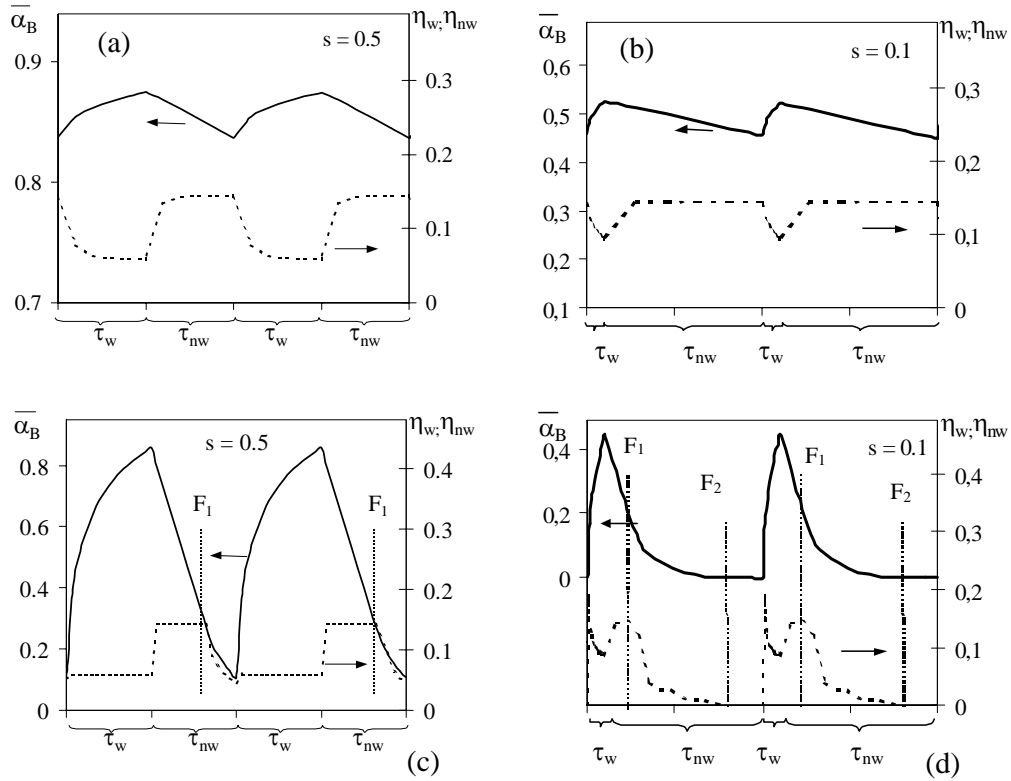


Figure II.2: Time evolution of the mean liquid reactant concentration within the catalyst and of the overall effectiveness factor during the wet and dry cycles. $\phi=20$; $Bi_{glA, \text{mean}}=10$; $Bi_{lsB, \text{mean}}=100$; $\delta=0.5$; $\xi=0.05$; $f_{\text{mean}}=f_w=1$; (a) Cycle period = 0.064, $s=0.5$; (b) Cycle period = 0.064, $s=0.1$; (c) Cycle period = 0.64, $s=0.5$; (d) Cycle period = 0.64, $s=0.1$

For intermediate cycle periods, in the order of a hundred seconds, variations of the mean liquid reactant concentration inside the catalyst are mild (Figures II.2 a-b). Its concentration is quite larger than the concentration of A ($\xi=0.05$), and a pseudo first order approach successfully represents the situation. When the split is 0.5, the overall effectiveness factor tends to asymptotic values both during the wet and dry cycles (Figure II.2a). There is a transient at the beginning of each cycle that can not be neglected. Its magnitude will depend on mass transport and reaction characteristics. For the particular set of parameters studied in Figure II.2a the transient period lasts less than 30% of τ_w for the wet period. During the dry period, the asymptotic value of η_{nw} is approached faster, in less than 15% of τ_{nw} .

For a lower split (Figure II.2b), the wet period is not long enough to attain a plateau. Also, the mean liquid reactant concentration inside the catalyst is lower due to a very short feeding time of B. However, for the set of parameters considered, starvation of B is still prevented since τ_{nw} is not long enough to consume all B.

Depletion of the liquid reactant is an important issue that arises specially for the case of strong internal mass transport limitations and prolonged dry periods. Therefore, Figures II.2c-d illustrate the time evolution of the effectiveness factor and the mean liquid reactant concentration inside the catalyst for a prolonged cycle period. Partial consumption of B can be attained (Figure II.2c) and complete depletion is observed for split 0.1 (Figure II.2d).

As liquid reactant depletion starts at the outer surface of the catalyst and proceeds toward the catalyst interior, two particular times can be observed:

- 1) The instant at which the liquid reactant concentration at the catalyst surface becomes zero; *i.e.*, partial depletion of B.
- 2) The instant when the liquid reactant concentration becomes zero in the whole particle; *i.e.*, complete depletion of B.

The fractions of the dry cycle required to attain both times will be called F_1 and F_2 hereafter. Their values depend on the system and cycling parameters.

The mean concentration of B largely depends on the extension of the wet period. When the dry cycle starts, the mean concentration of B decreases fast, especially until F_1 . Afterwards, the rate of decrease is lower due to a smaller effective volume for reaction. The overall effectiveness factor increases due to the reduction in the external mass transfer

resistance until another pseudo steady state, which ends in F_1 , as shown in Fig II.2c-d. Then, as B is consumed, a progressive decrease of the effectiveness factor is observed, until it finally becomes zero after F_2 (Fig II.2d). For the fraction of the dry cycle after F_2 , no reaction takes place. For this reason, with prolonged cycle periods, experimental enhancement factors lower than one can be obtained, as reported by Skala and Hanika (2002), Houserová et al. (2002), Massa et al. (2005) and Muzen et al (2005).

A comparison of the initial values of η_w (Fig. II.2c and II.2d) indicates that, for the smaller split considered, a transient state is observed in which η_w increases up to a maximum, related to the high initial loading of A inside the particle after a period without reaction. Then, η_w decreases towards the asymptotic value, but it cannot attain it due to the very short τ_w .

II.3. FACTORS AFFECTING THE REACTION OUTPUT

II.3.1. MASS TRANSFER

The influence of mass transport resistances on cycling performance is addressed. Figure II.3 represent the enhancement vs. split obtained varying the magnitudes of the Biot numbers for different Thiele modulus. Cycling effectively enhances reactor performance when internal and external mass transport resistances at steady state operation are considerable.

When external mass transport resistances are considerable, a maximum is observed in the enhancement vs. split curves. The existence of a maximum in the enhancement vs split curve has been found in numerous experimental results (see Table I.2). This maximum is predicted by the model arising from the longer dry cycles for smaller splits. On one side, a longer OFF period improves gaseous reactant access to the particle, increasing reaction rate. However, if the split is too small, total consumption of the liquid reactant will occur, as shown in Figure II.2a. Since reactant consumption is larger for higher Thiele modulus and given Biot numbers, the maximum is shifted to larger split values for larger values of ϕ . Likewise, the maximum will also appear at different splits if the Biots are modified for a

given Thiele modulus. When the external mass transport resistance is negligible, cycling has a poor influence on the enhancement.

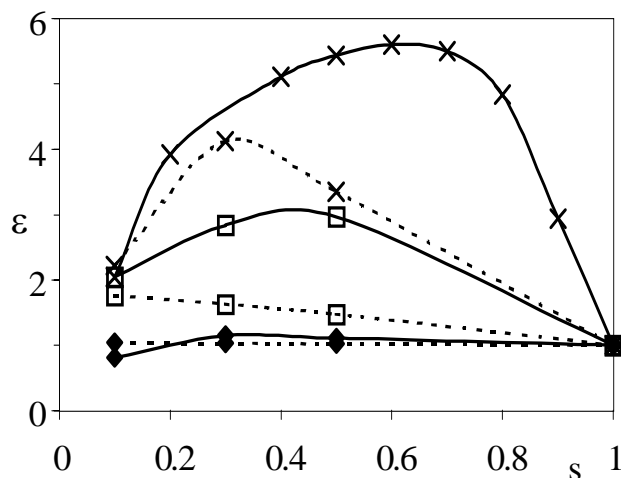


Figure II.3: Influence of the external mass transfer resistance on the enhancement for different Thiele modulus: (—) $\phi = 20$; (---) $\phi = 5$. (\diamond) $Bi_{glA, mean} = 100$; $Bi_{lsB, mean} = 100$; (\square) $Bi_{glA, mean} = 5$; $Bi_{lsB, mean} = 50$; (\times) $Bi_{glA, mean} = 1$; $Bi_{lsB, mean} = 1$; Cycle period = 0.64; $\delta = 0.5$; $\xi = 0.05$; $f_{mean} = f_w = 1$

II.3.2. WETTING EFFICIENCY

Many experimental studies of periodic operation of TBRs have been carried out in laboratory or pilot plant scale units under conditions of incomplete wetting of the catalyst. As discussed in Chapter I, external partial wetting of the catalyst has a strong effect on reaction outcome. Predicted reaction enhancements vs split for different external wetting conditions, determined for intermediate external mass transfer resistances, are presented in Figure II.4 for two values of the Thiele modulus.

When the catalyst is completely wet ($f_w = f_{mean} = 1$), the enhancement achieved while cycling can be considerable, especially at high Thiele modulus. Under steady state operation, the effectiveness factor will be relatively small. During the ON cycle, the higher Biots will result in higher effectiveness factors. In addition, when the liquid is OFF, the

effectiveness factor will also increase. Therefore, provided that B is not thoroughly consumed during the dry cycle, the enhancement achieved during cycling for the complete wetting situation is the highest possible.

Lets analyze the incomplete wetting condition, *i.e.* $f_{\text{mean}} = 0.4$ and f_w given by Eq. II-8. At the reference steady state, a large fraction of the particle is exposed directly to the gas environment, resulting in a relatively high effectiveness factor. During the ON cycle, wetting is larger and the effectiveness factor is lower than the steady state values, despite the increase in Biot numbers. Once the liquid is OFF, the effectiveness factor will increase. However, the enhancement during the OFF cycle will not be as relevant as the one achieved for the complete external wetting situation. Thus, for low values of the wetting efficiency, liquid flow modulation could actually be deleterious, as in the case of $\phi = 20$ (Figure II.4). As expected, when the internal mass transport resistances are reduced, $\phi = 5$, the influence of cycling is attenuated for both values of f_{mean} .

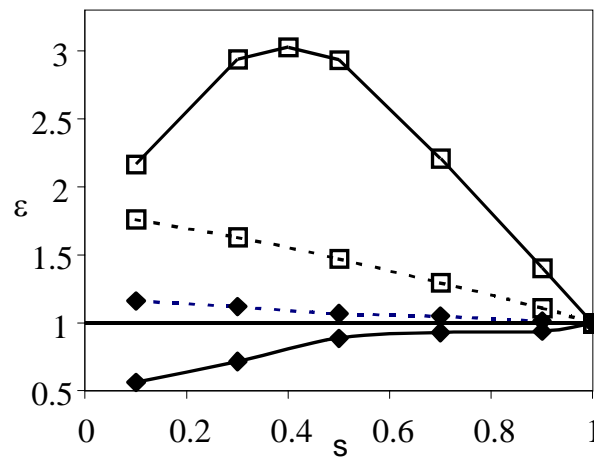


Figure II.4: Effect of wetting conditions on the enhancement factor for different Thiele modulus:

(—) $\phi = 20$ and (---) $\phi = 5$. (\square) $f_{\text{mean}} = 1$; (\diamond) $f_{\text{mean}} = 0.4$. Cycle period = 0.64; $\delta = 0.5$; $\xi = 0.05$;

$$Bi_{\text{glsA,mean}} = 5; Bi_{\text{lsB,mean}} = 50$$

II.3.3. RATIO OF REACTANT CONCENTRATION

The influence of the ratio of reactants concentrations, ξ , on the depletion times F_1 and F_2 should be emphasized, since it is particularly relevant for an integral reactor. The value of ξ increases along the reactor due to the conversion of the liquid reactant, and larger values of ξ remarkably decrease the length of the dry cycle required to attain partial or complete depletion of B, as seen in Figure II.5. Therefore, if a high conversion of the liquid reactant is required, for example in the case of catalytic wet oxidation of contaminated water, these characteristic times would be important limits to consider for a cyclic operation strategy.

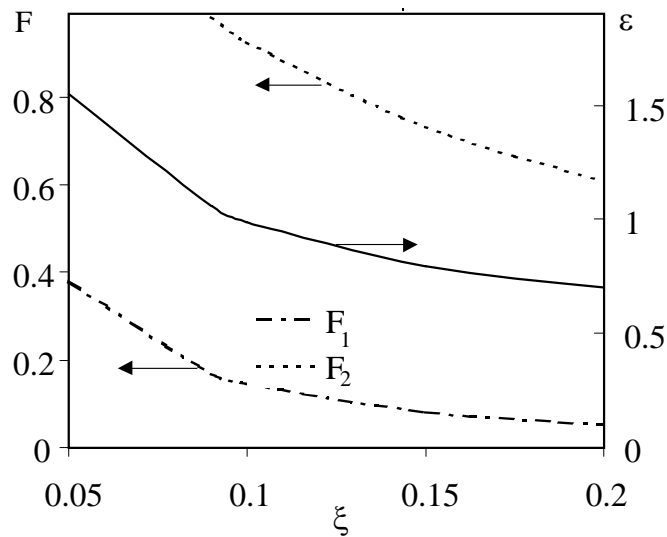


Figure II.5: Effect of the ratio of reactants on the length of the dry cycle required for partial or complete depletion of the liquid reactant inside the catalyst. Influence of ξ on the enhancement. Cycle period = 0.64; $s = 0.5$; $\phi = 20$; $Bi_{glS,A, \text{mean}} = 10$; $Bi_{lsB, \text{mean}} = 100$, $\delta = 0.5$;
 $f_{\text{mean}} = f_w = 1$

Figure II.5 also shows that ϵ decreases as the ratio of reactant concentrations

increases. This is due to the reactant depletion effect, thus an important conclusion can be inferred. For hydrogenation or oxidation processes, where α_A is almost constant along the reactor, an increase in ξ can be assimilated to an increase in conversion of B. Figure II.5 shows that, for a given liquid flow modulation strategy, the enhancement varies along the reactor, as the liquid reactant concentration decreases in the liquid bulk. Hence, to compare different modulation strategies used in an integral trickle bed reactor, initial concentration and conversion levels should be similar. For the same reason, enhancements obtained in a differential reactor will be completely different from those achieved in an integral reactor.

Starvation of the liquid reactant during steady-state has also been reported. Beaudry et al. (1987) and Harold and Ng (1987) were the first ones who introduced the concept of liquid reactant starvation as the reason for differences between model predictions and experiments for a gas-limited reaction in trickle-bed reactors. They argue that this situation is likely to appear for partially wetted catalysts, and would be reflected in an additional mass transfer resistance for the gaseous reactant through the dry area, since it has to cross the inner layer of catalyst without B, for the reaction to take place. Starvation at steady state conditions implies that the reaction is not taking place in the whole catalyst.

With the present model, starvation at steady-state conditions is predicted for the partial wetting situation when mass transfer resistances are harsh. The effect of liquid reactant depletion on the effectiveness factor for a partially wetted catalyst is illustrated in Figure II.6, where the Biot numbers have been set to very low values. The effectiveness factor is represented as a function of the ratio of reactants concentrations, ξ .

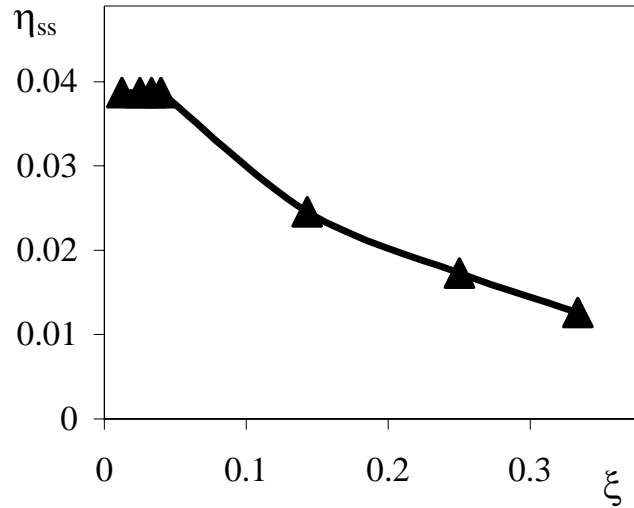


Figure II.6: Influence of the ratio of reactant concentrations on the effectiveness factor attained during steady-state operation. Effect of liquid reactant starvation. $Bi_{glA, mean} = 1$;

$$Bi_{lsB, mean} = 1; \phi = 20; \delta = 0.5; f_{mean} = 0.7$$

During periodic operation, depletion of the liquid reactant appears even at lower ratios of reactant concentrations, as illustrated in Figure II.7 for an intermediate cycle period.

The decrease of the effectiveness factor due to starvation for periodic operation can lead to poor enhancements since the liquid reactant is not fed during the dry cycle. However, as the effectiveness factor for the reference steady-state also diminishes, ε may still be larger than one for certain values of the cycling parameters. This arises from the extremely negative situation of a partially wetted catalyst under steady-state, which is running short of liquid reactant. The liquid velocity at the reference steady-state is lower than during the wet cycle; hence, the surface through which the liquid reactant is fed is smaller. Starvation would imply that there is part of the catalyst that is completely useless for the steady-state process.

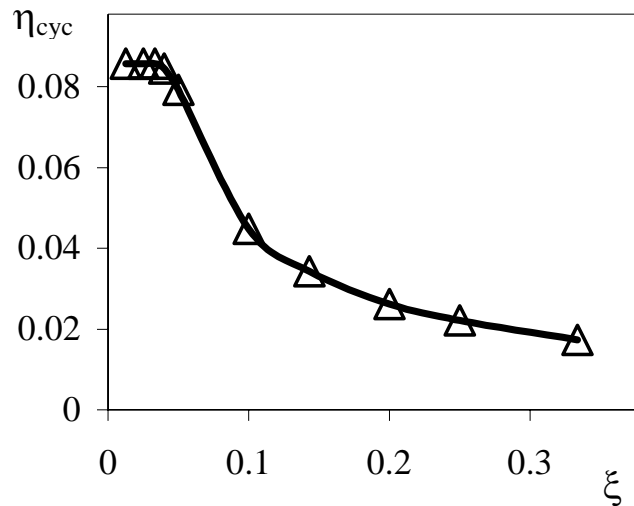


Figure II.7: Influence of the ratio of reactant concentrations on the effectiveness factor attained during periodic operation. Effect of liquid reactant depletion. $Bi_{glsA, mean} = 1$; $Bi_{lsB, mean} = 1$; $\phi = 20$; $\delta = 0.5$; $f_{mean} = 0.7$; Cycle period = 0.16 ; $s = 0.5$

Although periodic operation may have a positive effect even for conditions that lead to liquid reactant shortage, the enhancement factor, calculated from Eq. II.5 decreases as starvation starts, as observed in Figure II.8.

Even if enhancement factors larger than one can be attained for these extreme conditions of very high mass transfer resistances, this conclusion only holds for certain sets of conditions. The enhancement reaches values lower than one for many combinations of cycling parameters, particularly for conditions that leads to high external wetting for the reference steady state and also for very extended dry cycles, in which depletion will likely be severe.

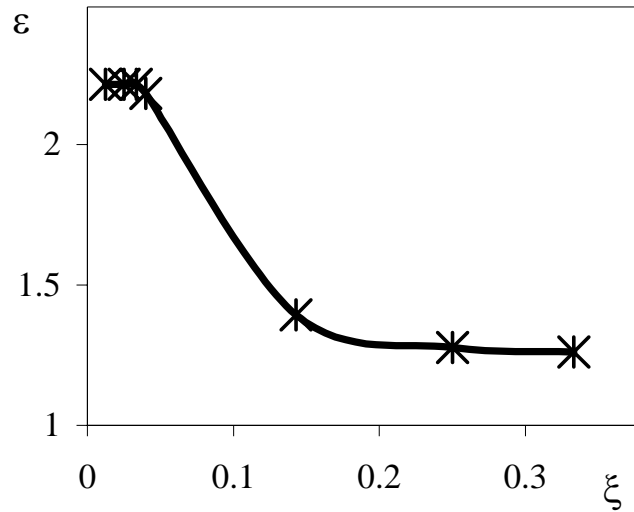


Figure II.8: Influence of the ratio of reactant concentrations on the enhancement attained due to periodic operation for conditions of liquid reactant starvation. $Bi_{glA, mean} = 1$; $Bi_{lsB, mean} = 1$; $\delta = 0.5$; $\phi = 20$; $f_{mean} = 0.7$; Cycle period = 0.16, $s = 0.5$

II.3.4. CYCLING PARAMETERS

As pointed out previously, when the rate-limiting reactant is present in the gas phase, reactor performance improvement over the optimal steady state can be attained when an ON-OFF cycling strategy is used. However, the success of periodic flow interruption depends (among other issues discussed previously) on cycle period and split, as seen in section II.2. The choice of an appropriate set of cycling parameters will largely determine reactor enhancement.

The effect of the cycle period on the predicted enhancement is illustrated in Figure II.9 for conditions typically found in laboratory and bench scale units. For large internal mass transport limitations, three regions may be appreciated, particularly for the lower split. At intermediate to low cycle periods (below 150 seconds; *i.e.*, below 0.08 in dimensionless units), the enhancement decreases as the cycle period increases. This trend is related to the relatively slow dynamics inside the particle. As shown in Figure II.2a, the transients before attaining asymptotic values for η_w and η_{nw} are not symmetrical. They are longer during the

wet period of the cycle. Their effect is more important as the cycle period is reduced. Then, η_{cyc} will approach to the asymptote of the dry cycle as the cycle period tends to zero. Since the wet period is longer for higher splits, the influence of cycle period is larger for this situation.

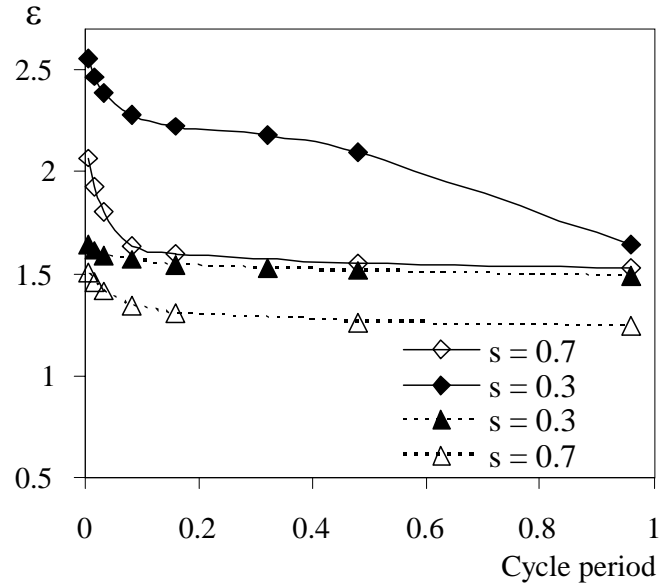


Figure II.9: Influence of the cycle period on the enhancement predicted by the model for different values of splits and incomplete wetting. $f_{\text{mean}} = 0.7$; $\delta = 0.5$; $\xi = 0.05$; $Bi_{\text{glsA, mean}} = 5$; $Bi_{\text{lsB, mean}} = 50$; Thiele modulus: (—) $\phi = 20$ and (---) $\phi = 5$.

When cycle periods are of the order of 150–750 seconds (0.1 – 0.4 in dimensionless units), the influence of the internal dynamics diminishes and the enhancement factor tends to level off at a constant value. For longer cycle periods, the influence of partial and complete depletion of the liquid reactant usually becomes the predominant factor and the enhancement markedly decreases. For a higher split, the effect of liquid reactant depletion appears for longer cycle periods, longer than those shown in the figure. Again, for low values of the Thiele modulus, the effects are less significant.

Many experimental contributions have found a maximum in the enhancement–period curve, even in isothermal or nearly isothermal explorations (Muzen et al., 2005;

Tukac et al., 2003; Khadilkar et al., 1999). Khadilkar et al. (1999) showed that reactor performance enhancement due to periodic operation for hydrogenation of diluted α -methyl styrene presented the highest value at cycle periods around a hundred seconds.

The present model does not predict a maximum in the enhancement vs. period curve. In fact, the predicted enhancement factor increases as the cycle period tends to zero, in agreement with other models found in the literature (Boelhouwer, 2001; Kouris et al., 1998). This fact arises from the prompt response of the system to a sharp decrease in external mass transfer resistance during the dry period, and a slower dynamic response to the increase in mass transfer resistance during the wet period.

At very short periods, the time required to drain the bed would be certainly greater than the extent of the dry cycle and the square-wave assumption used to estimate the liquid velocity and all the key parameters will not be efficient any more to represent the actual situation. Under such conditions, hydrodynamics and its interaction with external mass transport will affect markedly reactor performance.

II.3. PREDICTION OF EXPERIMENTAL TRENDS FOR CWAO

Simulation results obtained with the model are able to represent the events occurring at the particle scale, but cannot be strictly compared with experimental outcomes of an integral reactor. At this stage of modeling, the aim is mainly to interpret the interactions among the different factors affecting the behavior of a catalytic particle within a TBR subjected to liquid flow modulation. Therefore, the results can only be compared qualitatively to reported experimental results determined in integral TBRs. It helps identifying general tendencies for a periodically operated TBR.

In this section, the model is used to predict possible outcomes of a catalytic reaction considering particular experimental conditions corresponding to experimental investigations of periodic operation of TBRs reported in the literature. Experimental trends observed for intermediate and slow cycling operation are thus interpreted at the particle scale.

Two different reaction systems (representative of CWAO processes) are analyzed. The catalytic oxidation of organic pollutants in diluted aqueous solutions generally proceeds under nearly isothermal conditions. The liquid reactant is in excess since the solubility of

oxygen at low pressures is low; so, the reaction is frequently gas-limited. Recent experimental studies demonstrate that, under certain conditions, cycling can still contribute to improve the performances.

II.3.1. CATALYTIC OXIDATION OF ALCOHOLS

Muzen et al. (2005) investigated the effect of liquid flow modulation on the oxidation of ethanol and benzyl alcohol in aqueous solutions using a Pt/ γ -Al₂O₃ catalyst in a bench scale TBR. The operating conditions are detailed in Table II.2.

Table II.2: Operating conditions (Muzen et al., 2005)

Operating conditions	
Catalyst	Pt/ γ -Al ₂ O ₃
Particle diameter	3.1 mm
Mass of catalyst	0.4 kg
Bed diameter	0.04 m
Bed length	0.7 m
Temperature	70°C
Oxygen pressure	1 atm
Alcohol concentration	0.006 – 0.03 kmol/m ³
Cycle period	90-1800 s
Split	1/3, 1/2 and 2/3
Mean superficial liquid velocity	0.036 cm/s
Superficial gas velocity	3.3 cm/s

Actual experimental conditions employed for the oxidation of benzyl alcohol have been used for solving the model (see Table II.3) since some kinetic information was available and the reaction system fits better the model assumptions. The Thiele modulus

was determined using the kinetic constant calculated from experiments in a semibatch reactor and an estimated value for the effective diffusivity. The correlations of Goto et al. (1975) (see Sections I.1.2.1 and I.1.2.2) were employed to estimate overall volumetric gas-liquid and liquid-solid mass transfer coefficients. The wetting efficiencies were calculated according to the correlation of Herskowitz (1981) (Section I.1.1.3). Then, estimated wetting efficiencies are $f_{\text{mean}} = 0.7$ for $u_{l,\text{mean}} = 0.036$ cm/s and, considering the variations in liquid mass velocity for split 2/3 and 1/3, $f_w = 0.73$ and 0.78, respectively, during the ON cycle.

Table II.3: Set of conditions used in simulations.

Parameters	Range
$Bi_{\text{gl},\text{mean}}$	4.7
$Bi_{\text{ls},\text{mean}}$	36.5
f_{mean}	0.7
ϕ	6.5
δ	0.43
ξ	0.029

Time dependent behavior

Figure II.10 illustrates predicted instantaneous effectiveness factors for split 2/3 and different cycle periods. The effectiveness factor for the mean liquid velocity is also shown for comparison. In addition, the instantaneous mean concentration of the liquid reactant inside the catalyst is shown.

According to the model, the effectiveness factor tends to a value close to the one attained at steady state conditions during the wet period. This result arises from the combined effect of larger Biot numbers, which contribute positively to effectiveness factor during the wet period (η_w) counteracted by the negative influence of a slightly higher wetting efficiency, compared to the value for the mean liquid velocity; for example, $\eta_{\text{mean}} = 0.230$ and $\eta_w = 0.231$.

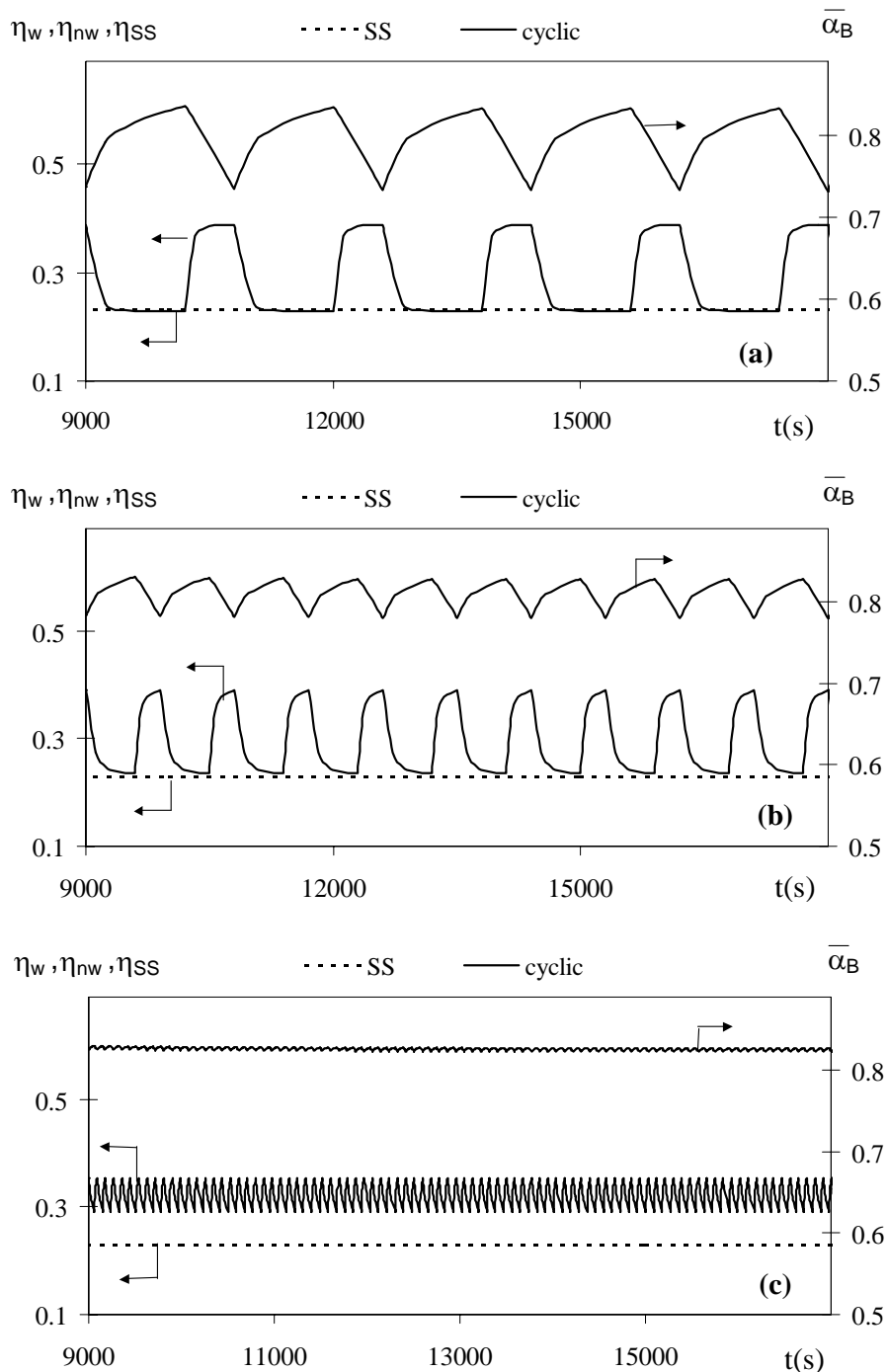


Figure II.10. Influence of the cycling strategy on the predicted instantaneous effectiveness factor and mean liquid reactant concentration inside the particle for the CWO of benzyl alcohol. Comparison with steady state behavior. Split = 2/3; for other parameters see Table II.3. (a) Cycle period = 0.96 (1800 s); (b) Cycle period = 0.48 (900 s); (c) Cycle period = 0.048 s (90 s).

The effectiveness factor during the dry cycle (η_{nw}) tends to the value characteristic of a completely dry particle and is responsible for the increase in the overall reaction rate. The mean liquid reactant concentration in the catalyst will finally determine the variations in the bulk concentrations in the integral reactor. The appearance of a sharp minimum in liquid reactant concentration at the end of the dry period anticipates a peak in conversion when the liquid starts to drain from the reactor after the dry cycle, as observed in the experimental work of Muzen et al, (2005). The shift in time naturally depends on the liquid flow rate and on the dynamics of the draining.

Mean liquid reactant concentration and effectiveness factor curves change their shape as the cycle period is decreased (Figures II.10b-c). This trend was also experimentally found by Muzen et al. (2005).

The mean liquid reactant concentration varies within a smaller range due to a shorter dry period that prevents liquid reactant large consumption. The effectiveness factor vs cycle period curve does not resemble any more a square wave as for the longer cycle periods (Figure II.10a). In contrast, it becomes saw-teeth like, generally tending to an upper limit for higher frequencies, and leading to larger improvements. When the cycle period is set to 90s (Figure II.10c), the effectiveness factor variations are reduced and the mean liquid reactant concentration tends to a constant value. The model predicts a “pseudo” steady state at a level different from the one at the mean liquid velocity.

The comparison between model and experimental trends leads to important conclusions. On one side, dynamics of mass transfer and reaction inside the particle clearly has a decisive effect on the system behavior for slow ON-OFF liquid flow modulation. For short cycle periods, hydrodynamic effects will be critical in the temporal variations of the governing parameters.

Time average behavior

Enhancements predicted by the model are evaluated. As observed, a negative trend in the enhancement vs. cycle period relation is found for the examined splits (1/3 and 2/3), but it is more pronounced for the larger one. Similar trends have been found in the experiments at moderate cycle periods for which other factors, not considered in the model,

would have negligible influence. The model nicely illustrates the subtle influence of mass-transfer dynamics on enhancement and how it is affected by different cycling parameters (Figure II.11). However, it fails to consider the effect of total depletion of the liquid reactant in this case, since it was applied for initial conditions with a large ratio of liquid to gas reactant concentrations.

In addition, as discussed for section II.3.4, the square-wave assumption generally accepted for describing variations in parameters for the cyclic operation, would not be valid for short cycle periods. Hence, the model does not predict the appearance of a maximum in the enhancement vs. cycle period curve observed in the experiments.

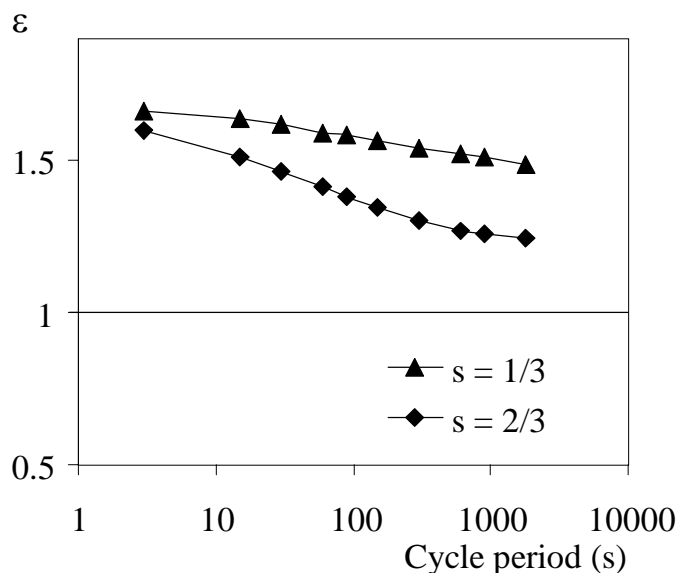


Figure 11. Estimated enhancement, predicted by the model, for the CWO of benzyl alcohol at the particle scale in a periodically operated TBR. $u_{l,\text{mean}} = 0.036$ cm/s; for other parameters see Table II.3.

II.3.2. CATALYTIC PHENOL OXIDATION

Massa et al. (2005) carried out the oxidation of phenol in aqueous solutions over a

CuO/ γ -Al₂O₃ catalyst in a laboratory scale Trickle Bed Reactor under steady state as well as periodic ON-OFF operation. The operating conditions are listed in Table II.4.

Table II.4: Operating conditions (Massa et al., 2005)

Operating conditions	
Catalyst	CuO/ γ -Al ₂ O ₃
Equivalent particle diameter	2.6 mm
Sphericity factor	0.87
Mass of catalyst	0.015 kg
Bed diameter	0.021 m
Bed length	0.07 m
Temperature	140°C
Oxygen pressure	7 atm
Phenol concentration	0.054 kmol/m ³
Superficial gas velocity	2.2 cm/s
Cycle period	3, 6 and 9 min
Split	1/6, 1/3, and 1/2
Mean superficial liquid velocity	0.005 cm/s
Superficial gas velocity	2.2 cm/s

Intraparticle gradients were evaluated by means of the Weisz modulus, ϕ_{we} , using the observed rates obtained at different liquid flow rates. In all the experiments, $\phi_{we} \gg 1$, which indicates that internal mass transport limitations are significant. The criterion proposed by Khadilkar et al. (1996) to determine the limiting reactant (see Section I.1.3.1) leads to the conclusion that the reaction was gas limited, $\gamma = 15 \gg 1$, calculated according to Eq.I-4. Additionally, the Mears' criterion for external mass transport control indicates that this resistance is also significant (Fogler, 1992). So, for these pellets, internal and/or external oxygen mass transport steps could be restrictive. The small liquid velocities employed in the study complicate the evaluation of the steady state Biot numbers through

available correlations, generally postulated for higher fluid velocities. Wetting efficiency was evaluated using the correlation developed by Larachi et al. (2001). This correlation predicts $f_{\text{mean}} = 0.17$. The values of δ and ξ under these operating conditions are 0.22 and 0.014, respectively.

Even though, the conditions examined in the model proposed may not entirely apply to the reaction system described in Massa et al. (2005), the model is useful to predict trends. The very small wetting efficiency and the relatively small effective diffusivity of the liquid reactant promote partial phenol depletion inside the catalyst. Hence, for the experimental conditions studied, cycling does not improve phenol conversion at large cycle periods and small splits. Only a small enhancement would be expected during cycling for short cycle periods and higher splits; that is, for relatively short dry periods. Predicted trends aided the interpretation of the experimental results of Massa et al. (2005) since the experimental trends found agree entirely with conclusions attained in section II.3.3. Indeed, for a reaction in which the external mass transport is the limiting step, no meaningful improvements with cycling are expected if wetting is rather low at the mean liquid flow rate and additionally, internal mass transport limitations are considerable, as shown in the lower curve of Figure II.4.

III. EXTENSION OF THE MODEL TO CATALYST WITH NON-UNIFORM ACTIVE SITES DISTRIBUTION

Results presented in Chapter II indicate that, under proper conditions, ON-OFF liquid flow modulation enhances the performance of a catalyst particle with a uniform distribution of active sites. Cycling outcomes depend on (but also modify) external and internal mass transfer characteristics. Thus, modification of catalyst properties could affect particle behavior while cycling. If the particle has a uniform distribution of active sites, changes in catalytic characteristics are properly represented by the Thiele modulus, as shown previously. When the distribution of active sites is not uniform, internal dynamics will also depend on the characteristics of the support.

An integrated approach to improve reactor performance should include the joint design of reactor, catalyst and mode of operation.

Hence, the aim of this chapter is to explore the performance of tailored catalysts during ON-OFF liquid flow modulation. More precisely, the behavior of particles in which the active sites are deposited in a thin layer close to the external surface (egg-shell) is deeply analyzed. Different width of active layers and permeable or impermeable cores will be considered in the analysis. Comparison of cycling performances of uniform and egg shell catalysts is presented.

III.1. MODEL DEVELOPMENT

A single reaction between a gaseous reactant (A) and a nonvolatile liquid reactant (B) within a porous solid catalyst is considered. Three catalyst particle configurations, with the same amount of active phase distributed in different reaction volumes, are examined (Figure III.1).

Two kinetic expressions are investigated: first-order with respect to each reactant, i.e. (1,1) and first order with respect to the gaseous reactant i.e.(1,0). Isothermal conditions are assumed, to focus the analysis on the mass transport and accumulation effects. Non

steady state mass balances for the gas and liquid reactants are formulated and solved for a spherical particle.

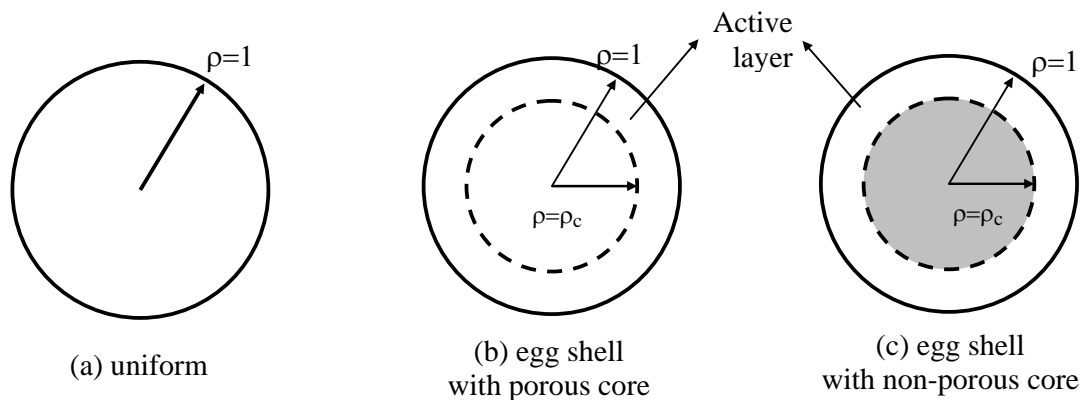


Figure III.1: Schematic indication of catalyst particle configurations.

External behavior during ON-OFF operation is described as a square-wave cycling. This hypothesis is valid mainly for intermediate to slow liquid flow modulation. For fast liquid flow modulation, the square-wave assumption may not represent properly the system, as discussed previously. Total internal wetting is considered during the whole cycle period. Major cycling enhancements are obtained when wetting is complete (as stated in the previous chapter). Therefore, it is assumed that the particle is completely wet at the reference steady state; that is, the steady state at the mean liquid velocity. Therefore, the external surface of the particle is completely wet during the wet cycle. The catalyst is assumed to be completely dry during the OFF cycle. Once the liquid flow stops, the particle is immediately exposed to the gaseous reactant. This approach is valid if the time required to drain the bed is smaller than the extent of the dry cycle. Then, mass transport resistances are considered negligible. This last assumption is supported by the significantly higher values of mass transfer coefficients in the gas phase (Tan and Smith, 1981), which would mostly determine the external resistances during the dry period of the cycle.

Even if these considerations limit the analysis to certain conditions, they strongly simplify the resolution time and many of the qualitative conclusions can be extended to external partial wetting during the wet cycle and steady state.

Taking into account these assumptions, non steady state mass balances for the gas and liquid reactants are formulated and solved for a spherical particle. Then, Eqs. II-1a and II-1b for a completely wetted catalyst particle are simplified as follows:

$$\frac{\partial \alpha_A}{\partial \tau} = \frac{\partial^2 \alpha_A}{\partial \rho^2} + \frac{2}{\rho} \cdot \frac{\partial \alpha_A}{\partial \rho} - \phi^2 \cdot \alpha_A \cdot \alpha_B \quad (\text{III-1a})$$

$$\frac{\partial \alpha_B}{\partial \tau} = \delta \cdot \left(\frac{\partial^2 \alpha_B}{\partial \rho^2} + \frac{2}{\rho} \cdot \frac{\partial \alpha_B}{\partial \rho} \right) - \phi^2 \cdot \xi \cdot \alpha_A \cdot \alpha_B \quad (\text{III-1b})$$

To compare the performance of a catalyst with an active phase uniformly distributed over the whole particle, with results obtained with an egg shell distribution, the following condition is imposed to the kinetic constant:

$$k_{es} = k_{un} \frac{V_{un}}{V_{es}} = k_{un} \cdot \frac{1}{(1 - \rho_c^3)} \quad \text{for } \rho_c \leq \rho \leq 1 \quad (\text{III-2a})$$

$$k_{es} = 0 \quad \text{for } \rho < \rho_c \quad (\text{III-2b})$$

where k_{un} and k_{es} are the kinetic constants for the uniform and egg shell distributions, respectively, and ρ_c is the dimensionless radius of the internal core of the particle without active phase (see Figure III.1). Accordingly, the Thiele modulus is defined as:

$$\phi^2 = \frac{k_{un} \cdot R^2 \cdot C_{B0}}{(1 - \rho_c^3) D_A} = \frac{\phi_{un}^2}{(1 - \rho_c^3)} \quad (\text{III-3a})$$

The catalyst with uniform activity corresponds to the specific case of $\rho_c = 0$.

Two differential equations for the catalyst with uniform activity, four differential equations for the egg shell catalyst with porous core and two differential equations for the egg-shell catalyst with non-porous core should be defined. Equations are solved with appropriate initial and boundary conditions.

Initial conditions are:

$$\tau = 0 \quad \forall \rho \quad \alpha_i = 1 \quad i = A, B \quad (\text{III-4a})$$

Boundary conditions for the wet period of the cycling are:

$$\rho = 1 \quad \frac{\partial}{\partial \rho} \alpha_A = \text{Bi}_{\text{gls},A} \cdot (1 - \alpha_A) \quad \frac{\partial}{\partial \rho} \alpha_B = \text{Bi}_{\text{ls},B} \cdot (1 - \alpha_B) \quad (\text{III-4b})$$

where,

$$\text{Bi}_{\text{gls},A} = \frac{\left(\frac{1}{\text{kl}_A \cdot a_{\text{gl}}} + \frac{1}{\text{ks}_A \cdot a_{\text{p}}} \right)^{-1} \cdot R^2}{3 \cdot D_A} \quad \text{Bi}_{\text{ls},B} = \frac{\text{ks}_B \cdot a_{\text{p}} \cdot R^2}{3 \cdot D_B}$$

Eqs. (III-4a) and (III-4b) are valid for all the catalysts. The following boundary conditions depend on the type of catalyst.

Catalyst with uniform activity:

$$\rho = 0 \quad \frac{\partial}{\partial \rho} \alpha_i = 0 \quad i = A, B \quad (\text{III-4c})$$

Egg shell catalyst with porous core:

$$\rho = 0 \quad \frac{\partial}{\partial \rho} \alpha_i = 0 \quad i = A, B \quad (\text{III-4d})$$

$$\rho = \rho_c \quad \alpha_i \Big|_{\rho_c^-} = \alpha_i \Big|_{\rho_c^+} \quad i = A, B \quad (\text{III-4e})$$

$$\rho = \rho_c \quad \frac{\partial \alpha_i}{\partial \rho} \Big|_{\rho_c^-} = \frac{\partial \alpha_i}{\partial \rho} \Big|_{\rho_c^+} \quad i = A, B \quad (\text{III-4f})$$

Egg shell catalyst with non-porous core:

$$\rho = \rho_c \quad \frac{\partial}{\partial \rho} \alpha_i = 0 \quad i = A, B \quad (\text{III-4g})$$

During the dry cycle, the boundary conditions are the same, except for Eq. (III-4b), which becomes:

$$\rho = 1 \quad \alpha_A = 1 \quad \frac{\partial}{\partial \rho} \alpha_B = 0 \quad (\text{III-4h})$$

The boundary conditions required for solving the model at steady-state are (III.4b) to (III.4g), depending on the catalyst employed.

Model is solved by explicit finite differences. Several discretization strategies were tested to verify convergence of the results. Details are presented in Appendix B.

III.1.1. EFFECTIVENESS FACTOR AND ENHANCEMENT DUE TO PERIODIC OPERATION.

From reactants radial profiles within the catalyst, instantaneous overall effectiveness factors are calculated as:

$$\eta_i = \frac{3 \int_{\rho_c}^1 \rho^2 \cdot \alpha_A \cdot \alpha_B \cdot d\rho}{(1 - \rho_c^3)} \quad i = w, nw, \text{mean} \quad (\text{III-5})$$

where the reference reaction rate, used to calculate overall effectiveness factors, is evaluated taking into account the bulk phase concentrations.

The time-average effectiveness factor (η_{cyc}) and the enhancement factor (ϵ) due to periodic operation are calculated according to Eqs. II-4 and II-5.

When zero-order kinetics with respect to B is assumed, *i.e.* (1,0), α_B is substituted in Eqs. III-1 and III-4, by the Heaviside function, $H(\alpha_B)$. The definition of Thiele modulus becomes:

$$\phi^2 = \frac{k_{un} \cdot R^2}{(1-\rho_c^3)D_A} = \frac{\phi_{un}^2}{(1-\rho_c^3)} \quad (III-6)$$

III.1.2. SIMULATION PARAMETERS

Parameters used in the simulation were evaluated as described in Section II.1.2 and are shown in Table III.1.

Table III.1: Set of conditions used in simulation.

Parameters	Range
P	300 – 3000 s (0.16 –1.60)
s	0.1 - 1
$Bi_{gls,mean}$	5
$Bi_{ls,mean}$	50
f_{mean}	1
ϕ	5 - 50
δ	1
ξ	0.05 –0.5

The range is selected to analyze limit conditions and taking into account those that have been used for experimental investigations reported in the literature. Steady state at the mean liquid velocity, as well as cycling results presented here, were evaluated at complete external wetting conditions ($f_{mean} = f_w = 1$), considering $Bi_{lsB,mean} = 50$ and $Bi_{glsA,mean} = 5$. The influence of these parameters on the behavior of a uniform catalyst particle has been evaluated in Chapter II.

Table III.2 summarizes the catalyst configurations studied here.

Table III.2: Characteristics of catalyst employed in the simulation

Catalyst	Distribution of activity	Active layer width^a	Non-active core
UN	Uniform	100	-
ES10P	egg shell	10	porous
ES1P	egg shell	1	porous
ES10NP	egg shell	10	non-porous
ES1NP	egg shell	1	non-porous

^a(as percentage of particle radius)

III.2. SIMULATED DYNAMIC PROFILES

Reactant concentration profiles inside the particle change with time and with the external conditions imposed. Invariant concentration profiles at the end of the wet and the dry cycles are achieved after 10 to 30 cycles, depending on operating conditions.

For (1,1) kinetic, gas (A) and liquid (B) reactant profiles inside catalysts UN and ES10P are shown in Figures III.2 a-d, at the end of both the wet and dry cycles. Figures III.3 and III.4 show spatial reactant profiles within the particle at the end of wet and dry cycles. These figures illustrate more clearly the concentration curves presented in Figure III.2. In Figure III.2a and c, the evolution of gaseous reactant profiles during the dry cycle is also shown.

For both catalysts during the wet cycle, as seen in Figures III.2a and c, the concentration of A at the catalyst surface is lower than the bulk concentration of A, due to the gas-liquid mass transfer resistance. Since the liquid-solid resistance is small, the liquid reactant concentration at the catalyst surface is close to the liquid bulk concentration.

During the dry cycle, the surface concentration of A equals the saturation value, since external mass transfer resistances become negligible for both catalysts. Reactant A is completely consumed for certain locations in the uniform catalyst, whereas in the egg shell catalyst, A is not depleted. For the egg shell, accumulation of A in the core of the catalyst is observed during the dry cycle. Although the local catalyst activity is increased due to the

higher number of active sites per unit volume, the active shell width is not thick enough to consume A in any point. During the wet cycle, the accumulated A diffuses towards the reaction zone, decreasing its internal concentration but it may not be totally consumed. Larger density of active sites and accumulation of A contribute to the overall reaction rate enhancement during the wet cycle.

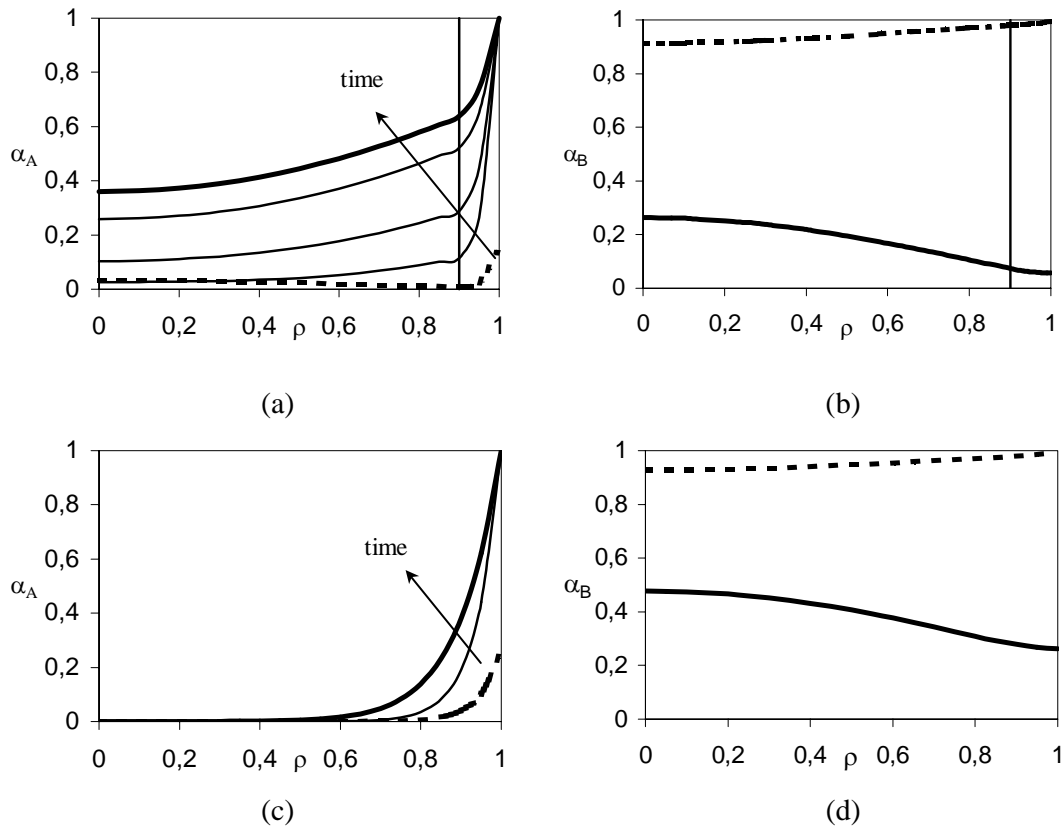


Figure III.2: Reactant concentration profiles during cycling for ES10P (a and b) and UN catalyst (c and d) at the end of wet (---) and dry (—) cycles. (1,1) kinetic. Cycle Period: 0.64; $\phi_{un}=20$; split =0.5; $Bi_{glsA}=5$; $Bi_{lsB}=50$; $\xi=1/20$; $\delta = 1$

The liquid reactant B is not fed during the dry period and it is also consumed more readily at the outer layer of the catalyst due to the higher concentration of A; hence, its

concentration decreases in that direction (Figures III.2b,d and Figure III.4). If the dry cycle is long enough, the concentration of B within the catalyst decreases considerably for certain locations. A region of the catalyst with a small concentration of B diminishes the overall effectiveness factor. Liquid reactant B is consumed more rapidly in the egg shell, due to the higher catalyst activity.

Accumulation processes are clearly visualized. Within both catalysts, the liquid reactant accumulates during the wet cycle. Conversely, the gas reactant accumulates during the dry cycle only for the egg shell catalyst. This fact had a remarkable importance on cycling performance, and will be discussed later.

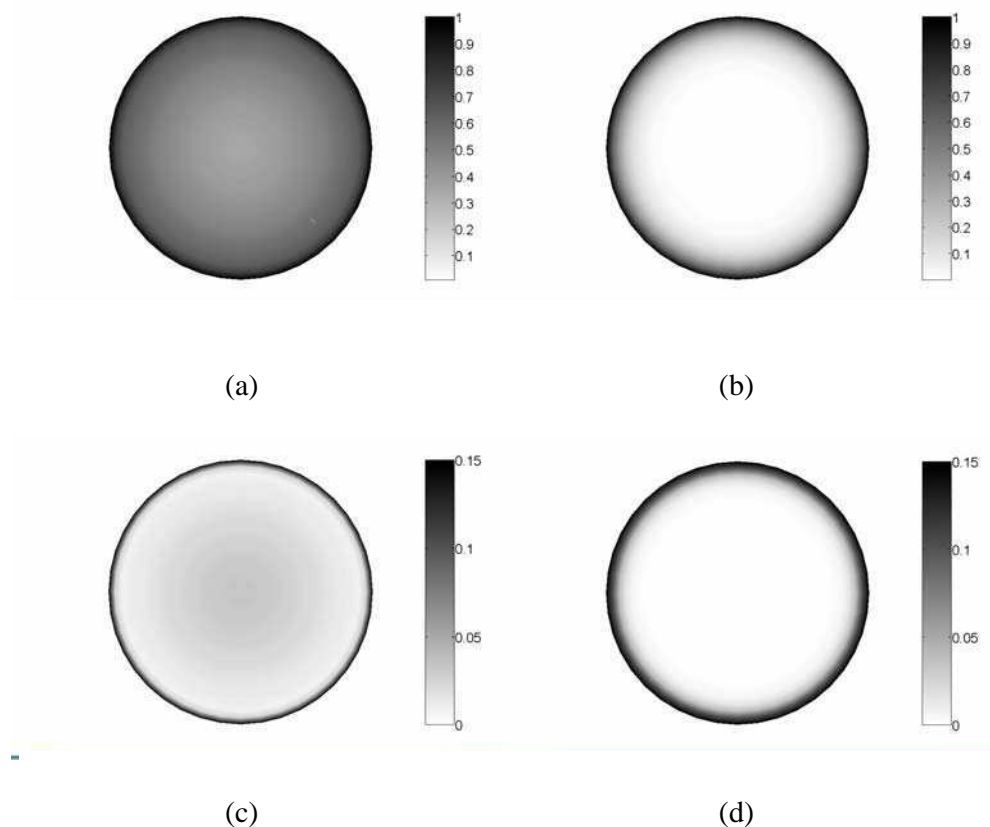


Figure III.3: Gas reactant A profile for the ES10P catalyst at the end of (a) the dry and (c) the wet cycle and for the UN catalyst at the end of (b) the dry and (d) the wet cycle. Conditions in Fig. III.2

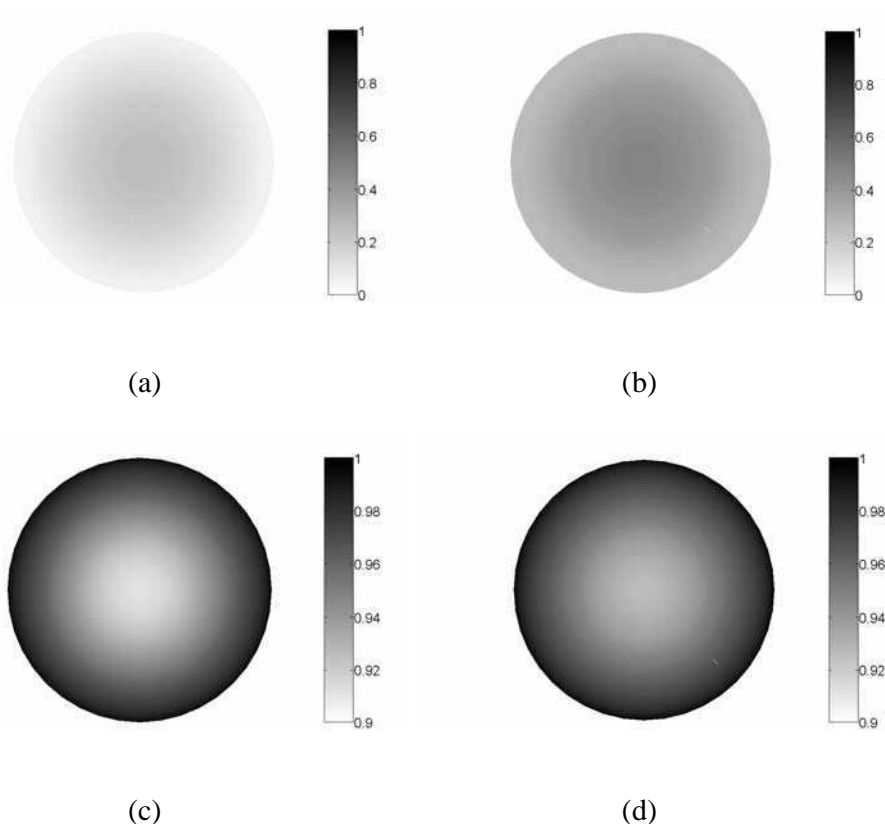


Figure III.4: Liquid reactant B profile for the ES10P catalyst at the end of (a) the dry and (c) the wet cycle and for the UN catalyst at the end of (b) the dry and (d) the wet cycle. Conditions in Fig. III.2

III.3. FACTORS AFFECTING THE REACTION OUTPUT

III.3.1. CYCLING PARAMETERS

The enhancement factor due to periodic operation (ϵ) for both catalysts is shown in Figure III.5a as a function of cycle splits for two different periods and (1,1) kinetic expression. A maximum is always present in the enhancement vs. split curve. This trend has been experimentally observed by several authors (Banchero et al., 2004; Lange et al., 1994; Skala et al., 2002), including those that used egg shell catalysts.

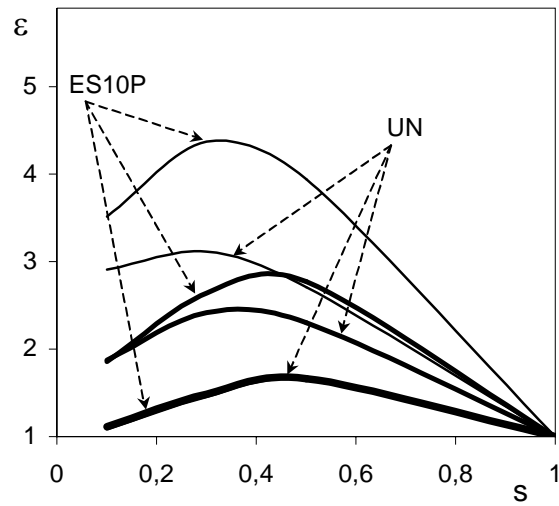
As the split diminishes, the duration of the dry cycle increases, favoring the access of A. However, if the split is small, replenishment of B during the wet cycle will not be

complete, and its concentration inside the particle will be lower. This will decrease the reaction rate and the enhancement will also diminish. The maximum moves toward smaller values as the period is reduced. When the dry period is too long (at higher periods or smaller splits), B concentration inside the particle becomes very small and the reaction rate drops off. Under these conditions enhancement due to cycling may be negligible.

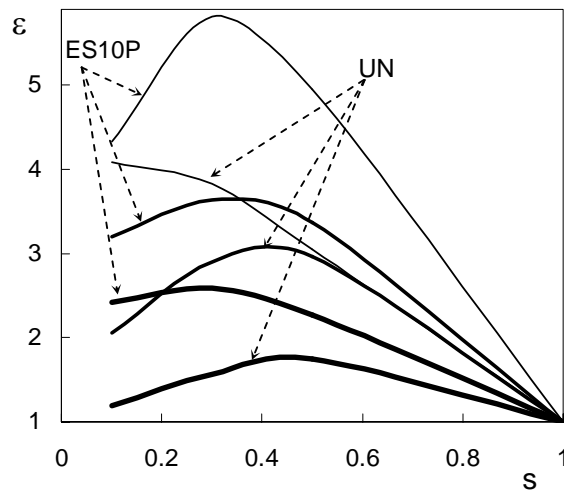
Comparison between both catalysts shows that the predicted enhancement for the egg shell catalyst is generally higher, although this type of configuration has a larger overall effectiveness factor for the reference steady-state. The last is calculated for a similar particle with complete external wetting and external mass transfer that corresponds to a liquid mean velocity, $u_{l,mean} = u_{l,w.s.}$. However, the difference between both catalysts depends on the period and the split.

Liquid flow modulation increases the mass transfer of A to the particle and leads to higher improvements for the egg-shell type catalysts. This may be attributed to the same reasons that induce differences between egg shell and uniform configurations at steady state conditions (Gavriilidis et al., 1993). However, this explanation reflects the results achieved with cycling only if B concentration does not decrease too much during the dry cycle within the reaction zone. This condition is fulfilled for short and intermediate cycle periods and relatively high splits.

For long cycle periods at any split (as indicated in the lower curve of Figure III.5a) or for very small splits, non-uniform and uniform cycling enhancements may be similar. The duration of the dry cycle negatively affects egg shell and uniform performances, but the effect is more pronounced for non-uniform catalysts. In them, during the dry cycle, reactant B slowly diffuses from the catalyst center to the reaction zone. The uniform configuration will have reaction inside the catalyst at relatively large rates, since A penetrates further during the dry period to regions where B is accumulated. The interaction of these two effects explains the curves illustrated in Figure III.5a and the shift in maximum values found for both types of catalysts.



(a) first order with respect to B



(b) zero order with respect to B

Figure III.5: Enhancement factor due to periodic operation (ϵ) vs. split for ES10P and UN catalyst for different cycle periods. (— $P=0.16$, — $P=0.64$, — $P=1.6$). $\phi_{un}=20$; $Bi_{gl,A}=5$; $Bi_{ls,B}=50$; $\xi=0.05$; $\delta = 1$

Comparison of outcomes obtained with different kinetic expressions was also done. Figure III.5b shows results for a reaction that is first order with respect to A and zero order

with respect to B. The curves are similar to those previously described, although variations are steeper because the kinetic does not depend on the liquid reactant concentration, thus the reaction rate does not decrease as B concentration diminishes. Explanations presented in Chapter II for the uniform catalyst are valid. The reaction rate stops only when the concentration of B equals zero, starting at the external border of the particle during the dry cycle. Concepts exposed to explain the results shown in Figure III.5a are valid to understand the curves in Figure III.5b. Comparison between both catalysts shows that, for the conditions examined, the egg shell catalyst presents a higher enhancement and the difference with the uniform catalyst is greater for the reaction that is zero order in B. This is explained taking into account the events occurring during the dry cycle when the concentration of B at the external border is relatively small. Therefore, reaction rate will decrease when the order depends on B, but will remain constant until α_B is zero, for a reaction that is zero order with respect to B.

III.3.2. INTERNAL MASS TRANSFER AND ACCUMULATION EFFECTS

From the discussion presented previously, it becomes clear that internal processes dynamic strongly affects the behavior of a catalytic particle. Hence, it has to be taken into account for modeling liquid flow modulation.

Figures III.6 and III.7 show the enhancement factor evaluated for different Thiele modulus and (1,1) kinetics. Catalyst design is considered by taking into account particles with characteristics presented in Table III.2.

Figure III.6 shows that the enhancement of completely porous catalysts (UN, ES10P and ES1P) increases for higher Thiele modulus, ϕ . Under the conditions studied, this trend is observed regardless of the catalytic site distribution. At smaller values of the Thiele modulus, the enhancement will be lower in any case. The maximum on the enhancement vs. split curve depends on the Thiele modulus (see section II.3.1) and its location moves towards higher splits for larger values of ϕ . Therefore, it can be verified that, for certain combinations of period and split, the tendency observed with Thiele modulus can reverse. For the conditions studied, egg shell catalysts present higher enhancements than uniform

catalysts. Comparison between egg shell catalysts indicates that the better enhancement is obtained for catalyst ES1P, which has the thinner active layer.

Results obtained with egg shell catalysts with non-porous core (ES10NP and ES1NP) are also shown in Figure III.6. These catalysts were used in models for a steady state system (Harold et al., 1987) and for liquid flow modulation (Stegasov et al., 1994).

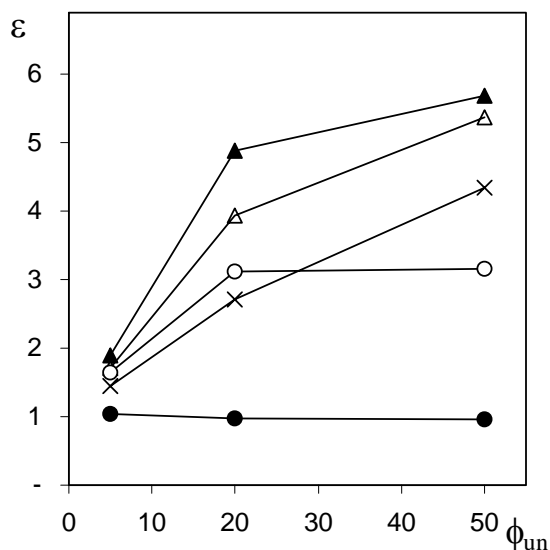


Figure III.6: Enhancement factor due to periodic operation (ϵ) for different catalyst distribution and Thiele modulus. × UN; △ ES10P; ▲ ES1P; ○ ES10NP; ● ES1NP. Cycle Period: 0.5; split = 0.5; $Bi_{gs,A} = 5$; $Bi_{ls,B} = 50$; $\xi = 1/20$; $\delta = 1$.

Performances of egg shell catalysts with porous and non-porous core show a remarkable difference, especially for the catalyst that holds the thinner active layer. When the core is porous, it acts as a reservoir of the liquid reactant and this fact is responsible for the different results observed so far. Between non-porous catalysts, differences arise from the higher storage capacity of the active layer of the ES10NP.

These results emphasize the influence of the inert core porosity of a catalyst, which should be taken into account for catalyst design and modeling of periodic operation. Even if

egg-shell type catalysts with porous and non-porous cores will render similar results for steady state operation, performance will be completely different for periodic operation. Therefore, the porous condition of the inert core should be clearly identified.

Another important factor to consider is the type of liquid flow modulation imposed. For ON-OFF operation (as analyzed here), during the OFF portion of the cycle, B comes exclusively from accumulation in the pores. In BASE-PEAK operation, the access of B from the exterior is reduced during the BASE portion of the cycle, but never runs down (Boelhouwer et al., 2001). Therefore, positive enhancement is likely, even for an egg shell with non-porous core catalysts.

An additional significant conclusion of the results shown in Figure III.6 is related to the modeling of periodic operation in TBRs. A frequent assumption is to ignore the accumulation inside the inert core for egg shell type catalysts. However, if the storage is ignored, the egg shell catalyst will resemble a non-porous core one. The accumulation inside the particle has a remarkable incidence and cannot be ignored when the catalyst is completely porous.

Figure III.7 presents the enhancement obtained with a ratio of reactants concentrations $\xi = 0.5$, while other conditions remain constant. Completely porous catalysts (uniform and egg shell) have similar enhancement values. Only for the higher Thiele modulus investigated, catalyst UN presents a slightly higher performance. As exposed previously, this can be explained by taking into account the storage of B during the wet cycle and its subsequent diffusion and reaction during the dry period. More significant differences are observed with non-porous core catalysts. Enhancement values are smaller than one, particularly for the ES1NP catalyst. In this case, the effectiveness factor at ON-OFF operation is even smaller than the effectiveness factor obtained for UN at steady state operation. Naturally, cycling is not recommended under these conditions.

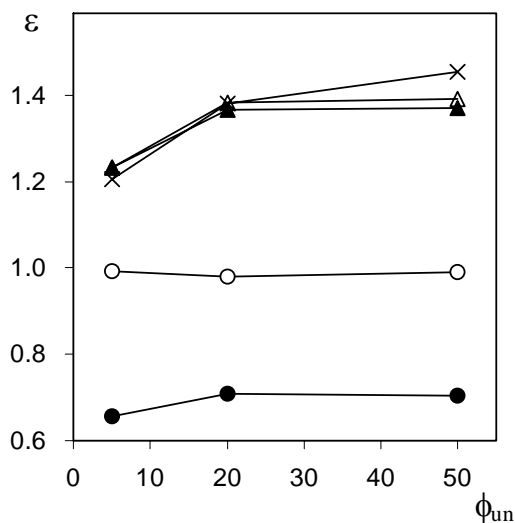


Figure III.7: Enhancement factor due to periodic operation (ε) for different catalyst distribution and different Thiele modulus. \times UN; Δ ES10P; \blacktriangle ES1P; \circ ES10NP; \bullet ES1NP. Cycle Period: 0.5; split = 0.5; $Bi_{gs,A} = 5$; $Bi_{is,B} = 50$; $\xi = 1/2$; $\delta = 1$.

III.3. FINAL REMARKS

Comparison between uniform and egg shell catalysts for steady state two phase systems has been extensively studied (Morbidelli and Varma, 1983). The analysis can be easily extended to three phase systems. For a first order kinetics, Morbidelli and Varma (1983) have presented analytical expressions to evaluate the performance of egg shell catalysts. Their results indicate that the egg shell catalysts will always have a better performance, in comparison with uniform catalysts. However, the ratio of both effectiveness factors obtained depends on the values of Thiele modulus and Biot numbers. For example, when internal and external resistances are large (i.e., Thiele = 50 and Biot = 5) and the egg shell catalyst has a thin active layer (active layer = 0.1 dimensionless), non uniform and uniform effectiveness factors differ slightly (4.8%). So, under these conditions, both catalysts will perform alike. On the other hand, if external resistances are negligible (large Biot numbers), and for Thiele = 50, the difference between effectiveness factor is quite important (94%). So, egg shell catalysts are clearly preferred under such conditions.

Periodic operation improvements are generally related to the temporal reduction of the external mass transport resistances. This may lead to substantial differences between uniform and egg shell catalysts performances during steady state or periodic operation.

Table III.3 compares effectiveness factors predicted by the model for different catalysts during steady state and ON-OFF liquid flow modulation, for a (1,1) kinetic. For steady state operation, egg shell catalysts will perform slightly better than uniform catalysts, especially at higher Thiele modulus, i.e. 20 or 50. However, during liquid flow modulation, the situation changes and egg shell catalysts present an important improvement in comparison with uniform catalysts. These results remark the importance of a simultaneous design of catalysts and type of operation.

Table III.3: Ratio of effectiveness factor between catalyst with egg-shell and uniform activity for steady-state or periodic operation.

Conditions: split = 0.5; $Bi_{ls,B} = 50$; $Bi_{gls,A} = 5$, $\xi = 0.05$

CASE	$\phi_{un} = 5$	$\phi_{un} = 20$	$\phi_{un} = 50$
$\eta_{ES10P} / \eta_{UN} (ss)$	1.2747	1.0760	1.0533
$\eta_{ES10P} / \eta_{UN} (P=0.16)$	1.5044	1.5677	1.2952
$\eta_{ES1P} / \eta_{UN} (ss)$	1.3792	1.651	1.0761
$\eta_{ES1P} / \eta_{UN} (P=0.16)$	1.7988	2.1195	1.4079

IV. HYDRODYNAMICS OF PERIODIC OPERATION IN TBRs.

The time evolution of the liquid holdup at different axial positions in a mini-pilot scale trickle bed reactor is approximately estimated from the response of a set of conductimetric probes that mimic the packing. The probes are located within the system, without disturbing the flow, to get further insights on the influence of modulating the liquid flow rate on the local time variation of the liquid holdup. In addition, by probing at different axial positions, the effect of the bed depth on the response to the imposed modulation can be analyzed.

IV.1. EXPERIMENTAL

A schematic diagram of the experimental installation used is shown in Figure IV.1.

The experimental setup basically consists in an acrylic column of 7 cm inner diameter and a total height of 220 cm. The actual packed bed length is 150 cm. The packing is supported, at the bottom of the column, by a rigid stainless steel screen. Beneath the screen, there is a gas-liquid separator that vents the gas and returns the liquid to a reservoir. The liquid enters the column at the top, through a liquid distributor made in acrylic. The distributor has 18 holes of 1 mm diameter. Gas is provided from a compressor and goes into the column at the top, above the liquid distributor. To mitigate the pressure modulation induced by the compressor, a lung with a pressure regulator and a flow control loop are installed in the gas line.

The liquid is fed from a reservoir with a peristaltic pump controlled by a rotor velocity regulator, which is commanded by a programmable logic controller (PLC). After traversing the column, it is separated from the gas and collected for recirculation. Gas flow rate is measured by a flowmeter and regulated by means of a needle valve.

The column is equipped with six conductimetric probes distributed at different heights (see #1 to #6 in Fig. IV.1). The first probe is located 22.5 cm from the top of the bed; the others are placed downstream, separated 23.5 cm in between. The probes are connected to a multi-channel conductimeter commanded by a personal computer.

Experiments are performed at atmospheric conditions. Air is used as the gas phase and distilled water or a 0.01M KCl aqueous solution, as the liquid phase. The liquid temperature is continuously recorded.

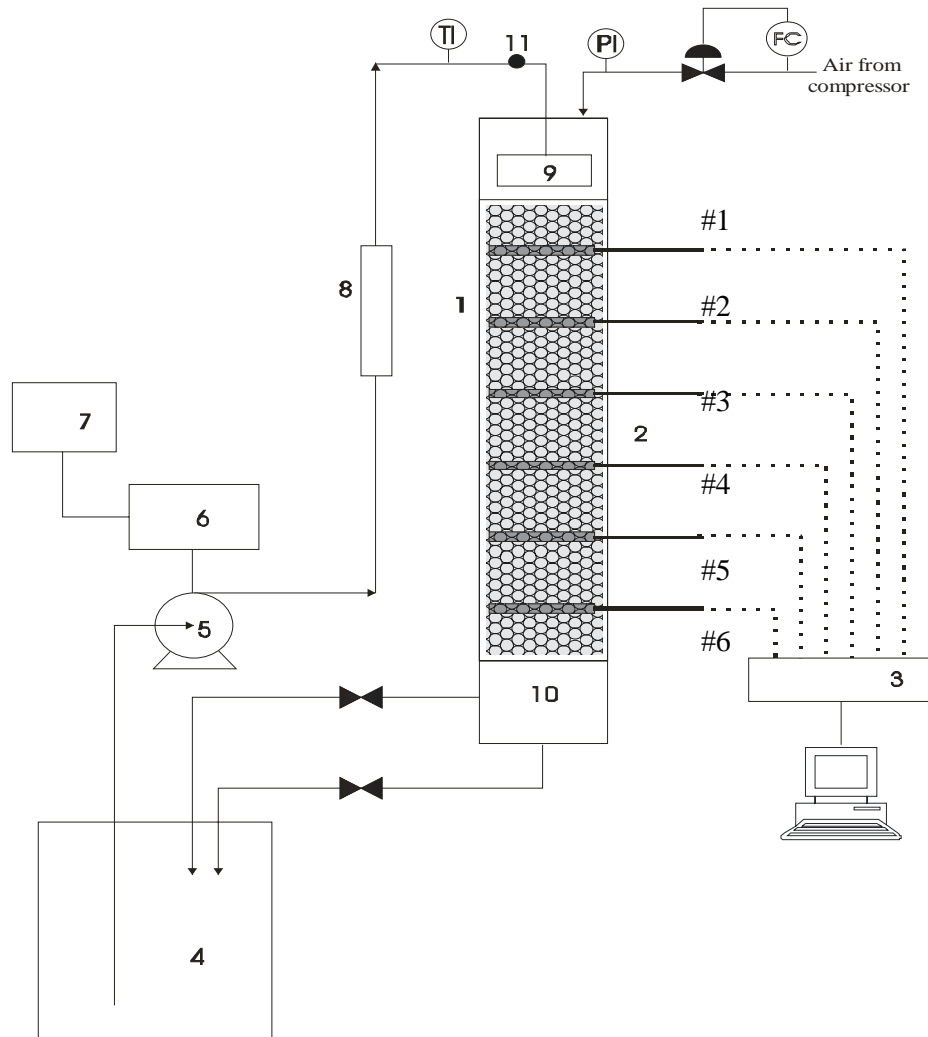


Figure IV.1: Schematic diagram of the experimental setup.

References: 1. Trickle Bed Reactor; 2. Conductimetric probes (#1 – #6); 3. Multichannel conductimeter; 4. Liquid reservoir; 5. Peristaltic pump; 6. Rotor velocity regulator; 7. Programmable Logic Controller; 8. Flowmeter; 9. Liquid distributor; 10. Gas-liquid separator; 11. tracer injection point.

The column is packed with commercial γ -Al₂O₃ spherical particles of 3.1 mm mean diameter. Void fraction of the packed bed is 0.39. Some characteristics of the packing are given in Table IV.1 (Horowitz, 1999). The tube to particle ratio is 22.6, well above the limit suggested in the literature to avoid wall effects; thus, channeling can be assumed negligible (Herskowitz, 2001).

Table IV.1: Characteristic of the packing used in the experiments

Particle	γ -Al ₂ O ₃ spheres (A 2-5 Rhone Poulenc)
Mean particle diameter	3.1 mm
Apparent density	1400 kg/m ³
Specific Area	250 m ² /g

All the experiments are performed under the trickle flow regime. Different gas and liquid velocities are examined, varying the split and the cycle period but always using an ON-OFF liquid flow modulation strategy. Explored operating conditions are listed in Table IV.2.

A detailed list of the explored conditions is given in Appendix C, referring to datafiles included in the enclosed CD.

Before starting the experiments, the column was always flooded with liquid to ensure complete internal wetting of the particles and to achieve reproducible observations. Then, the selected gas flow rate was set after adjusting the liquid flow rate to the one corresponding to the wet period, considering the desired mean liquid velocity, $u_{l,mean}$, and the cycling parameters. Afterwards, liquid flow modulation was imposed.

The liquid flow rate at the top of the column can be described almost as a square wave, since no dead time was noticed. The system was left at the desired cycling strategy during 10-20 minutes to reach an invariant cycling state before acquiring the signals. However, the invariant state was also checked directly from the measurements.

Table IV.2: Examined operating conditions

Temperature	$T = 20^{\circ}\text{C} (+/-2^{\circ}\text{C})$
Pressure	Atmospheric
Liquid density	$\zeta_l = 997 \text{ kg/m}^3$
Gas density	$\zeta_g = 1.2 \text{ kg/m}^3$
Liquid viscosity	$\mu_l = 8.9 \times 10^{-4} \text{ Pa.s}$
Gas viscosity	$\mu_g = 1.8 \times 10^{-5} \text{ Pa.s}$
Surface tension	$\sigma_l = 0.073 \text{ kg/s}^2$
Split	$0.17 < s < 1$
Cycle period	$5 \text{ s} < P < 900 \text{ s}$
Gas velocity	$u_g = 1.4 \text{ cm.s}^{-1} \text{ or } 3.0 \text{ cm.s}^{-1}$
Liquid velocity	$0.15 \text{ cm.s}^{-1} < u_l < 0.89 \text{ cm.s}^{-1}$

IV.1.1. CONDUCTANCE TECHNIQUE

As already mentioned, the column is equipped with six probes to measure the instantaneous conductance induced by the amount of liquid contained between the two electrodes that conform the probes. The actual position of each electrode is shown in Fig. IV.1 and has been described in the previous section. Each probe consists of two *lines* of 14 copper spheres, 4.6 mm diameter, tied with a copper wire (an illustration is shown in Fig. IV.2).

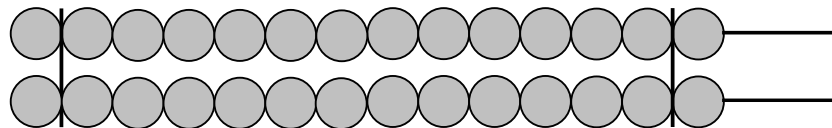


Figure IV.2: Details of the conductimetric probes.

The conductimetric probes are not too rigid, they have been manually located in the column as it was mounted and progressively filled. The separation between the two lines of copper spheres, maintained by two pieces of plastic, allows a few alumina particles to get in between. The responses of the six probes are acquired simultaneously with a sampling frequency of 200Hz using a multi channel conductimeter. The excitation frequency of the conductimeter is 10 KHz, which allows assuming that the signal has negligible capacitance components. The acquisition is prolonged for periods long enough to get at least two complete invariant cycles. For short cycle periods, several complete cycles have been recorded.

The response measured by each probe depends on the conductivity of the media contained within the two lines of tied copper spheres. That conductivity is strongly related to the amount of liquid contained and would therefore provide an approximate way of estimating the liquid holdup of the flowing liquid. Even though the conductance measured would not correspond to the one induced by a cross sectional average of the liquid present at a given height, it results from the average of a significantly long portion, since the total length of each probe is almost the column diameter. Excessive non-uniformities in the liquid distribution would affect the quality of the data.

When the column is flooded, the solid free space between electrodes is filled with the liquid electrolyte used, and the instantaneous conductance measured would follow an expression given by (Levine, 1995; Tzochatzidis et al., 1992):

$$\psi_{i,f} = \gamma_l A/L \tag{IV-1}$$

where γ_l is the conductivity of the liquid and A/L would be the effective cell constant for a given electrode.

When the gas and the liquid are flowing downwards through the bed, the conductance measured by the probes would approximately be given by:

$$\psi_i = \gamma_l \kappa A/L \tag{IV-2}$$

where κ is closely related to the liquid saturation. Actually, it represents a factor to consider the fraction of the cell area effectively wetted by the liquid and forming a gate between electrodes, through which the electrical circuit is closed. Therefore, to become independent of probe geometrical characteristics, and to eliminate errors in conductivity measurements, the instantaneous conductance is normalized with the conductance measured under conditions of flooding (Tzochatzidis et al., 1992) as:

$$\kappa = \frac{\psi_i}{\psi_{i,f}} \quad (\text{IV-3})$$

where ψ_i is the instantaneous conductivity signal and $\psi_{i,f}$ is the signal measured when the column is flooded.

IV.1.2. TRACING TECHNIQUE

The conductivity probes can be employed to measure the liquid holdup by a dynamic method using the stimulus-response technique. Stegmüller (1986) and Cassanello (1992) used similar (though shorter) electrodes to compute RTD curves in a TBR and in a Packed Bubble Column (PBC), respectively, for estimating the liquid axial dispersion and the liquid holdup from stimulus-response experiments. The response to a pulse injection was obtained with two electrodes inserted in the bed at two levels, defining an open-open vessel (Nauman and Buffham, 1983). They proposed flow models and the parameter of the models, *e.g.*, the Peclet number, and the liquid holdup were determined from a fitting in the time domain and from the moments of the curves.

In this case, a similar procedure is followed, a tracer pulse is injected into the fluid that enters the bed, and its concentration is continuously recorded employing the conductance probes inserted in the bed. Then, the Residence Time Distribution (RTD) curves are obtained at six different axial positions along the column. A 0.05M KCl aqueous solution is used as the tracer, while distilled water is circulating. This concentration is sharply reduced by dilution after entering the liquid stream and falls within the range of

linear relation between KCl concentration and conductance. Hence, concentration can be monitored by the conductivity probes. The filenames addressing the whole set of data are detailed in Appendix C.

The signals measured are used directly to get the Residence Time Distribution functions, $E(t)$, assuming that the tracer concentration is already well distributed all over the column section for the probes selected for the calculations. The density function $E(t)$ describes quantitatively the time that different fluid elements spend in the reactor. A pulse input of tracer is used to evaluate the $E(t)$ curve of the system, as follows,

$$E(t) = \frac{C(t)}{\int_0^{\infty} C(t) \cdot dt} = \frac{R(t)}{\int_0^{\infty} R(t) \cdot dt} \quad (\text{IV-4})$$

where $C(t)$ is the time variation of the tracer concentration and $R(t)$, the signal measured by the conductimeter for a given probe. The runs are always continued until all the signals return to the corresponding baseline, to ensure that the outlet tracer concentration is approximately zero.

The mean residence time that the tracer remains in the column is evaluated from the first moment of the RTD function as:

$$\theta_1 = \int_0^{\infty} t \cdot E(t) \cdot dt \quad (\text{IV-5})$$

Since the injection of a perfect pulse is not viable, the tracer concentration can be monitored at two points within the test section, provided the injection point is placed upstream. One of the probes close to the column entrance can be considered as the input and one close to the outlet as the output, defining an open-open vessel.

Figure IV.3 shows typical $E(t)$ curves for each electrode evaluated from the measured tracer concentration. For all liquid flow rates, the RTD curves have a tail that goes below the experimental error within reasonable time, except for very low liquid flow rates where tailing is significant. Hence, experiments at very low liquid velocities are subjected to higher error.

Evaluating $E(t)$ from the signals obtained with electrodes #1 and #6, as the input and the output, respectively, the mean residence time of the liquid within the section in between can be obtained from the difference between the ones calculated for each electrode, since mean residence times are additive (Nauman and Buffham, 1983):

$$\theta_{l_{(\#1-\#6)}} = \theta_{l_{\#6}} - \theta_{l_{\#1}} \quad (\text{IV-6})$$

Then, a mean liquid holdup for the test section can be evaluated from the mean residence time according to:

$$\varepsilon_1 = \frac{\theta_{l_{(\#1-\#6)}} \cdot Q_1}{\pi(D_c/2)^2 l_{(\#1-\#6)}} \quad (\text{IV-7})$$

where Q_1 is the liquid flow rate, D_c is the column diameter and $l_{(\#1-\#6)}$ is the distance between probes #1 and #6.

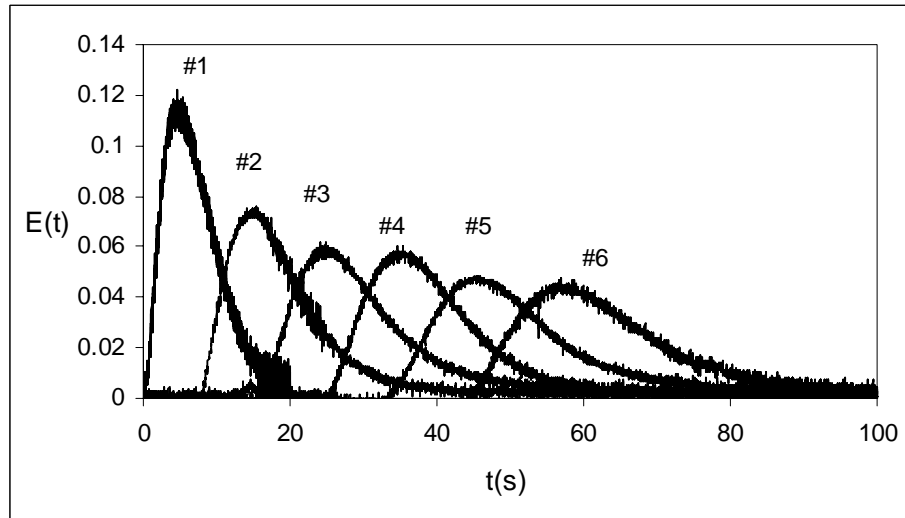


Figure IV.3: Residence time distribution function, $E(t)$, for each electrode.

Operating conditions: $u_l = 0.38$ cm/s; $u_g = 3.0$ cm/s

IV.2. RESULTS

IV.2.1. STEADY STATE EXPERIMENTS

Liquid holdups evaluated from RTD measurements for different sections of the reactor are shown in Figures IV.4. Electrode #1 is always considered as the input, while liquid holdup is evaluated considering the following outputs: #4, #5 and #6, to have a reasonable long test section. Each value is determined at least three times; reproducibility is within $\pm 2\%$. From the results, it arises that the liquid holdup does not vary significantly along the bed, within the range of operating conditions tested. Hence, liquid holdups calculated using the longest test section, between electrodes #1 and #6, are used for the subsequent analyses.

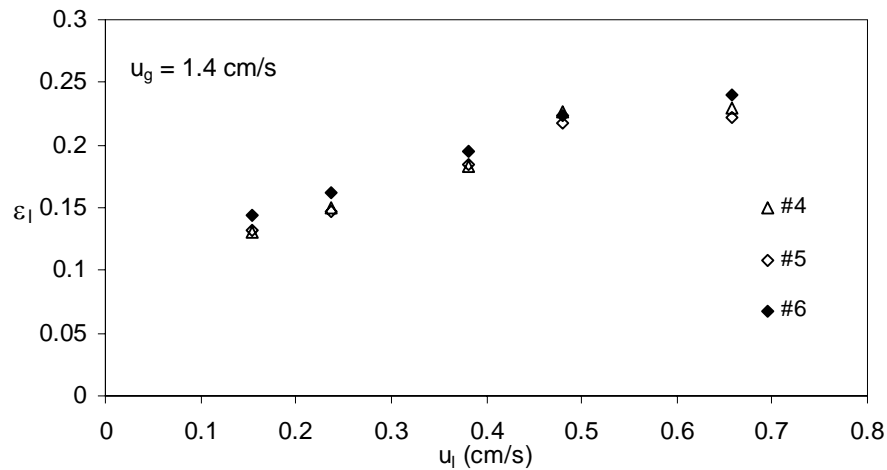


Figure IV.4a: Experimental liquid holdup obtained by tracer experiments as a function of the superficial liquid velocity for different bed lengths. $u_g = 1.4$ cm/s;

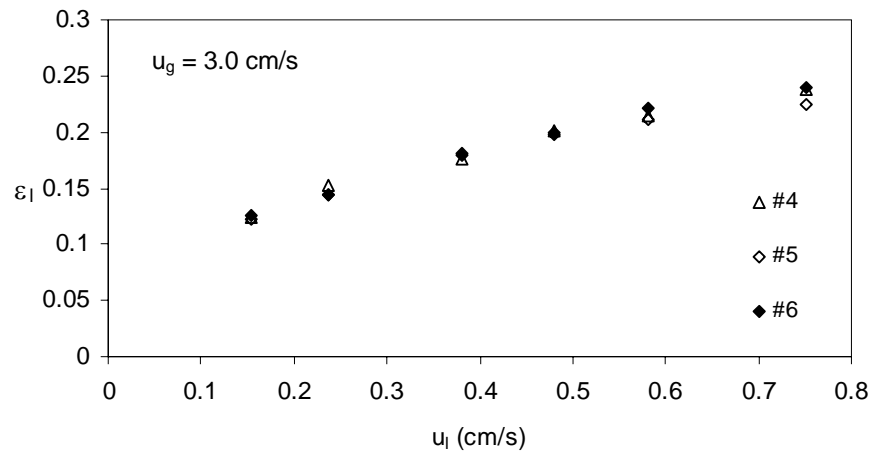


Figure IV.4b: Experimental liquid holdup obtained by tracer experiments as a function of the superficial liquid velocity for different bed lengths. $u_g = 3.0$ cm/s

Measured liquid holdups are represented as a function of the superficial liquid velocity, at different superficial gas velocities, in Figure IV.5. As expected, liquid holdup increases with increasing liquid flow rate, and decreases with increasing gas flow rate.

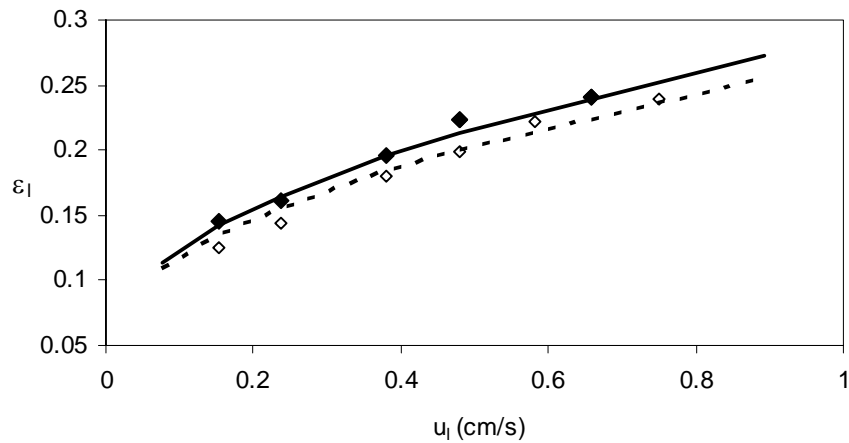


Figure IV.5: Comparison of the liquid holdup determined from the tracer experiments with the proposed fitting equation (Eq. IV-8).

These results fit the following relationship with respect to Re_l and Re_g :

$$\varepsilon_l = \varepsilon_s + 21.68 Re_l^{0.49} Re_g^{-0.10} \quad (IV-8)$$

where ε_s is the static holdup, calculated using the correlation of Saez and Carbonell (1985), which mainly depends on the Eötvös number. For the investigated conditions, $Eö = 1.286$, leading to an estimated static holdup of 0.047. Goodness of fitting is shown in Figure IV.5. The mean absolute relative error is 3% and the standard deviation calculated from experimental and predicted values is 5%.

Results obtained for $u_g = 3.0$ cm/s, and the corresponding fitting equation, are compared to correlations reported in the literature in Figure IV.6.

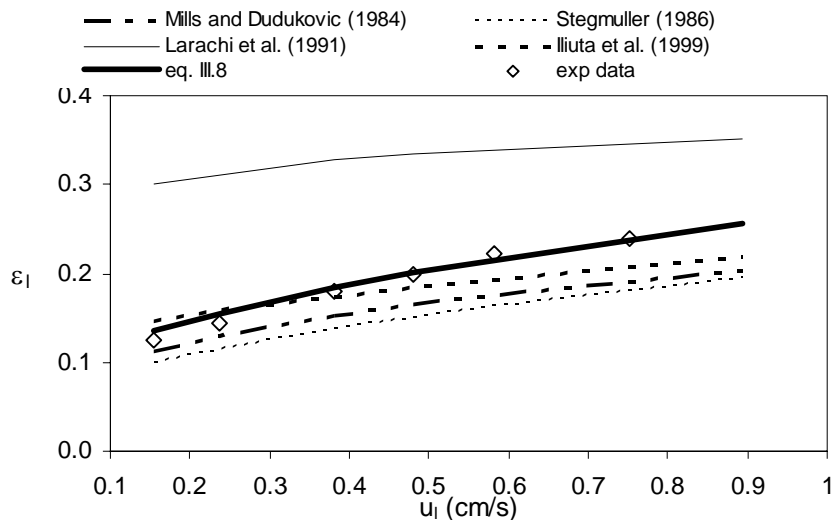


Figure IV.6: Comparison of experimental liquid holdups with those predicted from correlations available in the literature. $u_g = 3.0$ cm/s

Liquid holdup values predicted by the correlations of Larachi et al. (1991) and Lange et al. (1978) (not shown in the figure) are higher than those obtained experimentally in the present work. Stegmüller (1986) proposed a correlation, valid for $u_g = 4.3$ cm/s,

developed from experiments in a column with the same dimensional characteristics as the one used in this work, but packed with 5 mm glass spheres. The influence of liquid velocity predicted by the correlation of Stegmüller (1986) agrees with present results; however, predicted values are smaller. The correlation of Mills and Dudukovic (1984) predicts values slightly larger than those predicted by the correlation of Stegmüller (1986) and a similar trend with the superficial liquid velocity.

The general correlation of Iliuta et al. (1999), developed based on an extensive database of liquid holdup measurements in TBRs taken from the literature by using a combination of Artificial Neural Network and Dimensional Analysis, satisfactorily predicts the obtained results, even if the liquid velocity influence is slightly different.

The experimental data is confronted with the results predicted by the correlation of Iliuta et al. (1999) in Figure IV.7. The mean absolute relative error is 8% and the standard deviation calculated from experimental and predicted values is 5%.

Taking into account that the fit is good and that this correlation was developed based on an extensive database, its ability to extrapolate results for conditions different from those used to get Eq. IV-8 is expected to be better. Then, this general functionality will be considered to estimate liquid holdup values for analyzing results obtained with liquid flow modulation.

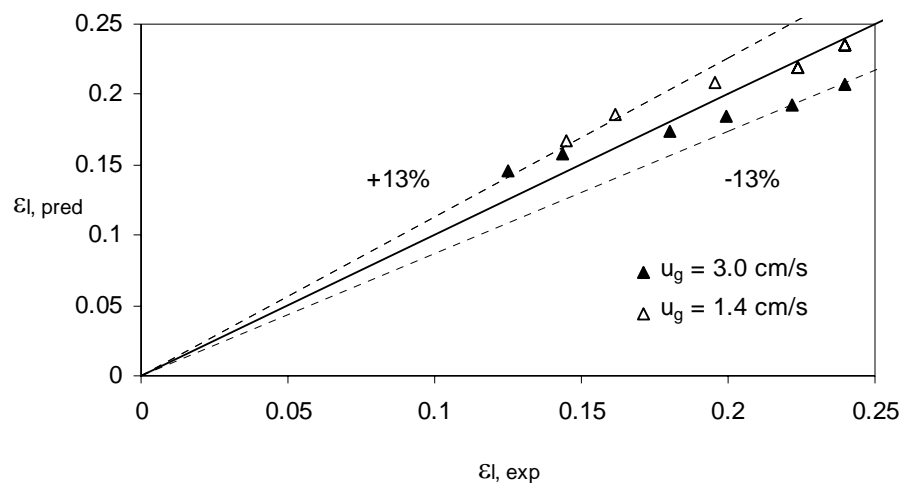


Figure IV.7: Comparison of the liquid holdups obtained from the tracer experiments with those predicted by the correlation of Iliuta et al. (1999).

IV.2.2. CYCLING EXPERIMENTS

Figures IV.8-9 show typical temporal variations of the normalized conductance, κ , determined from the response of the six conductimetric probes located at different heights in the column. The figures illustrate experiments at long cycle periods, particularly those that have long dry cycles, for given experimental gas and liquid mean velocities.

The name of files containing the measurements of the instantaneous conductance, ψ , obtained under steady state and periodic operation are detailed in Appendix C. Files with data under conditions of flooding, required to calculate the values of κ , are also listed. All the data files are included in an enclosed CD.

The liquid flow modulation is reflected in the shape of the curves. The liquid front (the time at which the probe gets in contact to a new wet period of the cycle) is displaced along the column. Even though there are some interactions among the signals, especially at the beginning of each period of the cycle, and instabilities until the liquid films paths are reestablished, the start/stop of the wet cycles induces very sharp variations in the probes responses. Since the liquid fronts are very sharp, the delay time required for the front to move between two different electrodes can be easily determined from the experiments.

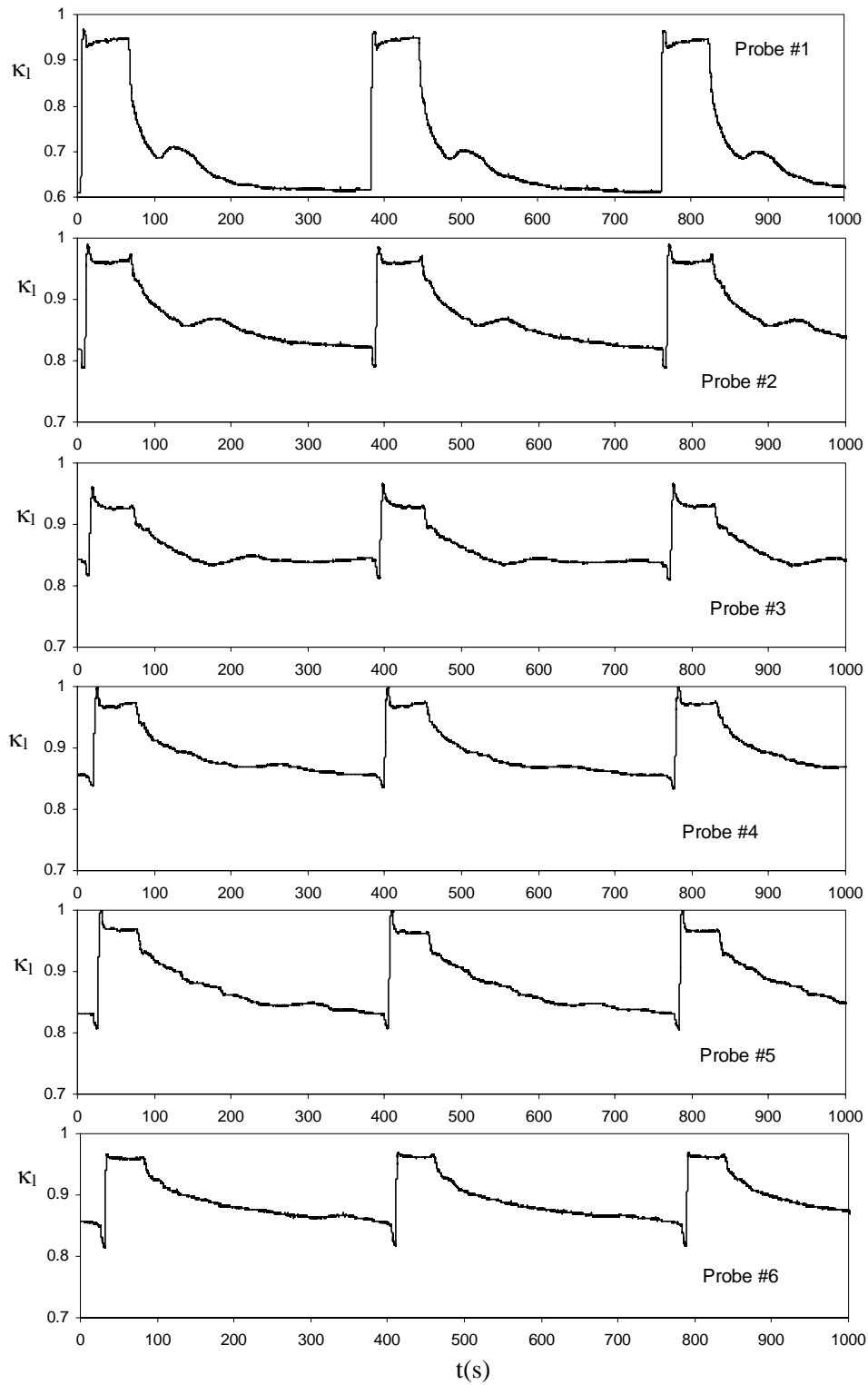


Figure IV.8: Time dependence of the normalized conductivity (κ). Operating conditions:
 $P=360$ s; $s=0.17$; $u_{l,ss}=0.15$ cm/s; $u_g=3.0$ cm/s.

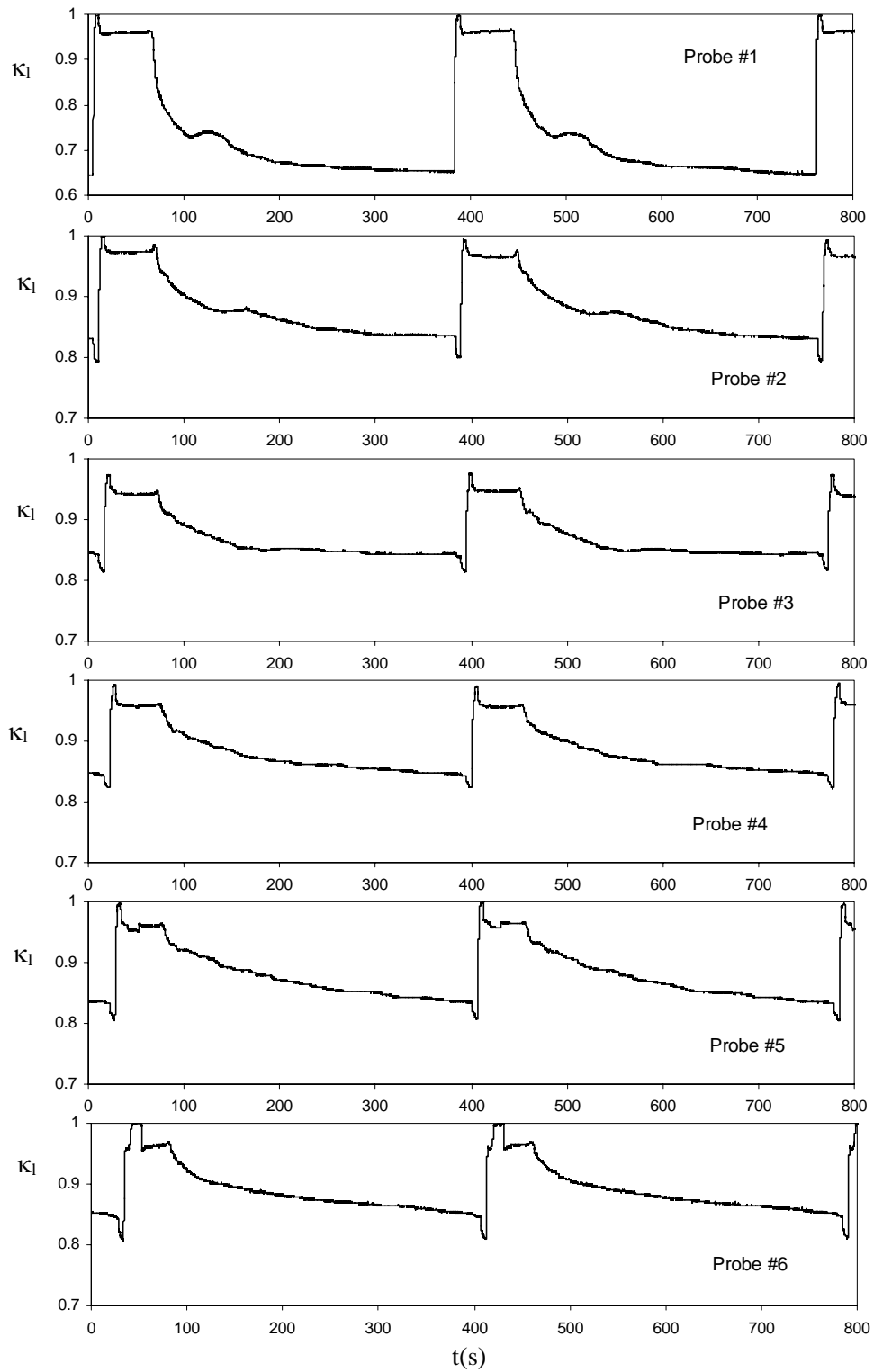


Figure IV.9: Time dependence of the normalized conductivity (κ). Operating conditions: $P=360$ s; $s=0.17$; $u_{l,ss}=0.15$ cm/s; $u_g=1.4$ cm/s.

The pulse velocity (u_p), as defined by Boelhouwer (2001), can be evaluated dividing the distance between probes (23.5 cm) by the corresponding time delay of the liquid front. Pulse velocities along the bed are calculated considering consecutive electrodes for different superficial gas and liquid velocities. Results are presented in Figures IV.10. They indicate that the pulse velocity remains almost constant along the column. As expected, pulse velocity increases with superficial liquid and gas velocities; the influence of the liquid velocity being more intense, in agreement with trends reported by Giakoumakis et al. (2005).

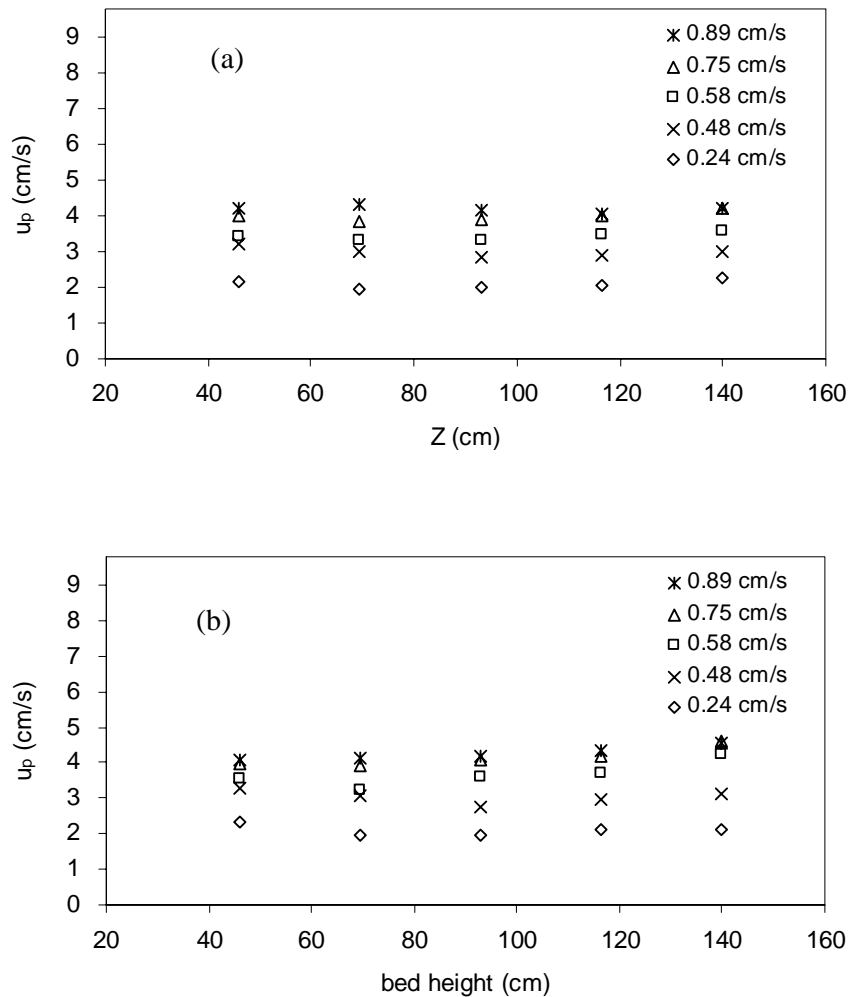


Figure IV.10: Pulse velocity as a function of the reactor bed length for different superficial liquid velocity. (a) $u_g = 1.4$ cm/s; (b) $u_g = 3.0$ cm/s

Considering the liquid front displacements and taking again electrodes #1 and #6, approximate mean liquid residence times, θ'_1 , are obtained for the #1–#6 test section. Correspondingly, approximate liquid holdups for the initial part of the wet period of the cycle have been calculated by an expression similar to Eq. IV.7:

$$\varepsilon'_1 = \frac{\theta'_{1(\#1-\#6)} \cdot Q_{1,w}}{\pi(Dc/2)^2 l_{(\#1-\#6)}} = \frac{u_{1,w}}{u_{P(\#1-\#6)}} \quad (\text{IV-9})$$

where $Q_{1,w}$ is the liquid flow rate during the wet period of the cycle.

Liquid holdups obtained from Eq. IV-9 are compared to those measured for steady state conditions using the method described in section IV.1.3. This comparison is shown in Figure IV.11. Trends are similar, even if the values predicted using the liquid fronts are lower than those evaluated from the RTD curves. At the same superficial liquid velocity, the liquid front travels downwards the column faster than the liquid does under steady state conditions. This is probably due to a less restriction to the liquid circulation as the wet fraction of the cycle period starts; in addition, a short transient during which the liquid builds-up should probably exist. However, the liquid holdup attained almost instantaneously is always larger than 60% of the liquid holdup at steady state conditions corresponding to $u_{1,w}$, and the similarity between estimated values is closer as the gas velocity is increased.

Another interesting feature of the curves shown in Figures IV.8-9 is that the normalized conductances approach stationary values when the wet and dry periods are long enough. Hence, the asymptotic values can be compared with measurements obtained at steady state conditions.

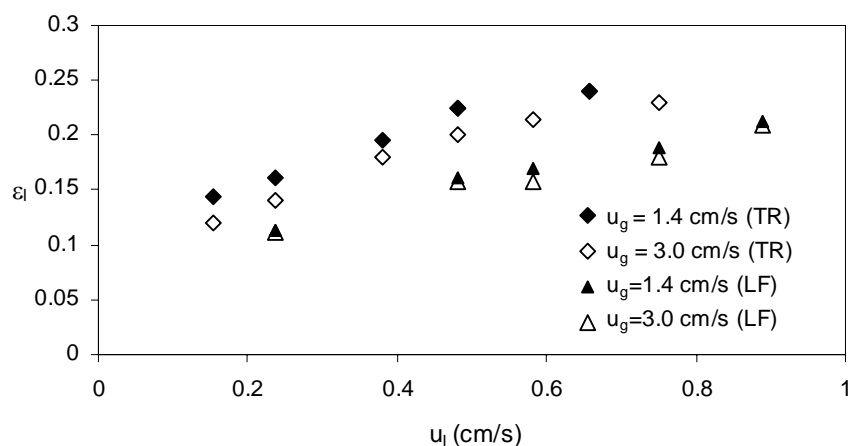


Figure IV.11: Experimental liquid holdup measured by tracer experiments (TR) and from the liquid front displacements (LF) as a function of superficial liquid velocities for different superficial gas velocities.

Figure IV.12a and b compares normalized conductance values measured for steady-state conditions with asymptotic values obtained during cycling, calculated as the average of the value measured for all the electrodes.

As observed, asymptotic values of average conductance measured for the wet cycle are quite similar to those measured under steady-state conditions at a liquid velocity equal to the one during the wet cycle. For low liquid velocities, small differences are apparent, likely due to the partial wetting of the solid and the higher probability for the liquid films to take new routes during periodic operation. This would determine that the mean liquid located between electrodes could be slightly different.

The average asymptotic conductance measured during the dry cycle always oscillates around the same value for different cycling parameters, indicating that it could be related to the static liquid holdup. As a whole, these results suggest that, for periods sufficiently long, the asymptotic average conductance measured for experiments with liquid flow modulation approach those of the corresponding steady-state condition.

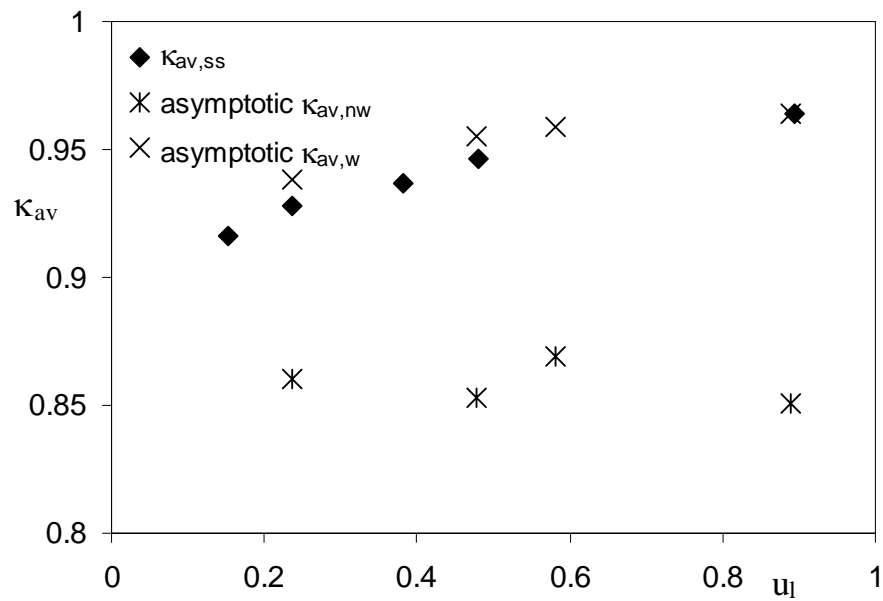


Figure IV.12a: Influence of the liquid superficial velocity on the average conductance, κ_{av} , measured for steady state conditions and the average of the asymptotic values attained during cycling conditions. $u_g = 1.4$ cm/s.

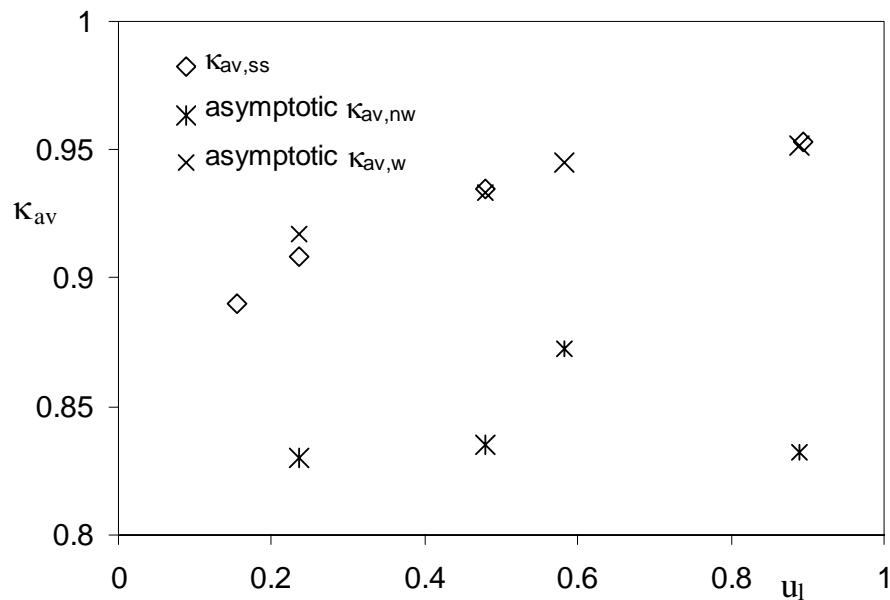


Figure IV.12b: Influence of the liquid superficial velocity on the average conductance, κ_{av} , measured for steady state conditions and the average of the asymptotic values attained during cycling conditions. $u_g = 3.0$ cm/s.

IV.2.2.1. CONDUCTANCE PROBES CALIBRATION

With the purpose of estimating the instantaneous liquid holdup measured for periodic operation at different column heights, the mean liquid holdups measured through the RTD experiments are related to κ , to determine appropriate calibration relationships.

Representative results of the normalized conductance, κ , as a function of mean liquid holdup measured by the tracing method are presented in Figure IV.13a-d and IV.14a-d for three electrodes at different axial positions and for the average of all the electrodes. The data value of κ calculated from the mean of asymptotic values obtained for long dry periods is assigned to the static liquid holdup, estimated by the correlation of Saez and Carbonell (1985).

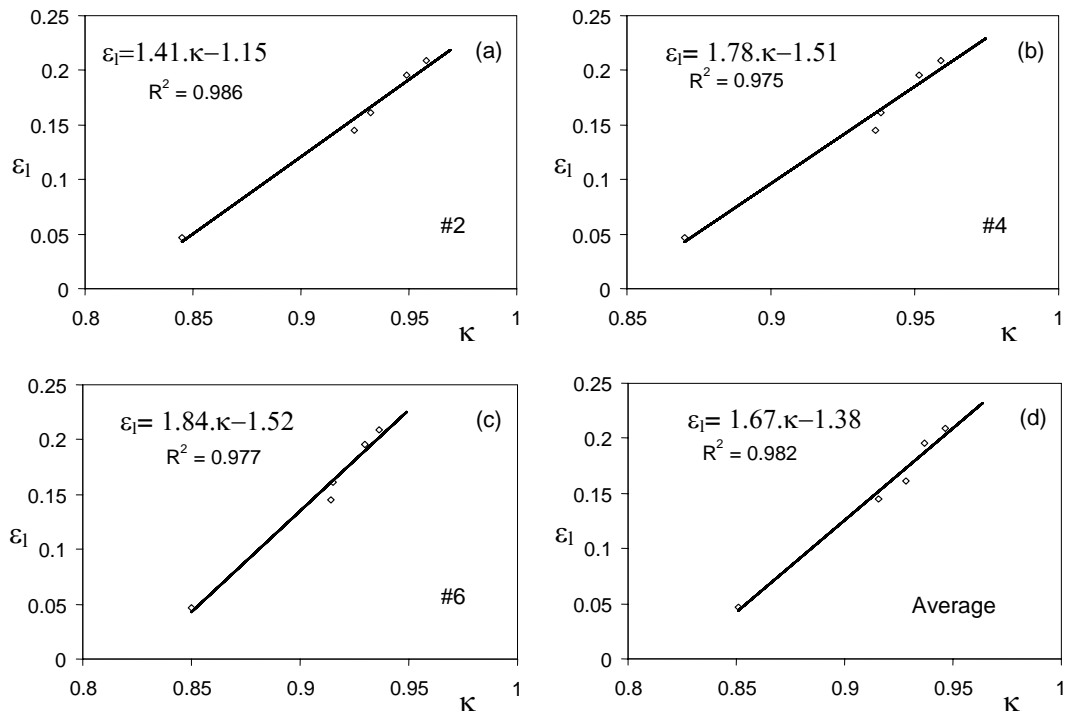
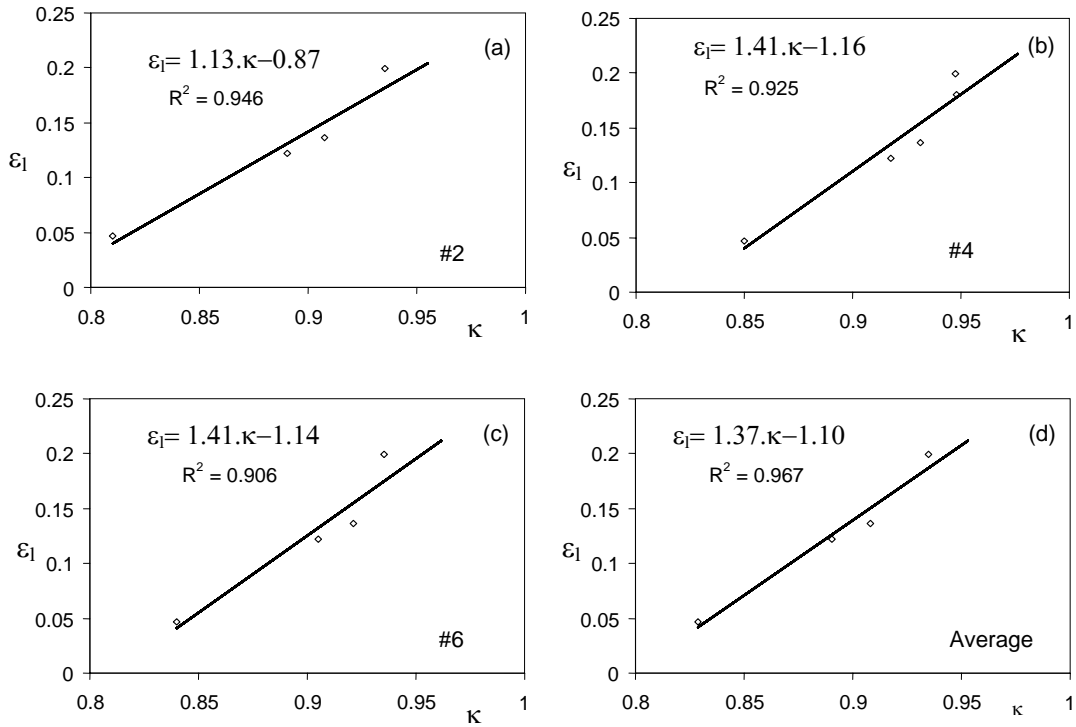
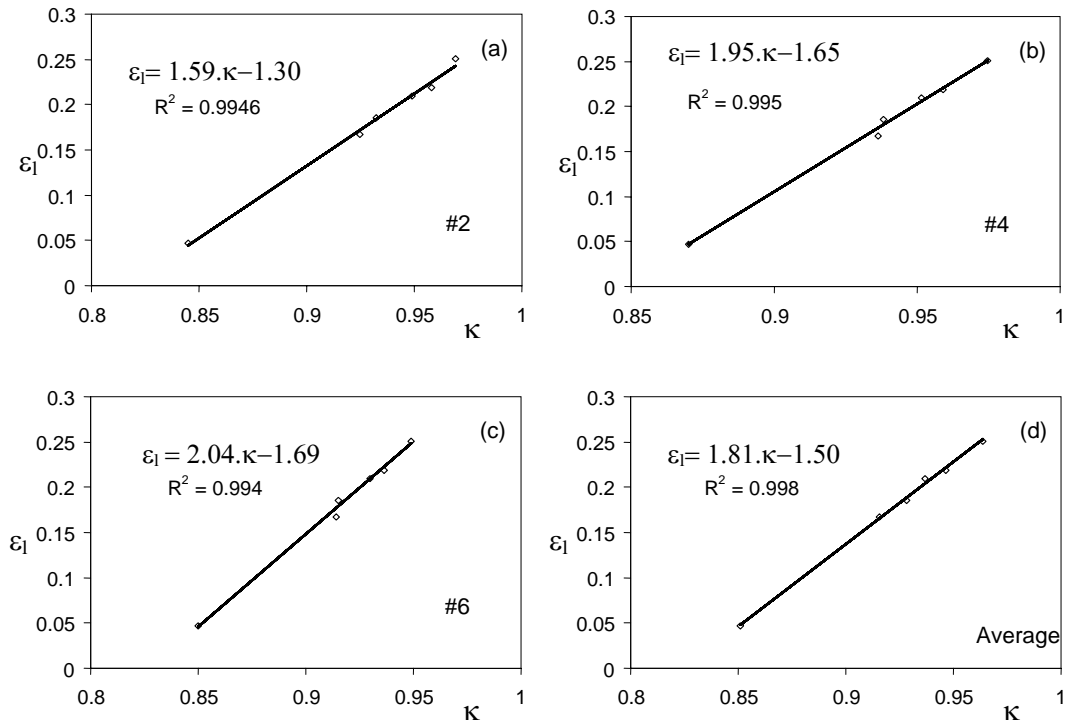


Figure IV.13: Experimental liquid holdup vs normalized conductance for $u_G = 1.4$ cm/s.


 Figure IV.14: Experimental liquid holdup vs normalized conductance for $u_G = 3.0$ cm/s.

 Figure IV.15: Estimated liquid holdup vs normalized conductance for $u_G = 1.4$ cm/s.

As observed, the experimental results are rather scattered and depart from the linear trend shown, mainly forced by the data corresponding to the static holdup. It is important in this case to be able to extrapolate outside the range for which the liquid holdup was experimentally obtained, since holdup values even as low as the static holdup are likely to characterize the dry period. Hence, the relationship between κ and the liquid holdups predicted by Iliuta et al. (1999) is also tested. Results are shown in Figures IV.15a-d and IV.16a-d for $u_G = 1.4$ cm/s and for $u_G = 3.0$ cm/s, respectively. In both cases, the linear fit is significantly improved with respect to the fitting obtained with the experimental results. Moreover, the value for the static holdup aligns very well in these cases.

It should be mentioned that the fitting to a straight line is good for all the electrodes, indicating that a linear relationship between the normalized conductance and the liquid holdup exists in the whole range. Hence, considering the goodness of fitting shown in Figures IV.15-16, it arises that instantaneous normalized conductances can be converted to liquid holdups to within a reasonable error.

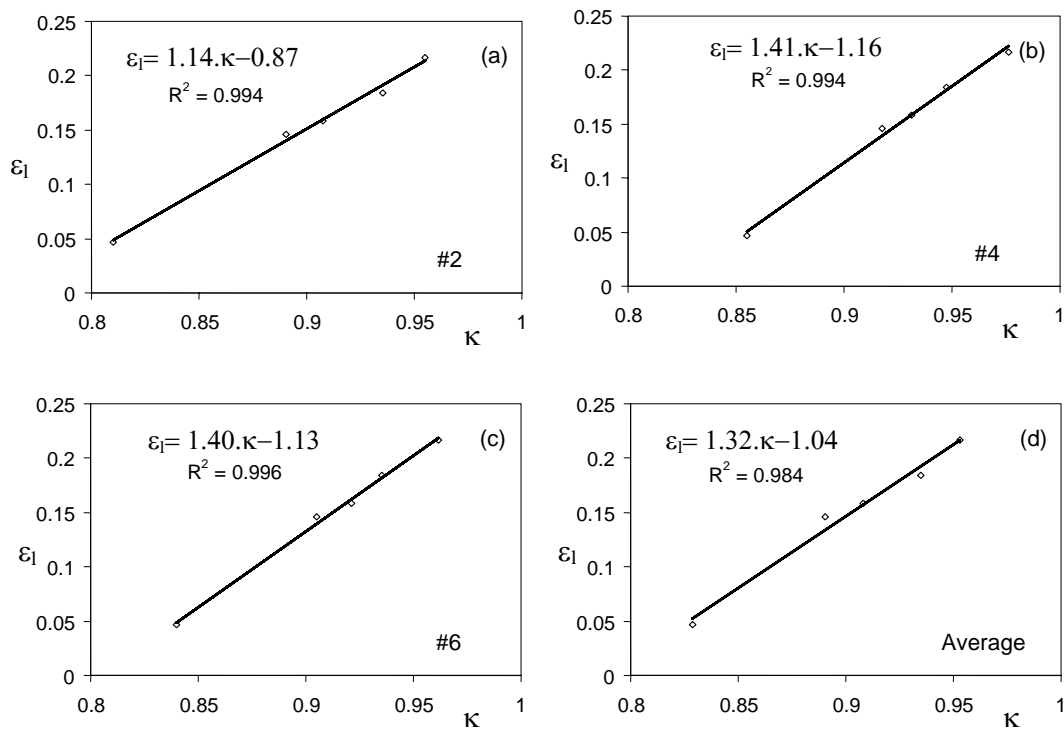


Figure IV.16: Estimated liquid holdup vs normalized conductance for $u_G = 3.0$ cm/s.

Even though the experimental results correspond to a mean value of the liquid holdup for the whole testing section, and therefore should be contrasted to a value of κ averaged along the column, different linear relationships have been found for each probe. These differences could be attributed to small local variations in liquid holdups and/or to a not totally uniform liquid distribution. It should be mentioned that the largest differences are apparent for the first electrode, where the liquid distribution is expected to be the worst. Hence, a different calibration equation is considered for each electrode instead of a single expression for all. The linear expressions considered are listed in Table IV.3.

Table IV.3: Calibration expressions for conductivity probes.

u_g (cm/s)	Electrode	Calibration linear fit
1.4	#1	$\varepsilon_l = 0.70\kappa - 0.41$
	#2	$\varepsilon_l = 1.59\kappa - 1.30$
	#3	$\varepsilon_l = 1.86\kappa - 1.50$
	#4	$\varepsilon_l = 1.95\kappa - 1.65$
	#5	$\varepsilon_l = 1.62 \kappa - 1.33$
	#6	$\varepsilon_l = 2.04 \kappa - 1.69$
3.0	#1	$\varepsilon_l = 0.51 \kappa - 0.28$
	#2	$\varepsilon_l = 1.14 \kappa - 0.87$
	#3	$\varepsilon_l = 1.50 \kappa - 1.16$
	#4	$\varepsilon_l = 1.41 \kappa - 1.15$
	#5	$\varepsilon_l = 1.13 \kappa - 0.88$
	#6	$\varepsilon_l = 1.40 \kappa - 1.13$

IV.2.2.2 INSTANTANEOUS LIQUID HOLDUPS UNDER CYCLING

The instantaneous conductance measured by each probe is converted into the instantaneous liquid holdup using the calibration relationships listed in Table IV.3. The simultaneous liquid holdup traces of the six conductimetric probes are presented in Figures IV.17-21 for experiments under periodic operation corresponding to $s=0.17$, $u_{l,mean} = 0.15$ cm/s and $u_g = 3.0$ cm/s.

The liquid holdup varies largely during both the wet and dry cycles. The square wave shape assumed for the liquid at the column entrance is significantly distorted along the column. The shape measured by the first electrode is always quite distinct than the others and shows the largest amplitudes in holdup. Normally, a liquid front is established very fast as the wet period starts. On the contrary, when the liquid flow is interrupted, the liquid holdup decreases slowly and progressively. Furthermore, a decrease in the extension of the plateau attained during the wet period is observed. The liquid holdup time profiles suggest that the liquid waves decay by leaving liquid behind them, in agreement with observations reported by Boelhouwer (2001). The modulation is observed in the six probes with almost the same frequency, as already evidenced from the pulse velocity shown in the previous section. Similar conclusions arise for experiments under periodic operation for different splits. For instance, results for $s = 0.65$ are shown in Figures IV.22-26.

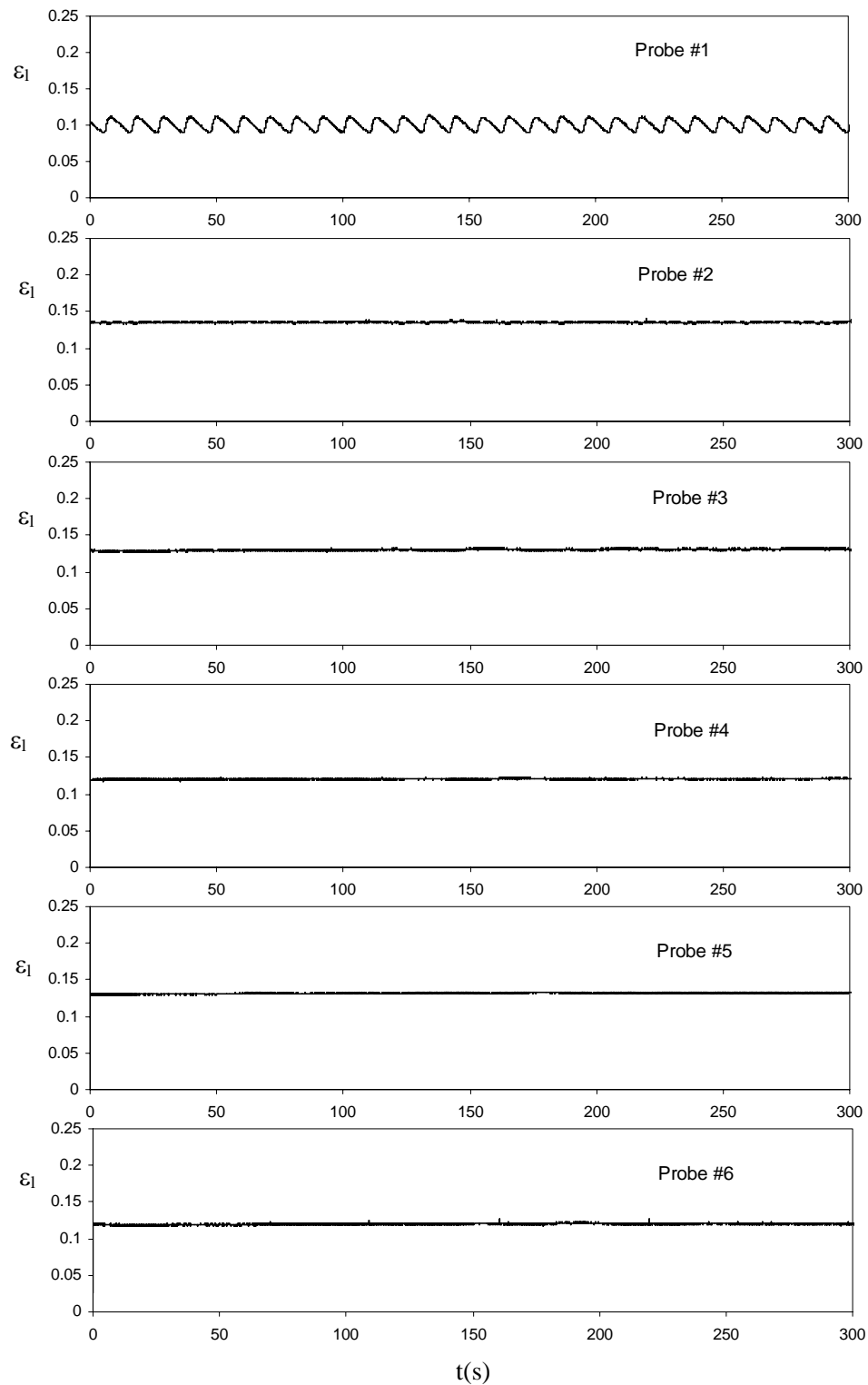


Figure IV.17 Estimated instantaneous liquid holdup vs time at different column heights.

Cycling conditions: $P=10$ s; $s=0.17$; $u_{l,\text{mean}}=0.15$ cm/s; $u_g=3.0$ cm/s.

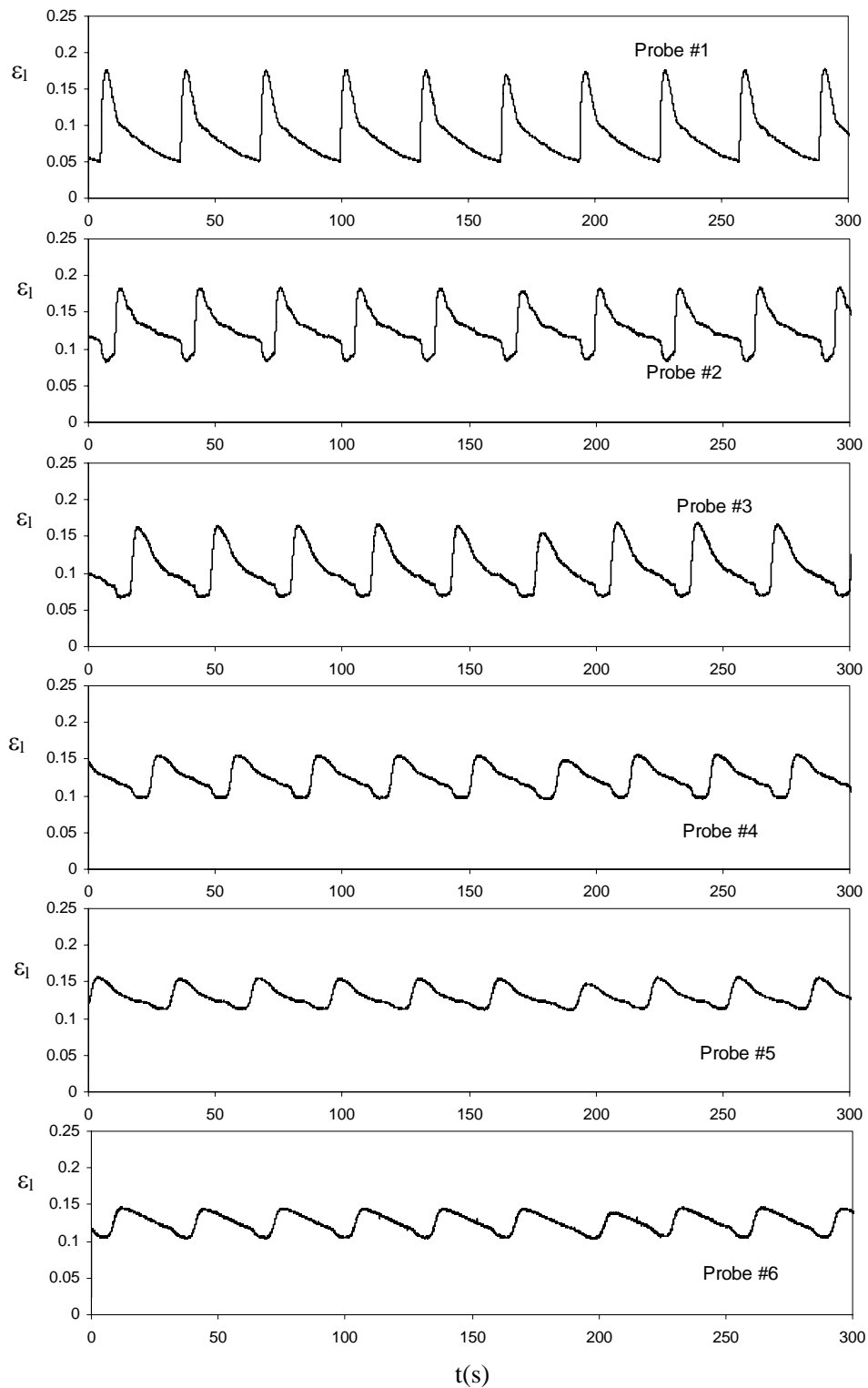


Figure IV.18 Estimated instantaneous liquid holdup vs time at different column heights.

Cycling conditions: $P=30$ s; $s=0.17$; $u_{l,\text{mean}}=0.15$ cm/s; $u_g=3.0$ cm/s.

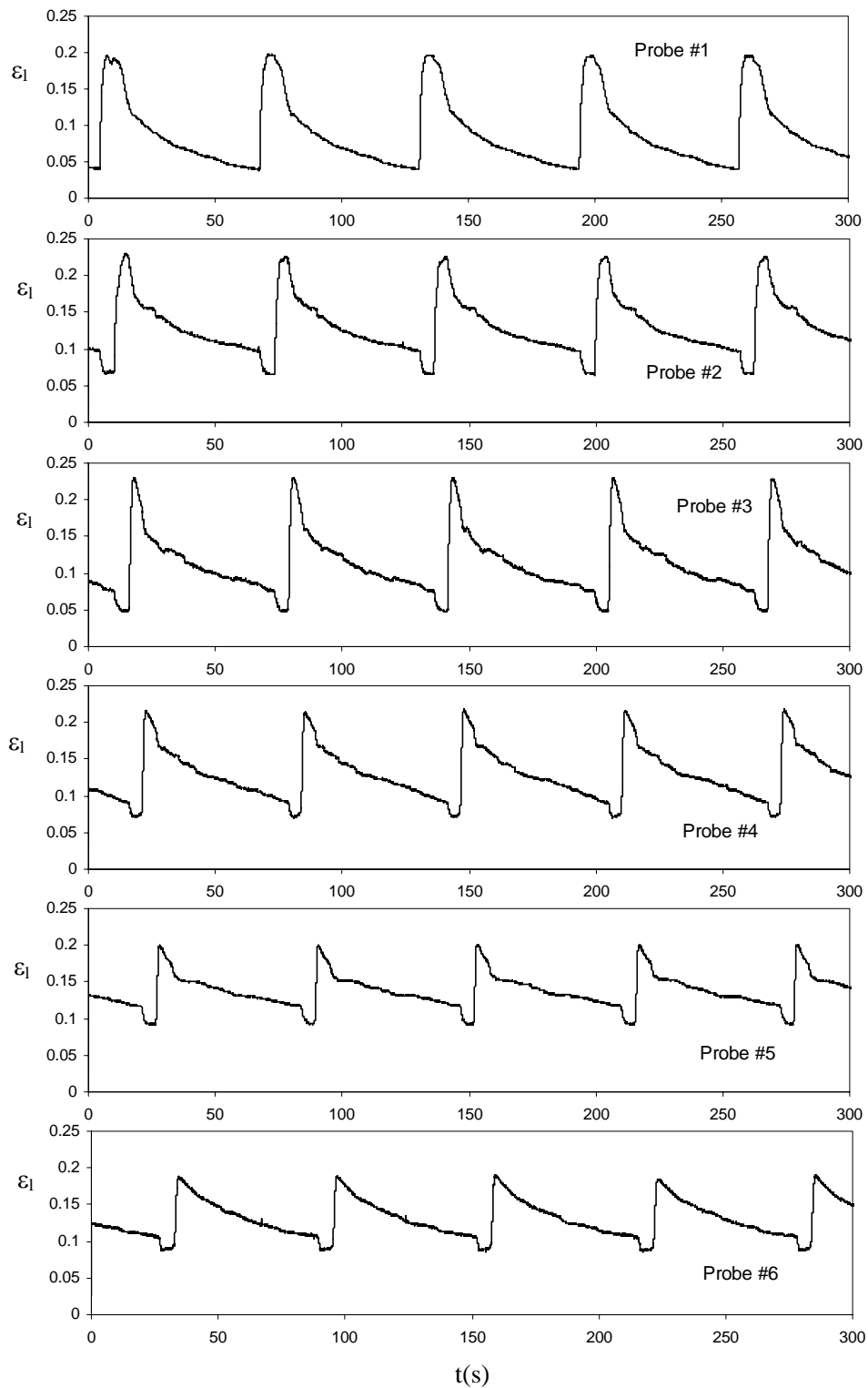


Figure IV.19 Estimated instantaneous liquid holdup vs time at different column heights.

Cycling conditions: $P=60$ s; $s=0.17$; $u_{l,mean}=0.15$ cm/s; $u_g=3.0$ cm/s.

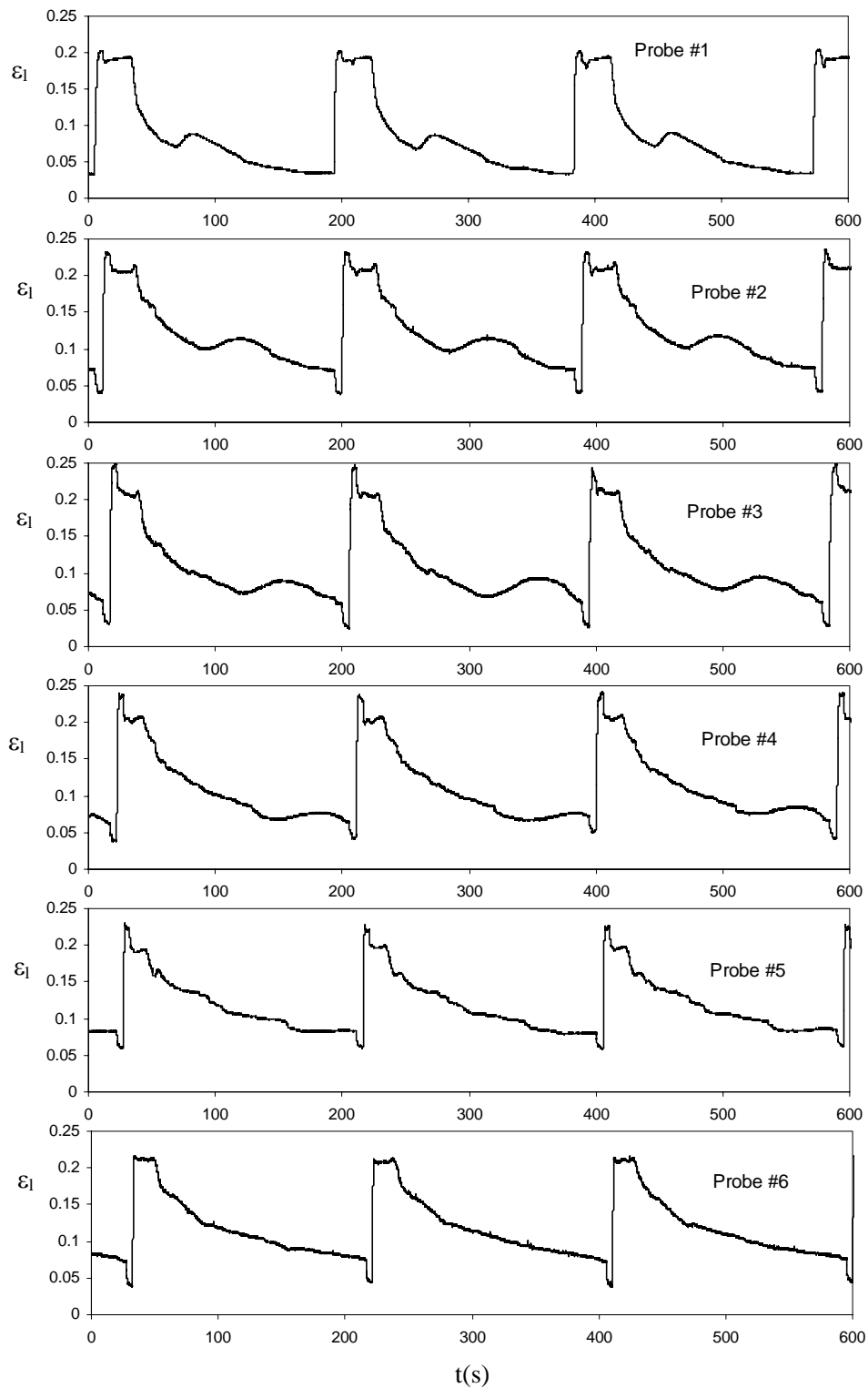


Figure IV.20 Estimated instantaneous liquid holdup vs time at different column heights.

Cycling conditions: $P=180$ s; $s=0.17$; $u_{l,\text{mean}}=0.15$ cm/s; $u_g=3.0$ cm/s.

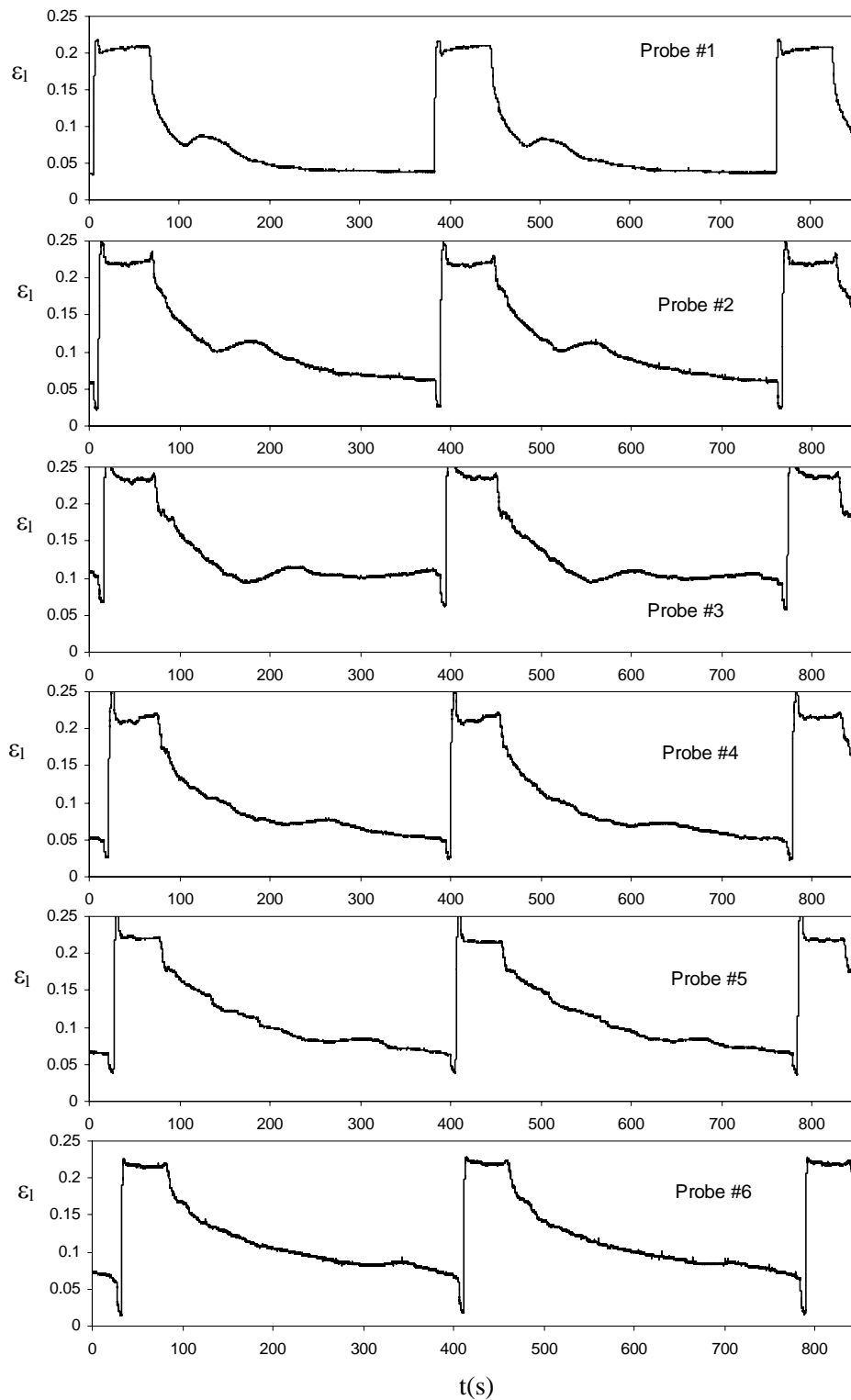


Figure IV.21 Estimated instantaneous liquid holdup vs time at different column heights.

Cycling conditions: $P=360$ s; $s=0.17$; $u_{l,mean}=0.15$ cm/s; $u_g=3.0$ cm/s.

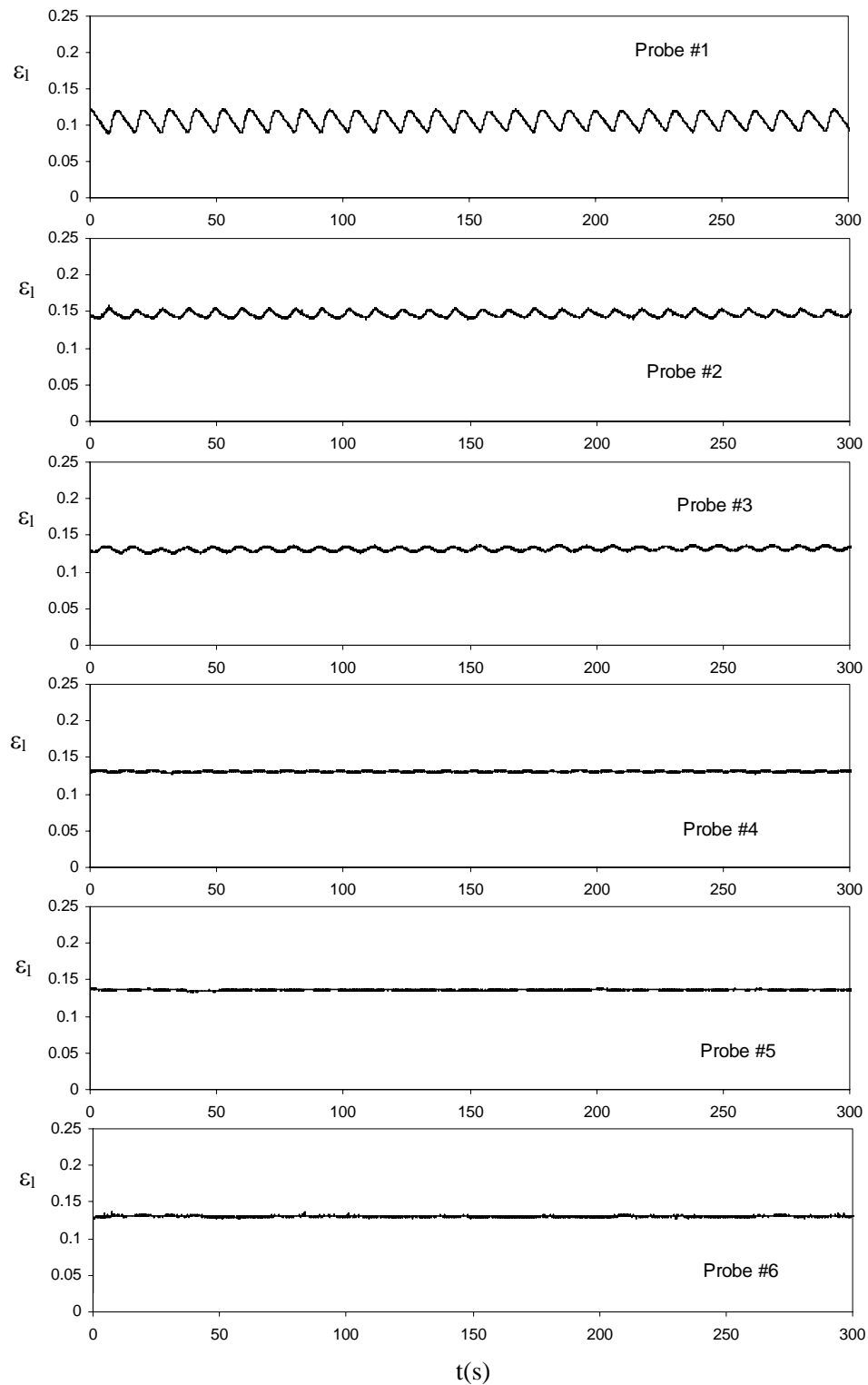


Figure IV.22 Estimated instantaneous liquid holdup vs time at different column heights.

Cycling conditions: $P=10$ s; $s=0.65$; $u_{l,\text{mean}}=0.15$ cm/s; $u_g=3.0$ cm/s.

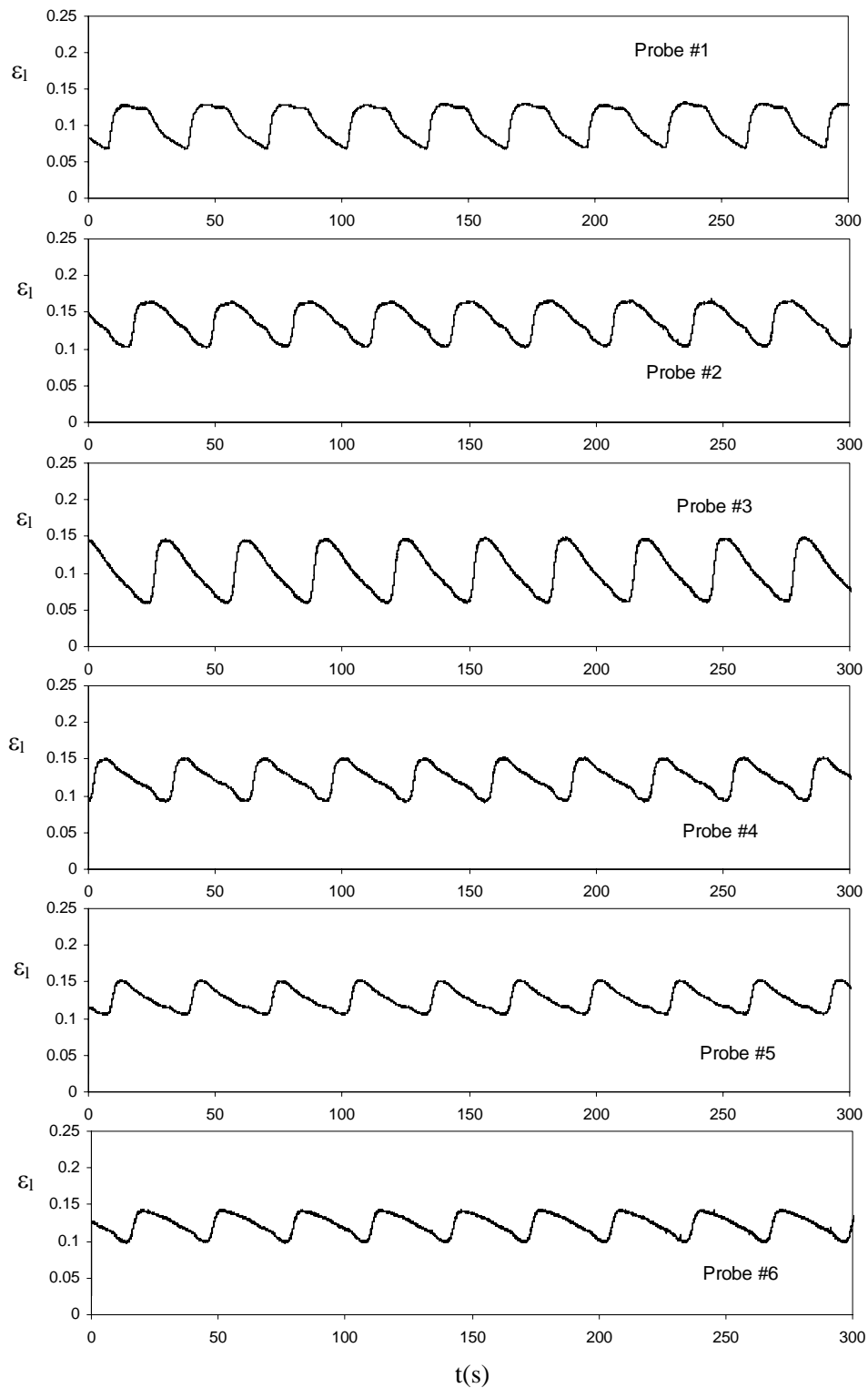


Figure IV.23 Estimated instantaneous liquid holdup vs time at different column heights.

Cycling conditions: $P=30$ s; $s=0.65$; $u_{l,\text{mean}}=0.15$ cm/s; $u_g=3.0$ cm/s.

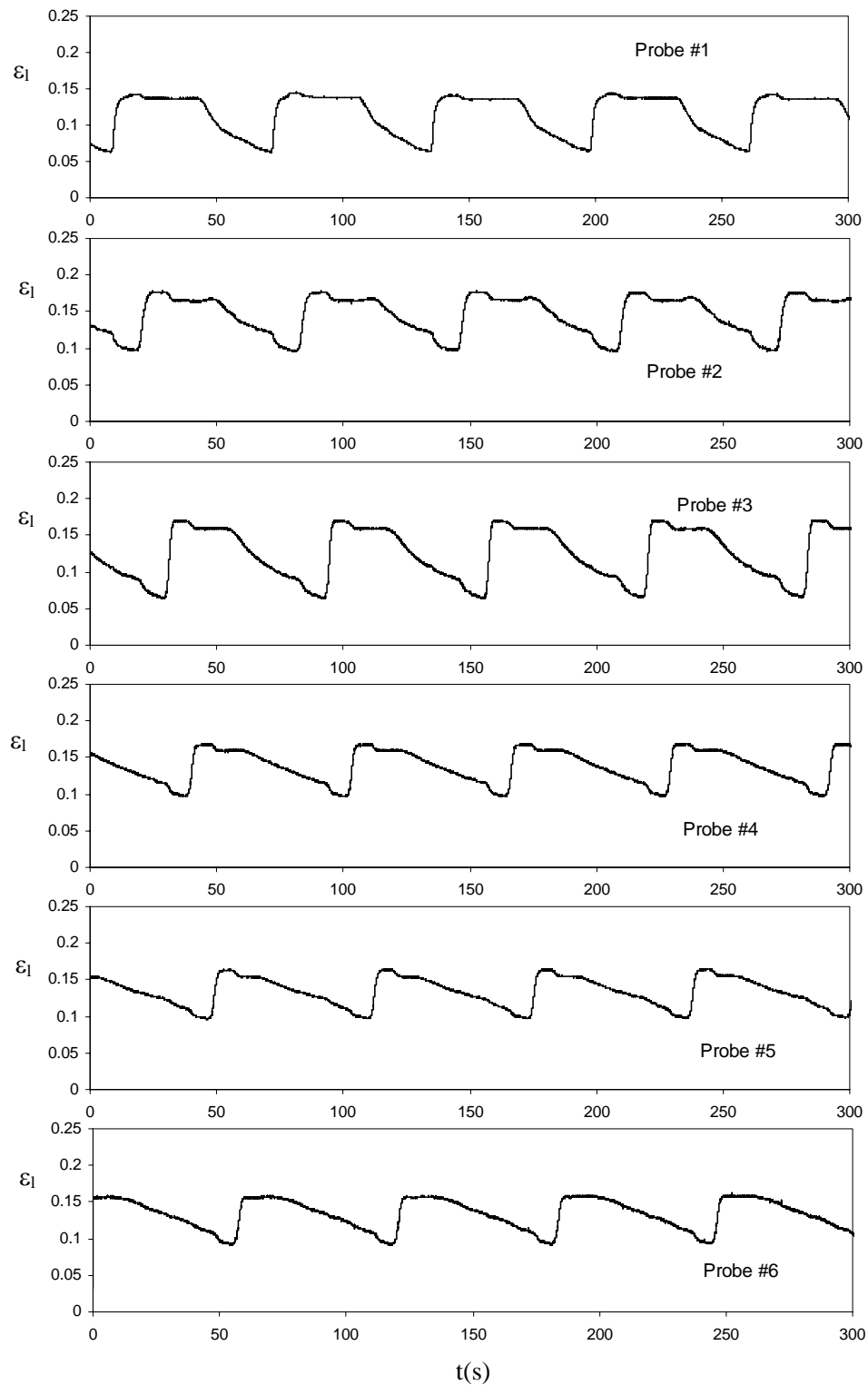


Figure IV.24 Estimated instantaneous liquid holdup vs time at different column heights.

Cycling conditions: $P=60$ s; $s=0.65$; $u_{l,\text{mean}}=0.15$ cm/s; $u_g=3.0$ cm/s.

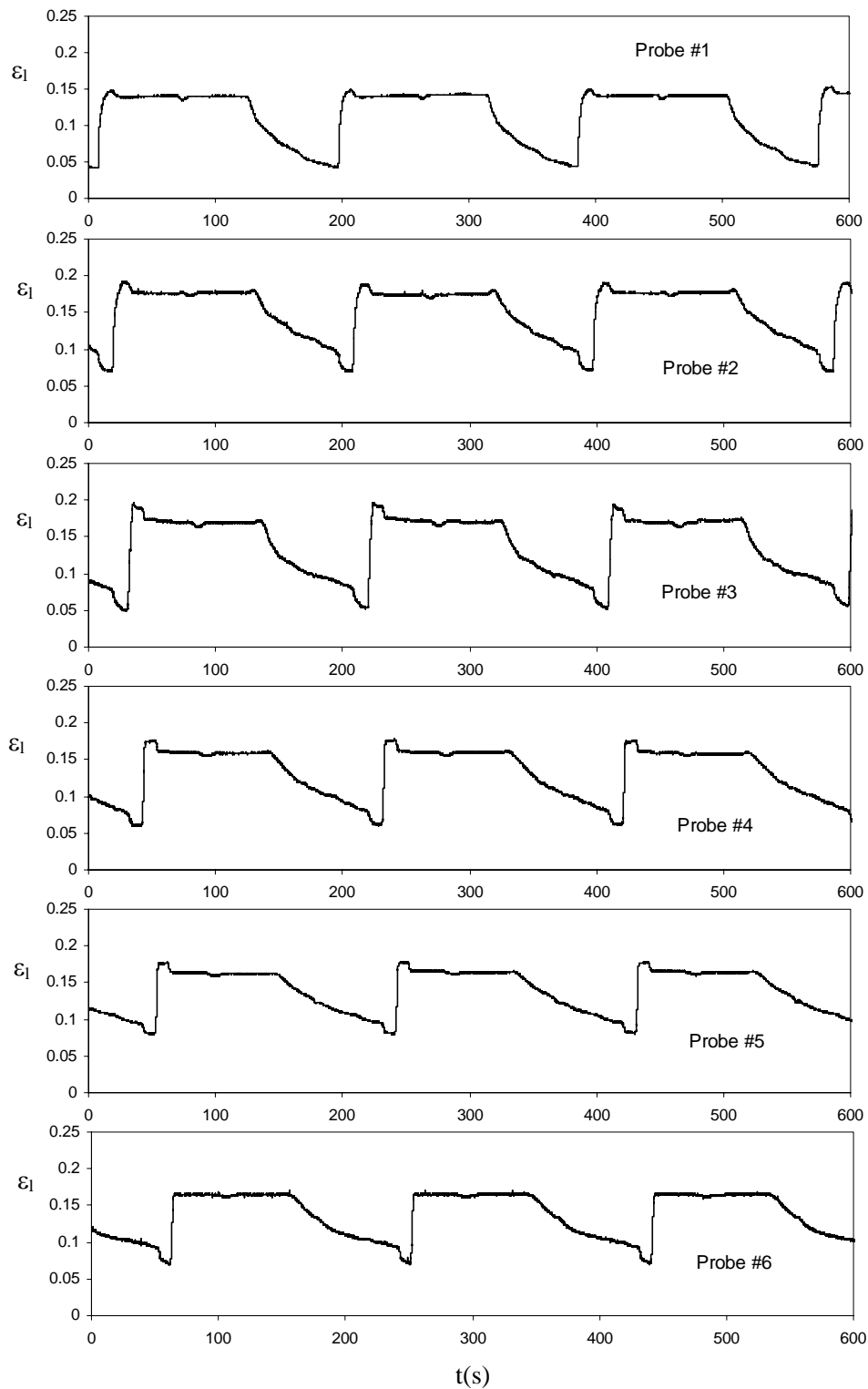


Figure IV.25 Estimated instantaneous liquid holdup vs time at different column heights.

Cycling conditions: $P=180$ s; $s=0.65$; $u_{l,mean}=0.15$ cm/s; $u_g=3.0$ cm/s.

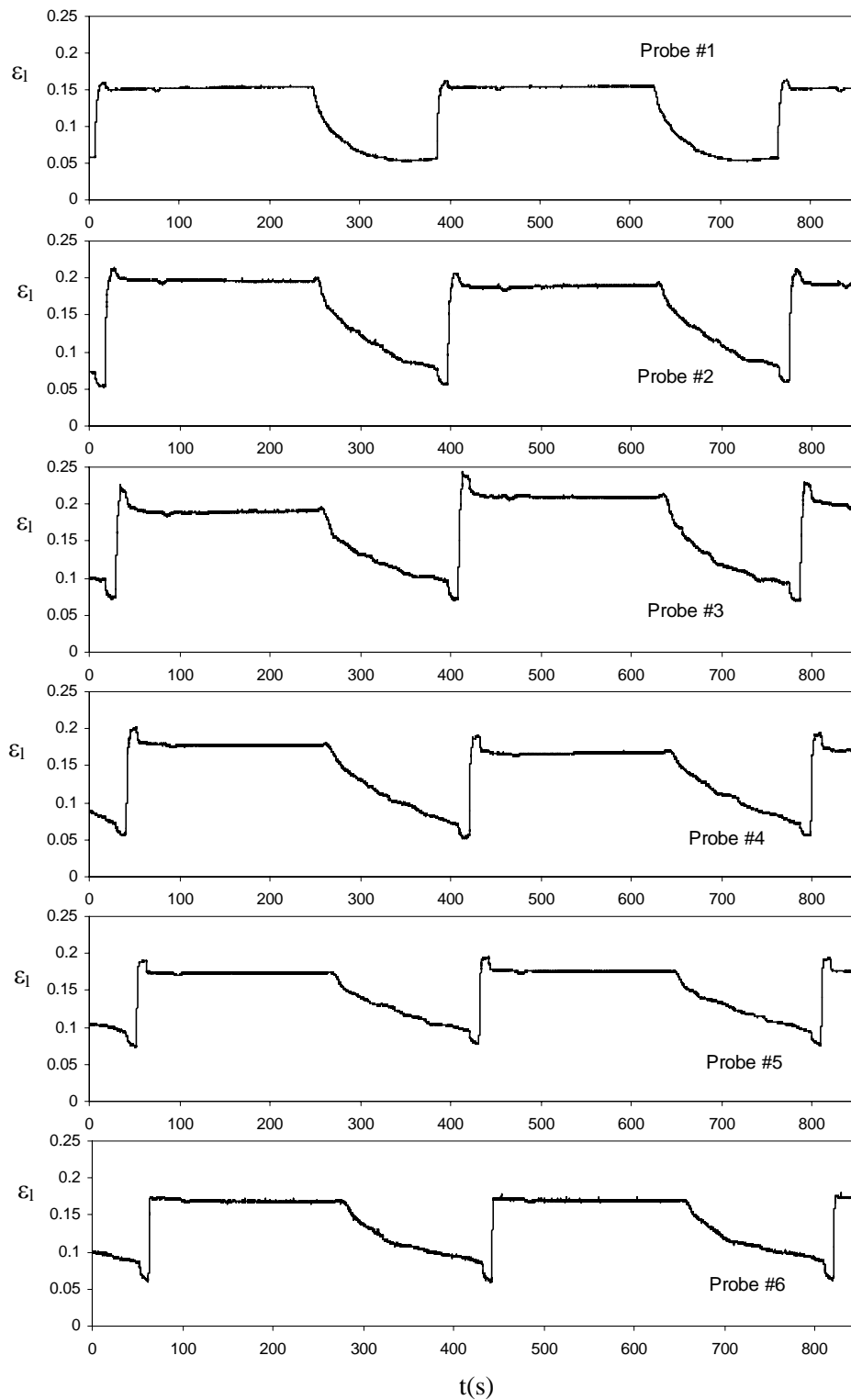


Figure IV.26 Estimated instantaneous liquid holdup vs time at different column heights.

Cycling conditions: $P=360$ s; $s=0.65$; $u_{l,\text{mean}}=0.15$ cm/s; $u_g=3.0$ cm/s.

It is worthy to note that, for a given set of parameters, *i.e.*, split, bed depth, gas velocity and mean liquid velocity, the time average liquid holdup ($\varepsilon_{l,av}$) remains almost constant for all the cycle periods (Figure IV.27). In all cases, the mean liquid holdup under ON–OFF liquid flow modulation is slightly lower than the one obtained at steady state at the corresponding mean liquid velocity, which is $\varepsilon_{l,mean} = 0.146$. Differences between both values apparently decrease with the split. However, the slight influence of the split disappears for longer bed depths.

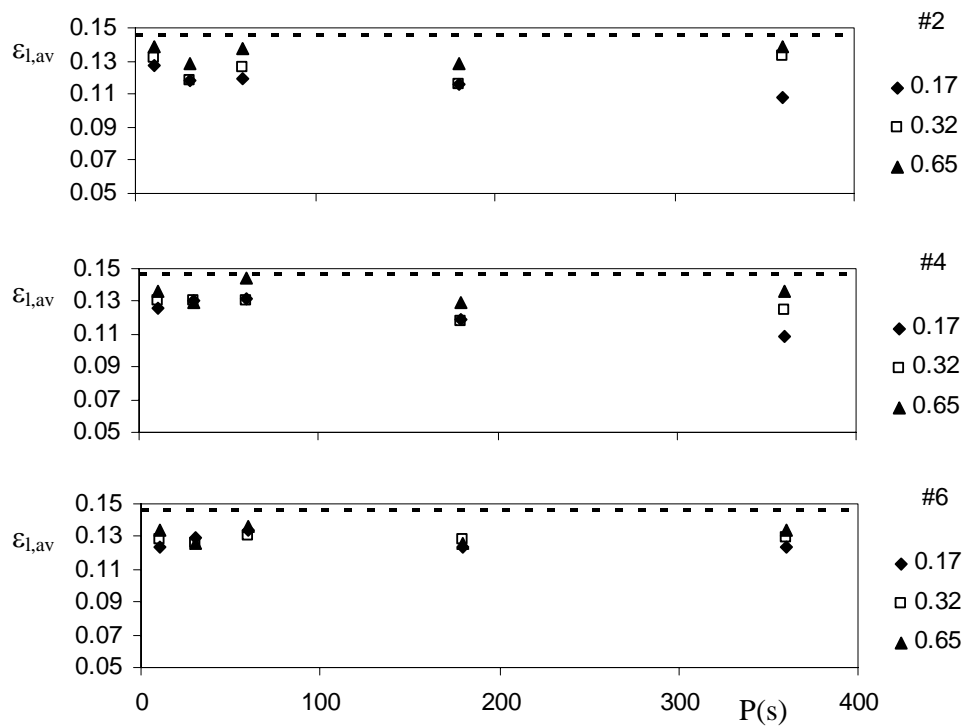


Figure IV.27: Time average liquid holdup as a function of cycle period for different splits and bed lengths. $u_{l,mean} = 0.15$ cm/s, $u_g = 3.0$ cm/s. Dotted lines correspond to $\varepsilon_{l,mean}$.

IV.2.2.2.1. EFFECT OF CYCLE PERIOD AND SPLIT

As clearly observed in Figures IV.17-26, the effect of the cycling parameters on the shape of the liquid holdup profiles is remarkable. The influence of the cycle period and split on characteristic values that the liquid holdup attains during each period of the cycle is analyzed in Figures IV.28-30.

For cycle periods in which a plateau for liquid holdup is attained within the cycle, the average asymptotic value that the liquid holdup reaches during the corresponding cycle is calculated. On the other hand, for the cycle periods where no plateau is clearly identified, the limit values measured before the cycle turns from wet to dry or *viceversa*, are evaluated using a statistic package included in M. Origin.

The ratios between the characteristic values of liquid holdup for the wet ($\varepsilon_{l,w}$) and the dry ($\varepsilon_{l,nw}$) periods of the cycle to the one for steady state at the mean liquid velocity ($\varepsilon_{l,mean}$) are calculated and represented as a function of the cycle period in the figures. The liquid holdup measured for the corresponding steady state at the liquid velocity for the wet cycle and the static liquid holdup are also shown.

Generally, the evaluated characteristic liquid holdup for each period of the cycle does not change strongly among the different electrodes distributed along the column. Moreover, if the cycle period is long enough, the liquid holdups tend to the same value whatever the cycle period. They approach the liquid steady-state holdup measured for a liquid velocity equal to the liquid velocity during the wet period or to the static liquid holdup for the dry period. However, only for the lower splits, and especially in the upper region of the column, the static liquid holdup is reached. For the majority of the experimental conditions examined, there is an excess liquid holdup over the static liquid holdup.

Giakoumakis et al. (2005) suggested that the transition between slow and fast modulation could be estimated considering the reactor length, the cycle period and the pulse velocity. If the cycle period is less than the ratio of the reactor length over the pulse celerity, the modulation would be fast. Hence, for the present bed length of 150 cm, the cycle period that would provide a limit between slow and fast modulation depends on the split, as the pulse celerity depends on the split. Transition limits are shown in Figures IV.28-30.

For long cycle periods, the pulses travel the whole column before a new pulse starts as indicated by the transition lines proposed by Giakoumakis et al. (2005).

For intermediate and low cycle periods, the liquid holdup during cycling departs from the steady state liquid holdup both during the dry and the wet period. The limit liquid holdup during the dry cycle tends to increase along the bed, while the one during the wet cycle tends to decrease along the bed. The transient behavior is relatively more important and a “quasi steady state” liquid holdup is hardly accomplished for any combination of cycling parameters.

For very short cycle periods, the liquid holdups during the wet and dry cycle approach each other, particularly as the bed depth increases. In the lower part of the column, liquid pulses are not clearly distinguished in the traces, not even after magnifying the scale. According to Boelhouwer (2001), the pulses are not stable and disappear.

The previous analysis suggests different qualitative limits between slow and fast cycling. Slow cycling can be defined as the one that leads to asymptotic values of the liquid holdup comparable to those of the steady state at similar velocities, *i.e.*, the steady state liquid holdup at a velocity equivalent to the one during the wet cycle and the static holdup, or at least a constant minimum liquid holdup for all the periods. Hence, from these experiments, we found that slow modulation conditions are attained for cycle periods longer than 60s. In contrast, fast modulation can be defined as the one that leads to similar limit liquid holdups for the wet and dry periods of the cycle, as in the case of cycle periods of 10s and less. In this case, a new “pseudo steady state” condition is apparently reached, with a characteristic average liquid holdup generally lower than the one measured at steady state with the mean liquid velocity, $u_{l,mean}$, calculated as $u_{l,w}/s$.

For intermediate cycle periods, differences between the liquid holdups during each period of the cycle are still significant. In addition, the asymptotic values are not reached. The behavior of the liquid holdup is eminently transient and approximations to pseudo steady state behaviors may probably not describe properly the situation to within a negligible degree of error.

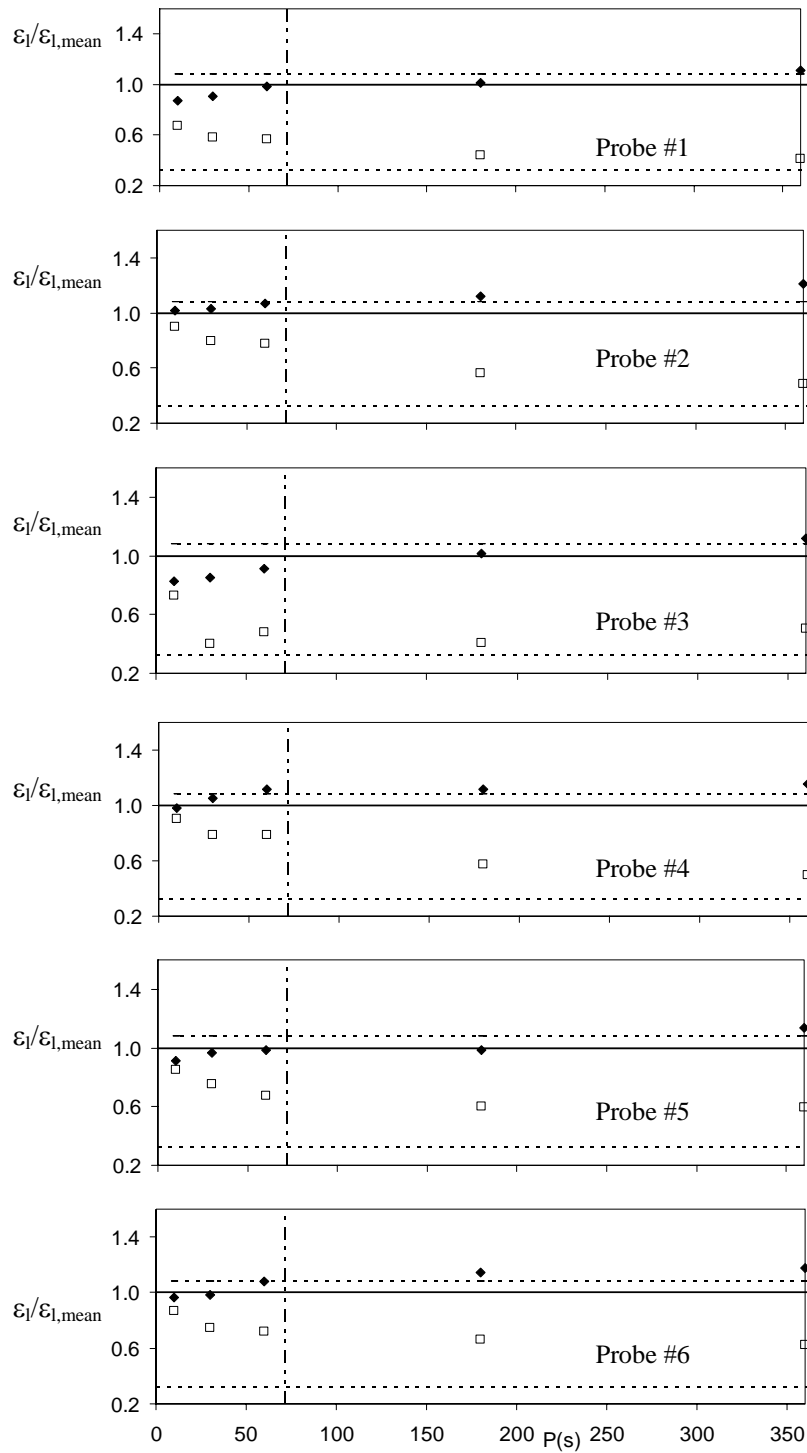


Figure IV.28: Effect of cycle period on asymptotic liquid holdups for both cycles. (◆) wet period of the cycle (□) dry period of the cycle. $s = 0.65$; $u_{l,mean} = 0.15$ cm/s; $u_g = 3.0$ cm/s. (---) values measured at steady state; (— — —) limit defined by Giakoumakis et al. (2005)

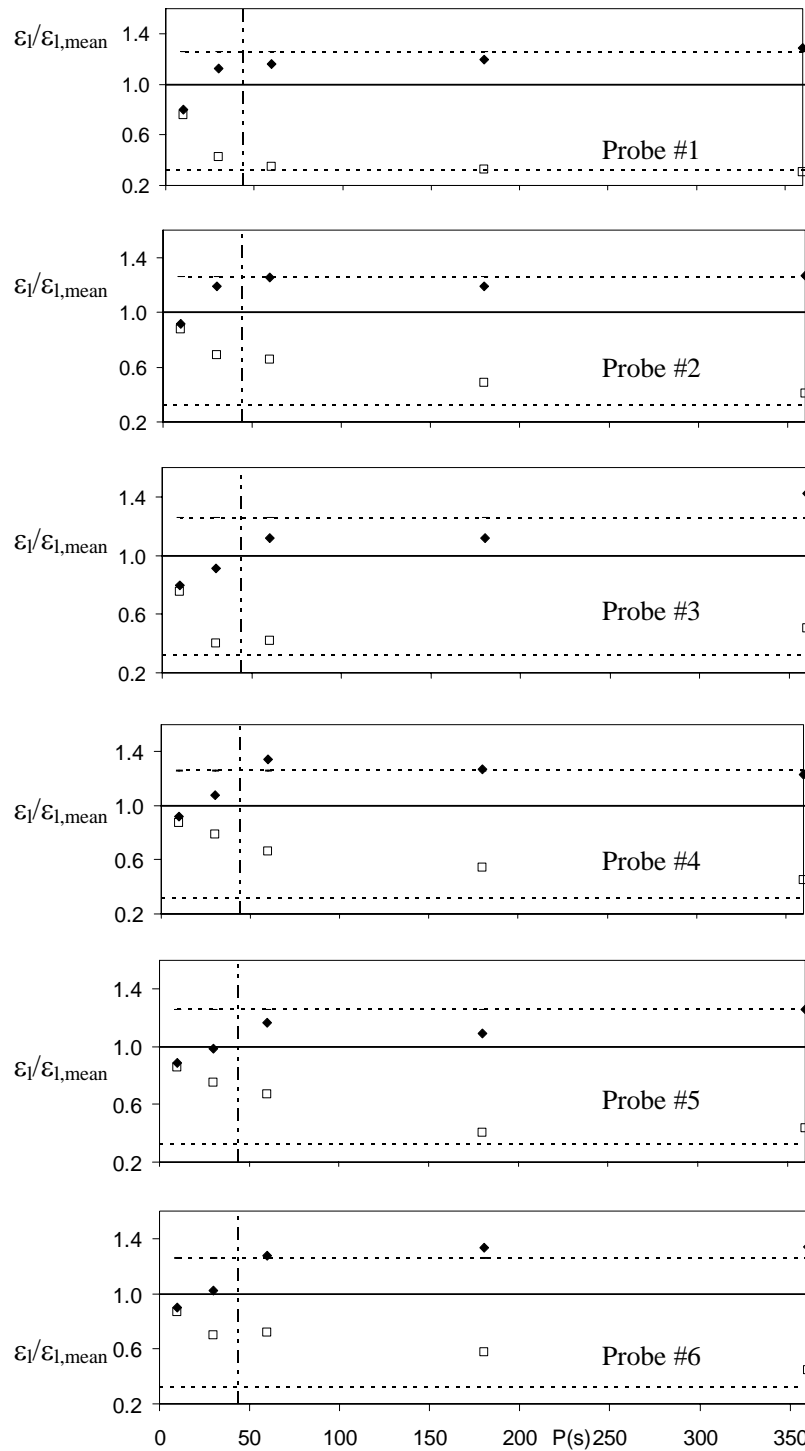


Figure IV.29: Effect of cycle period on asymptotic liquid holdups for both cycles. (\blacklozenge) wet period of the cycle (\square) dry period of the cycle. $s = 0.32$; $u_{l,mean} = 0.15$ cm/s; $u_g = 3.0$ cm/s. (---) values measured at steady state; (— — —) limit defined by Giakoumakis et al. (2005)

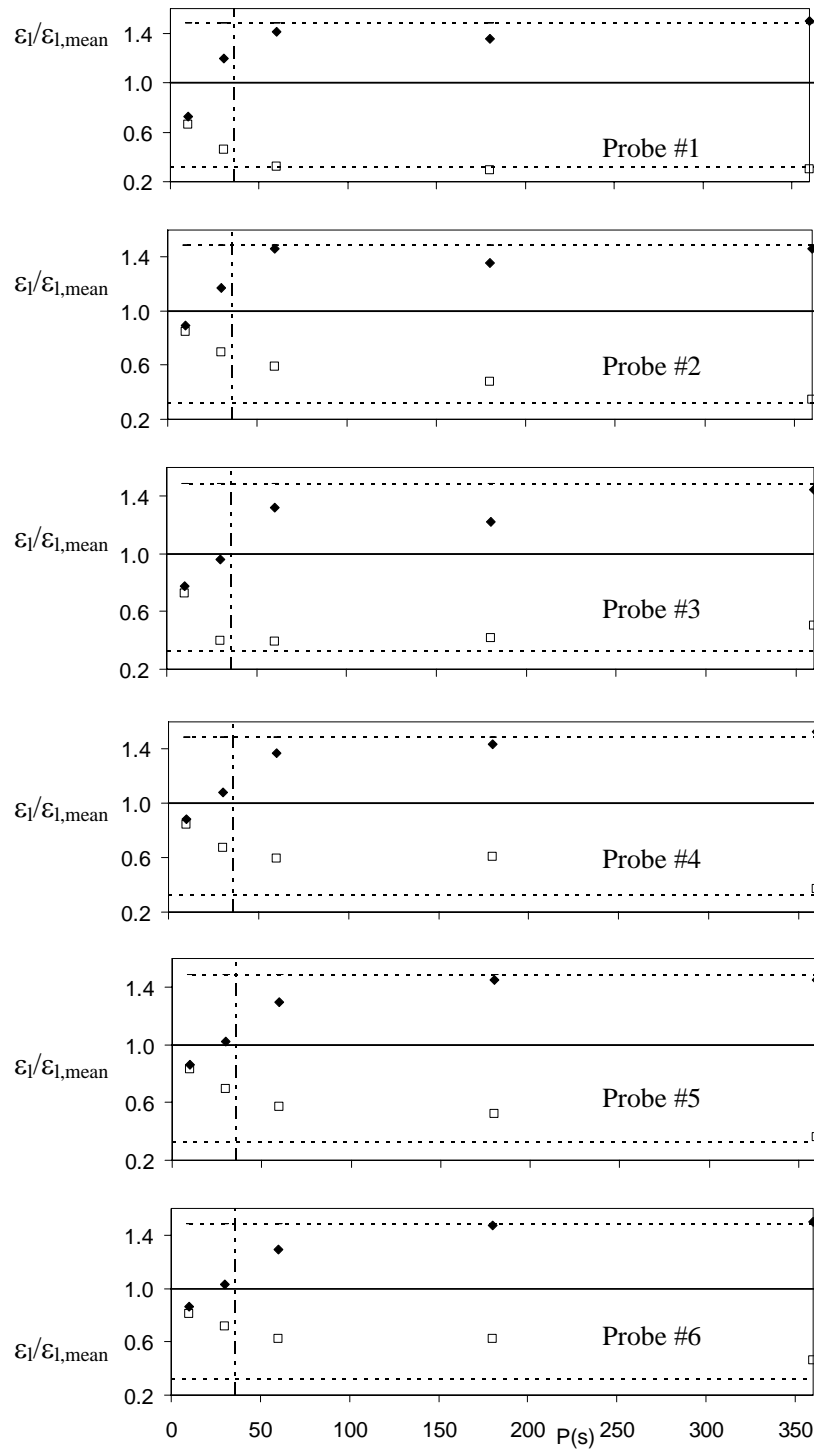


Figure IV.30: Effect of cycle period on asymptotic liquid holdups for both cycles. (\blacklozenge) wet period of the cycle (\square) dry period of the cycle. $s = 0.17$; $u_{l,mean} = 0.15$ cm/s; $u_g = 3.0$ cm/s. (---) values measured at steady state; (— · — · —) limit defined by Giakoumakis et al. (2005)

To quantify the variations between peaks and troughs, Giakoumakis et al. (2005) defined the liquid pulses intensity as the ratio between the standard deviation of liquid holdup and the time average liquid holdup:

$$I_p = \frac{\varepsilon_{l,sd}}{\varepsilon_{l,av}} \quad (\text{IV-10})$$

This parameter is considered to quantify pulse attenuation. In general, pulse intensity decreases with cycle period, as shown in Figure IV.31. For long cycle periods, pulses remain quite stable along the bed, especially for higher splits. As long as the cycle period decreases, pulse decay along the bed is evidenced (note the magnification of the scale of Fig. IV.31d). The influence seems to be more marked as the split decreases. For very short periods, pulse intensity tends to zero and thus, pulses fade away in the lower part of the column whatever is the split.

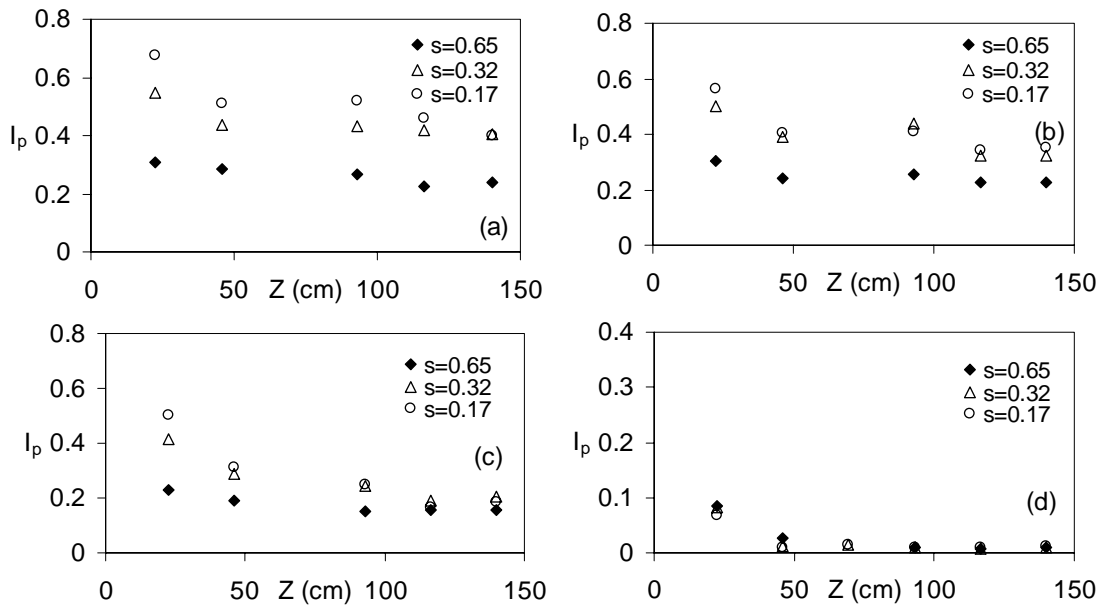


Figure IV.31: Pulse intensity as a function of bed length for different splits. $u_{l,mean}=0.15$ cm/s; $u_g=3$ cm/s (a) $P=360$ s; (b) $P=180$ s; (c) $P=60$ s; (d) $P=10$ s.

This is in agreement with observations of Boelhouwer (2001), who has remarked that the frequency of the liquid feed for periodic operation is limited to rather low values due to the instability of pulses. Although, and in coincidence with appreciations of Giakoumakis et al. (2005), it should be mentioned that the general statement put forward by Boelhouwer (2001) should be taken with care, and be grounded in more both hydrodynamic and reaction experiments. Even if the pulse intensity tends to zero and the holdup traces do not show a waving behavior, the instabilities in the liquid films may still have influence from the liquid feed perturbations, which are not reflected visually in the holdup traces. These local dynamic behaviors are not easily quantified and extracted from average values.

IV.2.2.2.2. EFFECT OF THE GAS VELOCITY

Similar qualitative conclusions obtained in the previous section arise from experiments under periodic operation for $u_g=1.4$ cm/s. The time required to drain the bed is longer; then, limits for slow and intermediate cycling shift towards longer cycle periods. Results suggest that limits between the different types of liquid flow modulation depend on the different factors examined, split, gas and mean liquid velocity. The transition region between slow and fast modulation, *i.e.*, the intermediate cycle periods, can then be broad.

As it was already mentioned, liquid holdup decreases with superficial gas velocity. Additionally, pulse intensity increases when the superficial gas velocity decreases, the highest possible being the one attained at $u_g = 0$ (not shown in the figures). For cycle periods greater than 180s (Figure IV.32a), this trend is clearly observed, particularly for the split $s= 0.17$. As cycle period decreases, the influence slowly disappears (Figures IV.32b-d).

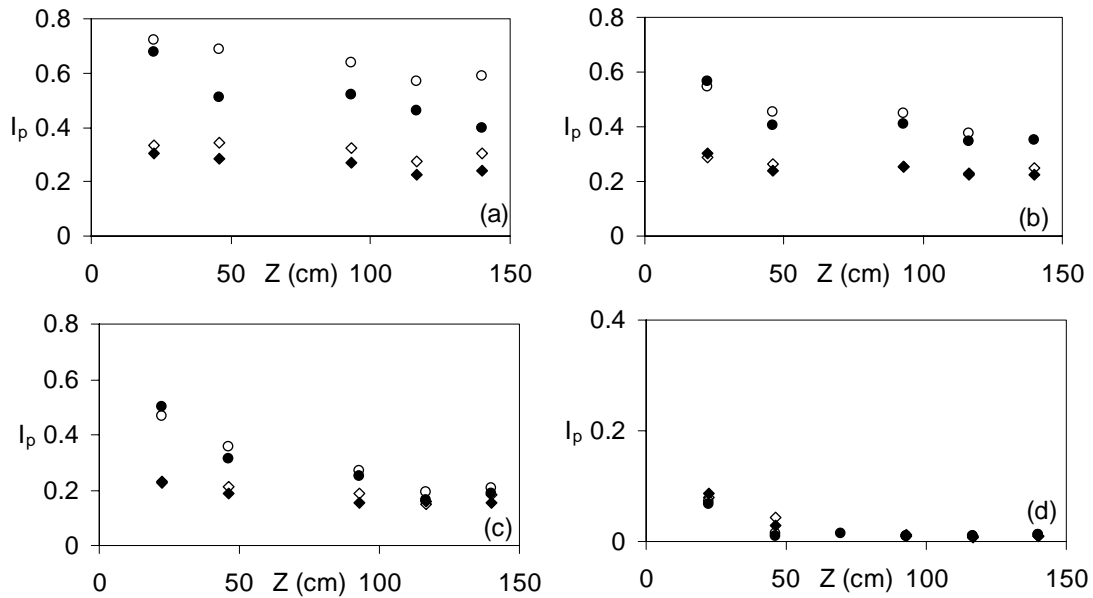


Figure IV.32: Pulse intensity as a function of bed length for different splits and superficial gas velocities, $u_{l,mean} = 0.15$ cm/s. (a) $P=180$ s; (b) $P=100$ s; (c) $P=60$ s; (d) $P=10$ s.

(\blacklozenge) $s=0.65; u_g=3.0$ cm/s; (\diamond) $s=0.65; u_g=1.4$ cm/s; (\bullet) $s=0.17; u_g=3.0$ cm/s; (\circ) $s=0.17; u_g=1.4$ cm/s.

IV.2.2.2.3. EFFECT OF THE MEAN LIQUID VELOCITY

For higher mean liquid velocities, higher liquid holdups are attained during the wet cycle. Besides, the liquid holdup during the dry cycle is also higher and longer cycle periods are required to reach the static liquid holdup. The time average liquid holdup increases for all cycle periods at $u_{l,mean} = 0.38$ cm/s and it is close to the corresponding liquid holdup attained under steady state operation ($\epsilon_{l,mean} = 0.174$).

Figure IV.33a-d points out that the mean liquid velocity has a negligible effect on the pulse intensity for almost all the examined operating conditions, except for the lowest cycle period shown. This trend is attributed to the low interaction between liquid and gas within the examined experimental conditions. Hence, the waving trace of the liquid holdup arises from a succession of wet and dry periods that do not increase significantly the interstitial fluid velocities; thus, not disturbing the free circulation of the other fluid. At very

short cycle periods and for a split of 0.65, it seems that a higher mean liquid velocity improves the liquid waves along the column.

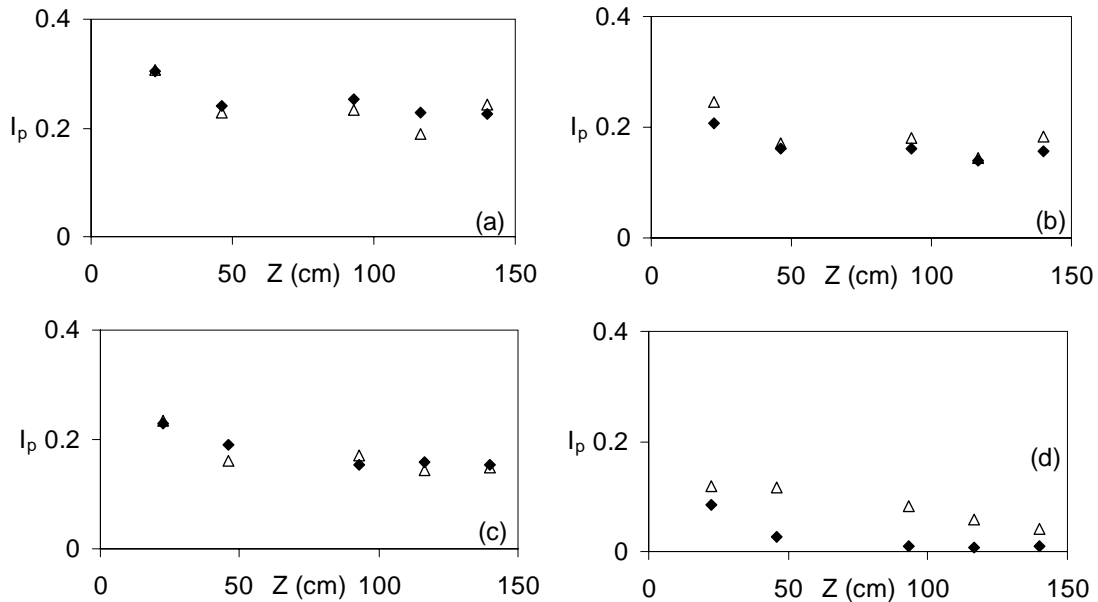


Figure IV.33: Pulse intensity as a function of bed length for different splits and mean superficial liquid velocities, $u_g = 3.0$ cm/s, $s = 0.65$. (a) $P = 180$ s; (b) $P = 100$ s; (c) $P = 60$ s; (d) $P = 10$ s.

(◆) $u_{l,mean} = 0.15$ cm/s; (Δ) $u_{l,mean} = 0.38$ cm/s.

This effect has also been observed by Giakoumakis et al. (2005) for cycle periods in the range of 4 to 8 s and at higher gas flow rates than those considered in the present work. These authors related this fact to a relatively higher interstitial gas velocity, which tends to homogenize liquid holdup variations along the column. The conditions examined in this work are far from pulsing or “pseudopulsing” flow as defined by Giakoumakis et al. (2005). The effect in this case does not seem to be related to the interstitial gas velocity. Moreover, larger pulse intensities are found for the lower gas velocity at the same mean liquid velocity (not included in the figure). For conditions shown in Figure IV.33d, the increase in pulse intensity due to a higher mean liquid velocity may likely arise from an increased liquid-

solid interaction and liquid film waving behavior due to inertia, which is more important for thicker liquid films.

IV.2.2.3. CORRELATION OF LIQUID HOLDUP UNDER PERIODIC OPERATION

To develop a methodology for estimating the time variation of the liquid holdup along the column during slow and intermediate ON-OFF liquid flow modulation, so as to use this information for modeling the behavior of a trickle bed reactor, a simple approach is presented. Taking into account that the transient behavior of the liquid holdup is mainly during the dry period of the cycle, since the increase in liquid holdup during the wet cycle is almost instantaneous, the approach is focused to represent the liquid holdup time profile during the time lag subsequent to the liquid flow interruption. When the liquid flow is halted, the signal decays in an almost exponential way. Hence, the time variation of ε_l was fitted to the following first order exponential decay expression:

$$\varepsilon_l = v_0 \cdot e^{\left(\frac{-t}{\chi}\right)} + v_1 \quad (\text{IV-11})$$

where t is the time and χ , v_0 and v_1 are constants obtained by fitting the experimental decays with Eq. IV-11. The characteristic parameter χ is dimensional and it should be expressed in the same dimension as the time. It is related to the rate of decay of the liquid holdup after liquid flow interruption. The lower is χ , the more abrupt is the drop of ε_l with time. From the analysis carried out in the previous section, it arises that the value of χ depends on the mean liquid velocity, the superficial gas velocity, the cycle period, the split, and the bed length.

The draining curves are fitted to Eq. IV-11 using Origin v7. Figures IV.34a-c show representative results of the goodness of fitting of the experimental data.

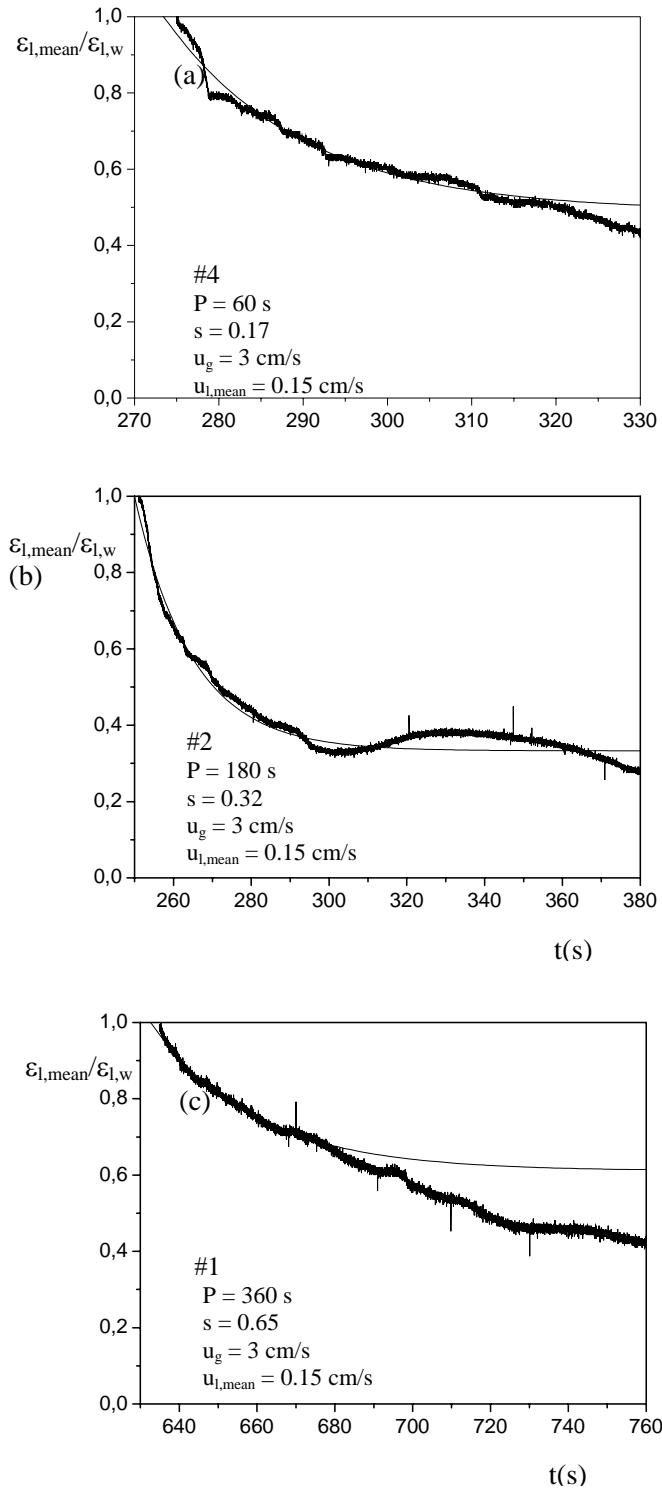


Figure IV.34: Fitting of liquid holdup decay during the dry cycle to Eq. IV-11.

The majority of the data fit the experimental decay as shown in Figure IV.34a-b. Figure IV.34c illustrates an example of the worse fitting obtained. Generally the worse fittings found were for electrode #1, where the decay is sharper and the liquid distribution is worse. For these cases, the initial part of the decay was given priority with respect to the asymptotic region.

The dimensional correlation proposed to relate the characteristic parameter χ with the variables that affect the liquid holdup decay is:

$$\chi = v_2' z^{v_3'} s^{v_4'} P^{v_5'} u_{l,\text{mean}}^{v_6'} u_g^{v_7'} \quad (\text{IV-12})$$

where v_2', v_3', \dots, v_7' are constants, s and P are the cycling parameters and z is the bed depth. Introducing the following dimensionless numbers:

$$Z = \frac{z}{L} \quad \Pi = \frac{P \cdot Q_{l,\text{mean}}}{V} = \frac{P \cdot u_{l,\text{mean}}}{L}$$

$$\text{Re}_{l,\text{mean}} = \frac{\zeta_l \cdot u_{l,\text{mean}} \cdot 2 \cdot R}{\mu_l} \quad \text{Re}_g = \frac{\zeta_g \cdot u_g \cdot 2 \cdot R}{\mu_g}$$

with L , the total bed length, R , the particle radius and ζ and μ , the density and viscosity of each fluid.

Then, equation IV-12 can be rewritten as:

$$\chi = v_2' \left(\frac{z}{L} \right)^{v_3'} s^{v_4'} \left(\frac{P \cdot u_{l,\text{mean}}}{L} \right)^{v_5'} \text{Re}_{l,\text{mean}}^{v_6'} \text{Re}_g^{v_7'} \quad (\text{IV-13})$$

A non-linear multivariate regression analysis was carried out using MathCad to estimate the coefficients v_i (see Appendix D). The expression obtained is:

$$\chi = e^{6.30} \left(\frac{z}{L} \right)^{0.49} \left(\frac{P \cdot u_{l,ss}}{L} \right)^{0.39} s^{0.18} \text{Re}_l^{-0.92} \text{Re}_g^{-0.21} \quad (\text{IV-14})$$

where χ is expressed in seconds. This correlation is valid within the conditions listed in Table IV.4. Figure IV.35 presents the value of χ estimated from experimental data vs. the one predicted by Eq. IV-14. The mean absolute relative error is 15% and the standard deviation calculated from experimental and predicted values is 12%.

Table IV.4: Validity range for the correlation proposed to estimate the characteristic parameter χ .

Variable	RANGE
Temperature	T = 20°C (+/-2°C)
Pressure	Atmospheric
Split	0.17 < s < 1
Cycle period	60 s < P < 900 s
Gas velocity	1.4 cm.s ⁻¹ < u _g < 3.0 cm.s ⁻¹
Liquid mean velocity	0.15 cm.s ⁻¹ < u _{l,mean} < 0.38 cm.s ⁻¹

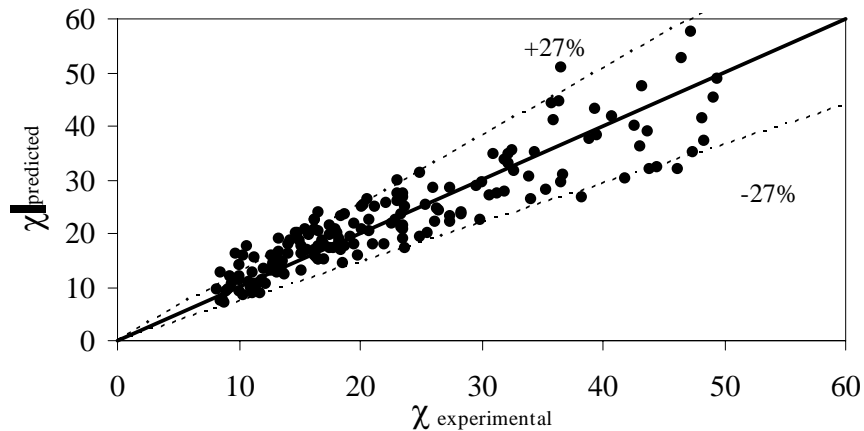


Figure IV.35: Predicted vs. experimental χ .

Developed correlation is used to analyze the influence of the different factors examined on the decay rate of the liquid holdup during the dry period of the cycle. General trends are presented in Figures IV.36-39.

Liquid drainage rate tends to decrease along the bed, especially for long cycle periods and low gas and mean liquid velocities. This is related to the decrease in pulse intensity, which is more evident for small splits.

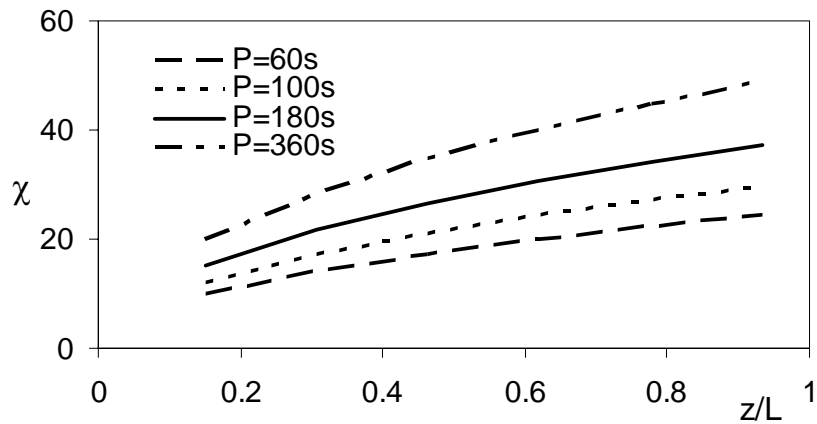


Figure IV.36: Effect of the cycle period on χ . $s=0.65$; $u_{l,\text{mean}} = 0.15$ cm/s, $u_g = 3.0$ cm/s.

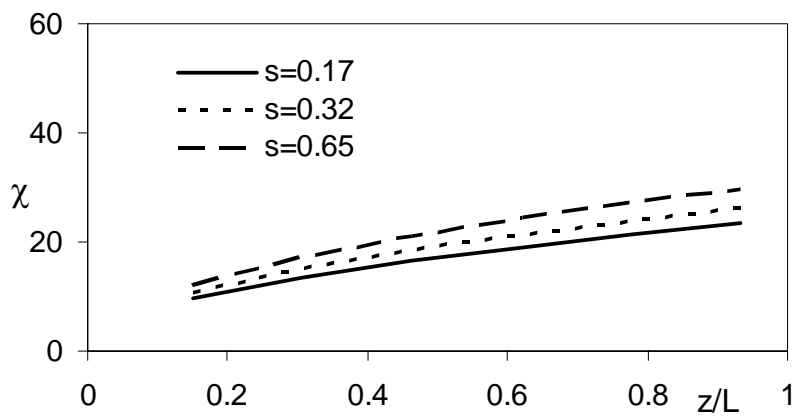


Figure IV.37: Effect of the split on χ . $P=100$ s; $u_{l,\text{ss}} = 0.15$ cm/s, $u_g = 1.4$ cm/s.

At a given cycle period, liquid holdup during the dry cycle decreases faster for lower splits (that is, for a higher $u_{l,w}$).

For cycling experiments performed with higher superficial gas velocities, remarkably higher decay rates are found, as shown in Figure IV.38. This is likely due to an increased gas-liquid interaction; *i.e.*, a more intense effect of the gas-drag on the liquid draining from the column.

The liquid holdup decreases faster when working with a higher mean liquid velocity, as shown in Figure IV.39. Larger mean liquid velocities imply larger velocities during the wet period, with the associated inertial effects that are reflected in a sharper draining velocity when the liquid feed is interrupted. All the effects are more evident for longer cycle periods.

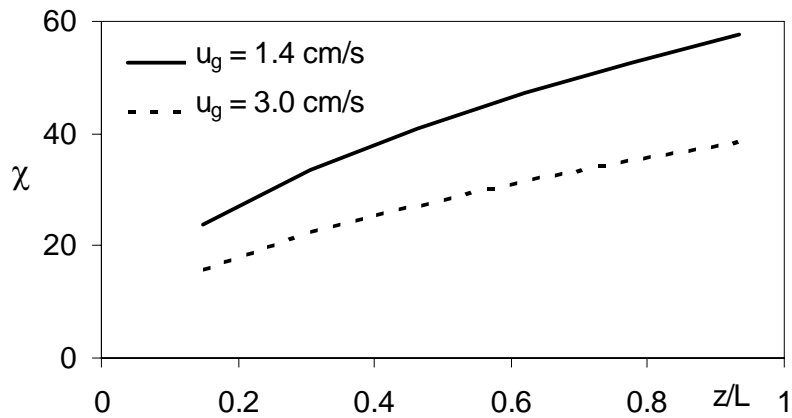


Figure IV.38: Effect of the superficial gas velocity on χ . $P = 360$ s; $s=0.65$; $u_{l,mean} = 0.15$ cm/s.

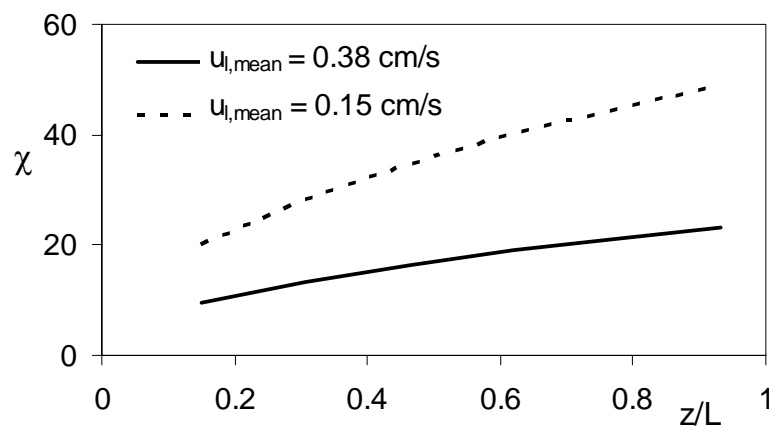


Figure IV.39: Effect of the mean superficial liquid velocity on χ . $P = 360$ s; $s=0.65$; $u_g = 3.0$ cm/s.

After calculating an estimation of parameter χ , it can be related with the liquid holdup as follows:

$$\frac{\varepsilon_l}{\varepsilon_{l,w}} = \frac{\varepsilon_{l,\min}}{\varepsilon_{l,w}} + \left(1 - \frac{\varepsilon_{l,\min}}{\varepsilon_{l,w}}\right) e^{\left(\frac{-t(s)}{\chi}\right)} \quad (\text{IV-15})$$

where $\varepsilon_{l,\min}$ is the liquid holdup achieved at the end of the dry cycle. For long cycle periods, $\varepsilon_{l,\min}$ can be reasonably replaced by the value of the static holdup. Liquid holdup during the wet period, $\varepsilon_{l,w}$, can be taken as the liquid holdup characteristic of steady state operation at a liquid velocity equal to $u_{l,w} = u_{l,\text{mean}}/s$. This value has been estimated using the correlation of Iliuta et al. (1999c). The same $\varepsilon_{l,w}$ can be used for the whole bed length. Figure IV.40 presents a comparison of liquid holdup decay predicted by Eq.IV-15 with the experimental data obtained for $P = 180\text{s}$, $s=0.17$, $u_{l,\text{mean}}=0.15\text{ cm/s}$ and $u_g=3\text{ cm/s}$. The fit is reasonably good and suggests that it can be used as an approximation to account for the decay region of the local instantaneous liquid holdup for modeling slow liquid flow modulation.

The correlation proposed was also compared with additional experiments to check if predictions could be interpolated without introducing an excessive error. Representative results are shown in Figure IV.41. This comparison shows that this approach predicts successfully experimental data obtained at slow liquid flow modulation within the range of operating conditions examined.

Figures IV.40 and IV.41 illustrate that the liquid holdup decay takes more time for longer bed depth, which results from the reduction in the extension of the liquid holdup plateau attained during the wet period. This effect was observed in the experiments even for very long cycle periods and was also reported by Boelhouwer (2001).

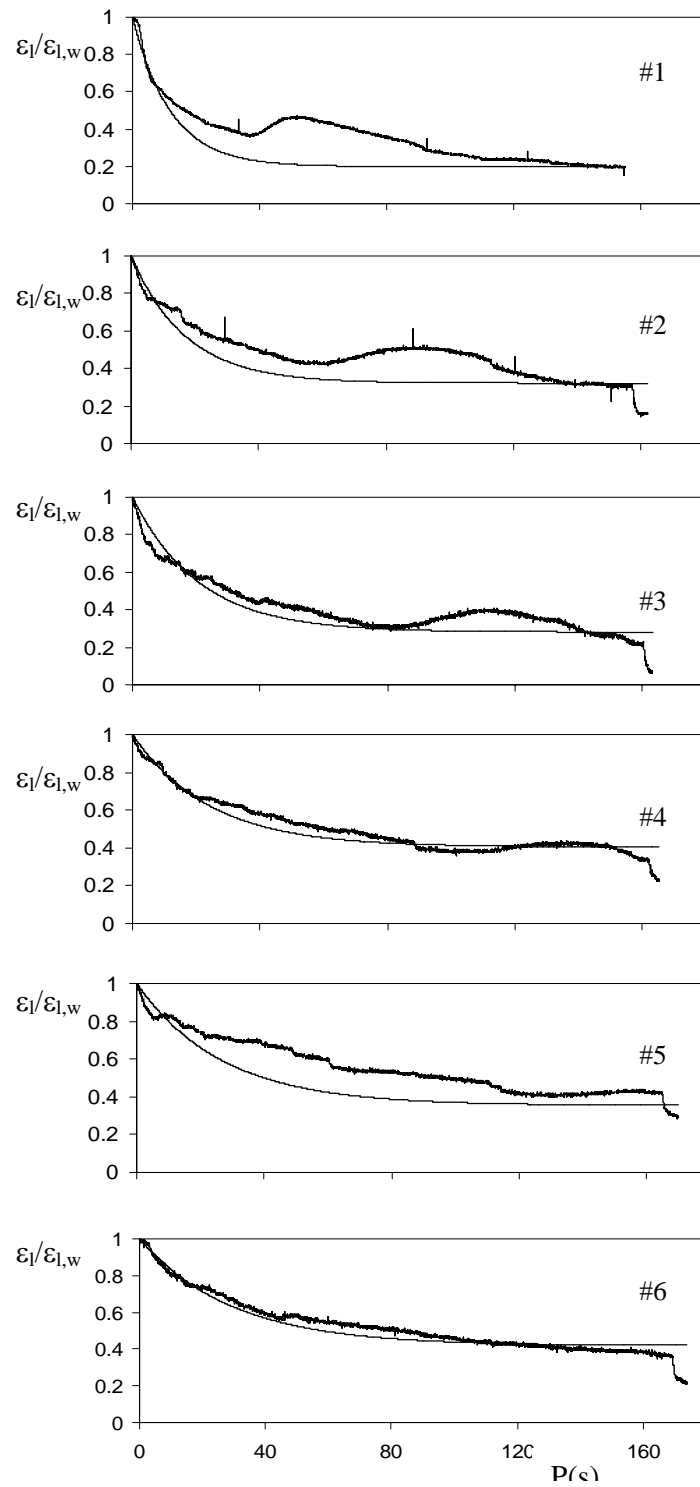


Figure IV.40: Simulated and experimental $\epsilon_I/\epsilon_{I,w}$ as a function of time. $P=180s$; $s=0.17$;
 $u_{l,mean}=0.15$ cm/s; $u_g=3.0$ cm/s

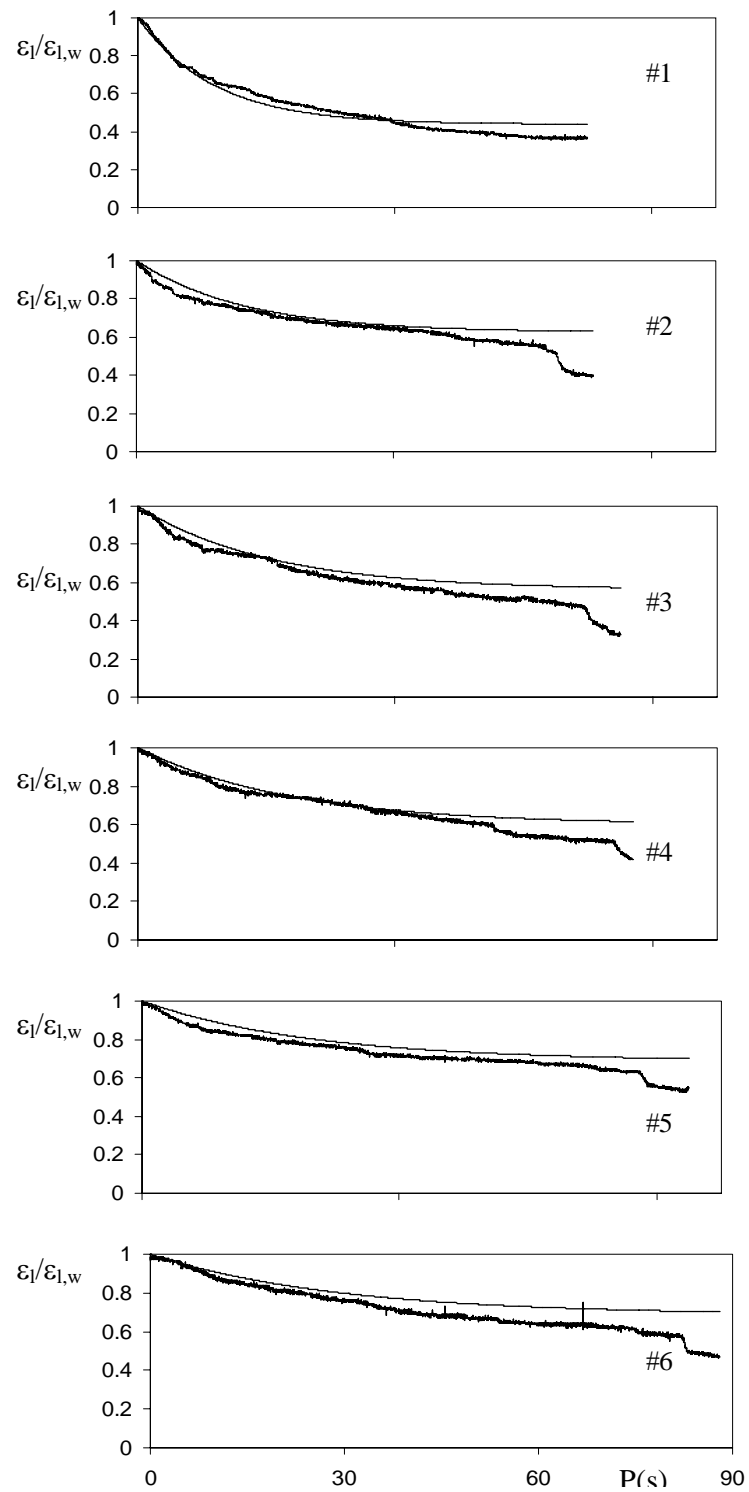


Figure IV.41: Simulated and experimental $\varepsilon_i/\varepsilon_{i,w}$ as a function of time. $P=180$ s; $s=0.65$;

$$u_{l,\text{mean}}=0.25 \text{ cm/s}; u_g=3.0 \text{ cm/s}$$

V. CONCLUSIONS

The ON-OFF liquid flow modulation strategy of periodic operation of trickle bed reactors has been studied by following two routes:

- ✚ The formulation and resolution of a comprehensive model, aimed at the particle scale, to describe the course of a gas-liquid reaction taking place within an isothermal heterogeneous porous catalyst subjected to alternating periods of zero and a given liquid velocity.
- ✚ A systematic characterization of the time evolution of the liquid holdup at different axial positions within a mini-pilot scale cold mock-up of a trickle bed reactor operation with ON-OFF liquid flow modulation.

The main conclusions arising from the work are summarized in the following sections.

V.1. MODELING PERIODIC OPERATION OF TRICKLE BED REACTORS AT THE PARTICLE SCALE

The approach followed for the modeling successfully aids the interpretation of many of the experimental trends obtained by several authors at intermediate to long cycle periods, characteristic of “slow” cycling. The enhancement vs. split curve presents a maximum at intermediate splits. Its location depends on system parameters.

In slow liquid flow modulation, the dynamics inside the catalyst particle and the accumulation of reactants largely determines reaction rate and should not be neglected in modeling the process. The model fails to predict experimental results for low cycle periods, characteristics of “fast” cycling, where the square-wave assumption considered to describe hydrodynamic and mass transport coefficient variations is no longer valid.

Present model contributes to define liquid flow modulation strategies that lead to improvements in reactor performance. Liquid flow modulation will not improve significantly reactor performance if mass transfer limitations are negligible or if the external

wetting efficiency is low, for the reference steady state. In addition, the ratio of reactant concentrations remarkably affects the possibility of enhancement. Therefore, experimental comparison among different cycling strategies should consider this parameter. Hence, great care should be taken while extrapolating results obtained in a differential reactor.

In brief, model results indicate that cycling will effectively enhance performance if the system has the following steady state characteristics:

- important internal and external mass transport resistances
- large external wetting of the particle

In addition, a suitable cycling strategy should avoid depletion of the liquid reactant.

V.1.1. EFFECT OF PERIODIC OPERATION ON CATALYSTS WITH DIFFERENT ACTIVE SITE DISTRIBUTIONS

The model was extended to study the impact of ON-OFF liquid flow modulation on the performance of different catalysts configuration. Egg shell catalysts present a better cycling performance in comparison with uniform catalysts. However, as in steady state operation, performance depends on working conditions, catalytic properties and on the type of liquid flow modulation imposed.

Even for conditions that lead to similar performance of egg shell and uniform catalyst under steady state operation, considerable differences may arise when liquid flow modulation is imposed. This is more relevant when internal and external mass transport resistances are significant.

Comparison between performances of egg shell catalysts with porous and non-porous inert core brings about interesting conclusions. At steady state, the nature of the inert core has no incidence on performance. However, with liquid flow interruption, differences become significant. The liquid reactant accumulates in the permeable core during the wet cycle and then diffuses and reacts during the dry cycle. As a result, the porous condition of the inert core should be clearly identified.

To sum up, internal limitations can be overcome with an appropriate catalyst design, whereas external resistances may be reduced with liquid flow modulation. Consequently,

catalyst design and mode of operation are related issues that need to be defined jointly to attain a significant performance enhancement.

V.2. EFFECT OF ON-OFF LIQUID FLOW MODULATION STRATEGY ON LIQUID HOLDUP TIME PROFILES MEASURED AT DIFFERENT BED DEPTHS

The time evolution of the liquid holdups within a min-pilot scale column packed with porous alumina particles generally used as catalyst supports were obtained through a conductimetric technique with minimal perturbations of the liquid flow.

Liquid holdups time variations are significantly modified along the column. The waving character of the liquid holdup measured close to the column top is attenuated along the bed and the degree of attenuation depends on the gas and liquid velocities and the cycling parameters, cycle period and split.

Pulse velocities, as defined by Boelhouwer (2001) and Giakoumakis et al. (2005), remain approximately constant for the whole bed length and depends on the gas and liquid velocities, the last inducing the largest effect.

From the analysis of characteristic liquid holdups attained during the wet and dry periods of the cycle, three regions can be distinguished:

- A region of slow liquid flow modulation, characterized by the attainment of asymptotic values of liquid holdups during the wet and dry cycles. The holdup reached during the wet period is roughly coincident with the one corresponding to the steady state liquid holdup for a liquid velocity equal to the one during the wet period, whatever the tested split. The static liquid holdup is approached only for dry cycle periods longer than 300s, within the experimental conditions tested. Otherwise, the attained asymptotic value is always larger than the static liquid holdup.
- A region of fast liquid flow modulation, characterized by similar limit values of liquid holdups attained for both the wet and dry period of the cycle. The waving trace of the liquid holdup is appreciated only in the upper part of the column, and the amplitude of the waves tends to zero in the lowest part, resembling a new “pseudo steady-state”. The average liquid holdup, determined from the whole trace is slightly

lower than the steady-state liquid holdup for a liquid velocity equal to the mean liquid velocity.

- A transition region between slow and fast liquid flow modulation, characterized by liquid holdup traces eminently transient, from which no asymptotic values are approached at any moment. For this region of cycle periods, a “quasi steady-state” approximation is not valid for any period of the cycling. The range of cycle periods comprised in this region can be significant. The transition limit suggested by Giakoumakis et al. (2005) falls always within this region, although it is closer to the zone defined as slow liquid flow modulation for high splits, and to the zone defined as fast liquid flow modulation for low splits.

Pulse intensities defined as Giakoumakis et al. (2005) generally decrease along the column, likely due to liquid axial dispersion, particularly since it is a bed of porous particles. For slow liquid flow modulation, the decrease is almost negligible. The holdup traces could be roughly assimilated to a deformed square wave and remain similar along the column, except for differences in the liquid holdup decay during the dry period of the cycle and for a slight decrease in the width of the plateau attained during the wet period.

For cycle periods in the transition region, the decrease in pulse intensities along the bed is significant. The holdup traces never look like a square wave, except for the closest position to the column entrance and for the highest split tested. The holdup traces resemble a saw-teeth wave or a triangular wave and the amplitude markedly decrease along the column.

For fast liquid flow modulation, cycle periods of 10s or less in this system, the pulse intensity depends particularly on the mean liquid velocity. For a low mean liquid velocity, the pulse intensities fall to zero everywhere in the column except close to the entrance. The holdup traces apparently reach a new steady-state situation, although dynamic characteristics of the fluctuations may not be equivalent to those characteristics of a steady-state operation. For a higher mean liquid velocity, the pulse intensities are significantly different from zero and decrease more progressively along the column.

To incorporate part of the measured hydrodynamic information into the model developed at the particle scale, it is useful to have a simple tool to recover the liquid holdup traces, at least for slow liquid flow modulation. In this case, the asymptotic value of the

liquid holdup during the wet period of the cycle is reached almost instantaneously, while during the dry period, the liquid holdup slowly decrease with time towards another asymptote, close or larger than the static liquid holdup. Hence, for slow modulation, the transient behavior is restricted mostly to the dry period of the cycle.

To describe the liquid holdup decay, a first order exponential decay function was proposed and the parameter to characterize the decay was determined by fitting in the time domain. Periods longer than 60s were considered since asymptotic values during both periods of the cycle were attained for these conditions with the three tested splits.

The characteristic parameter χ , used to describe the holdup decay was correlated with the variables that affect the decay, the gas and the liquid velocities, the cycle period, the split and the bed depth. Parameter χ depends particularly on:

- i) the gas velocity due to an increase in the gas-liquid interaction
- ii) the liquid velocity due to the increased inertial effects
- iii) the cycle period, associated to the extension of the dry period.
- iv) the split, related to the larger liquid velocity during the wet period for lower splits to get the same mean liquid velocity
- v) the bed depth, related to the amount of liquid retained along the column.

Using the developed correlation to estimate the characteristic parameter χ , the liquid holdup decay during the dry period of the cycle can be recovered using estimated holdups for the asymptotic values, in order to use this information for modeling the reaction outcome under slow liquid flow modulation at the particle scale and to extend the model to the integral reactor.

The relevance of internal processes (reaction, diffusion and accumulation) and external transport on overall performance has been highlighted. Internal limitations can be overcome with an appropriate catalyst design. External resistances may be reduced with liquid flow modulation. To elucidate whether periodic operation will lead to significant performance enhancement, internal processes had to be considered. To decide cycling strategies, a proper description of reactor hydrodynamics is required. The appropriate representation of both processes provides a useful tool to understand experimental studies and to set suitable conditions for reactor design and its operation.

APPENDIX A

A.1- DIMENSIONAL MASS BALANCES

Concentration profiles for a spherical particle considering radial and angular variations in the θ direction are evaluated in the model proposed in chapter II. Symmetry with respect to the angle Φ is considered. The wetting efficiency, is introduced in the model with respect to a critical value of the angle, θ_f , as $2f = 1 - \cos(\theta_f)$ as shown in Figure 1.

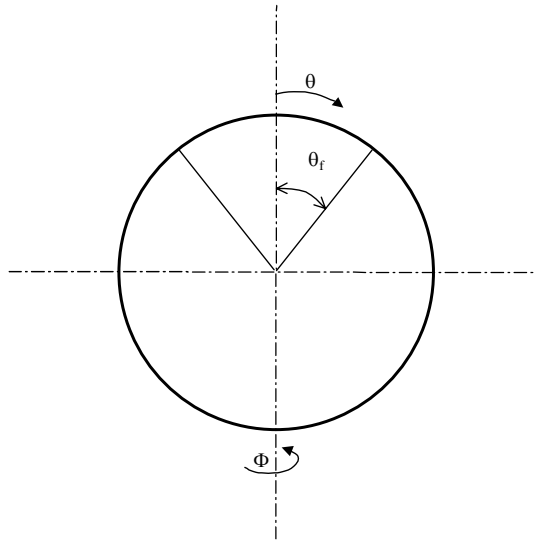


Figure A.1: Schematic indication of the critical angle that defines the wetted area of the catalyst for the model

According to the assumptions made in section II.1, the dimensional differential mass balances, boundary and initial conditions for both reactants inside the catalyst are:

$$\varepsilon_p \cdot \frac{\partial C_A}{\partial t} = D_A \left(\frac{\partial^2 C_A}{\partial r^2} + \frac{2}{r} \cdot \frac{\partial C_A}{\partial r} + \frac{\cot \theta}{r^2} \frac{\partial C_A}{\partial \theta} + \frac{1}{r^2} \frac{\partial^2 C_A}{\partial \theta^2} \right) - k \cdot C_A \cdot H(C_B) \quad (\text{A-1a})$$

$$\varepsilon_p \cdot \frac{\partial C_B}{\partial t} = D_B \cdot \left(\frac{\partial^2 C_B}{\partial r^2} + \frac{2}{r} \cdot \frac{\partial C_B}{\partial r} + \frac{\cot \theta}{r^2} \frac{\partial C_B}{\partial \theta} + \frac{1}{r^2} \frac{\partial^2 C_B}{\partial \theta^2} \right) - b.k.C_A \cdot H(C_B) \quad (\text{A-1b})$$

where $H(C_B)$ is the Heaviside function.

Initial and boundary conditions for the wet period of the cycling are:

$$t = 0 \quad C_i = 1 \quad i = A, B \quad (\text{A-2a})$$

$$r = 0 \quad \frac{\partial}{\partial r} C_i = \text{finite} \quad \text{if } 0 \leq \theta < \frac{\pi}{2} \text{ and } \frac{\pi}{2} < \theta \leq \pi \quad i = A, B \quad (\text{A-2b})$$

$$\frac{\partial}{\partial r} C_i = 0 \quad \text{if } \theta = \frac{\pi}{2} \quad i = A, B \quad (\text{A-2c})$$

$$r = 1 \quad \frac{\partial}{\partial r} C_A = \left(\frac{1}{kl_A \cdot a_{gl}} + \frac{1}{ks_A \cdot a_p} \right)^{-1} \cdot (1 - C_A) \quad \text{if } \theta \leq \theta_f \quad (\text{A-2d})$$

$$\frac{\partial}{\partial r} C_B = ks_B \cdot a_p \cdot (1 - C_B) \quad \text{if } \theta \leq \theta_f$$

$$C_A = 1 \quad \frac{\partial}{\partial r} C_B = 0 \quad \text{if } \theta > \theta_f \quad (\text{A-2e})$$

$$\theta = 0 \text{ or } \theta = \pi \quad \frac{\partial}{\partial \theta} C_i = 0 \quad i = A, B \quad (\text{A-2f})$$

A.2- FINITE DIFFERENCE APPROACH.

The method basically consists in replacing each derivative in the equation by a discretization (usually truncated Taylor series). The dimensionless reactant concentration, α , is a finite and continuous function of the independent variables ρ , θ and τ and it does not depend on the variable Φ (Figure A.1). The plane ρ - τ , is subdivided into sets of equal rectangles of sides $\Delta\rho$ and $\Delta\tau$, as shown in Figure A.2.

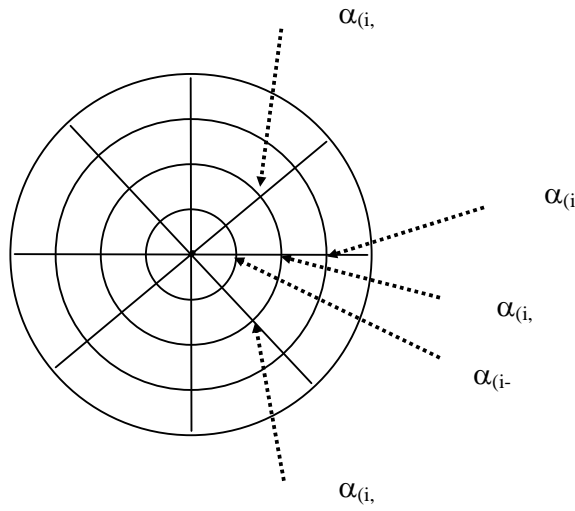


Figure A.2: Schematic discretization within the spherical particle.

According to Figure A.2, the value of α at the representative mesh point is denoted as: $\alpha_{i,j}$. Forward differences formulas were used for the temporal derivatives and central difference approximations were applied to the diffusion terms. Then, for each reactants, the explicit approximation are written as follows,

$$\frac{\partial \alpha}{\partial \tau} = \frac{\alpha_{i,j+1} - \alpha_{i,j}}{\Delta \tau} \quad (\text{A-3a})$$

$$\frac{\partial^2 \alpha}{\partial \rho^2} = \frac{\alpha_{i+1,j} - 2\alpha_{i,j} + \alpha_{i-1,j}}{\Delta \rho^2} \quad (\text{A-3b})$$

$$\frac{\partial \alpha}{\partial \rho} = \frac{\alpha_{i+1,j} - \alpha_{i-1,j}}{\Delta \rho} \quad (\text{A-3c})$$

The system is solved by an explicit method. Although this method is computationally simple, the time step is necessarily very small, because the process is valid (i.e. convergent and stable) only for $0 \leq \Delta \tau / \Delta \rho^2 \leq 1/2$ and $0 \leq \Delta \tau / \Delta \theta^2 \leq 1/2$. Additionally, $\Delta \rho$ and $\Delta \theta$ must be kept small in order to attain a reasonable accuracy.

As explained in section II.1, the mass balances, initial and boundary conditions are adimensionalized and results in Eqs. I-1a and I-1b. For non-zero values of r , there is no difficulty in expressing each derivative in terms of standard finite difference approximation, but as $\rho=0$, the right side appears to contain singularities. It can be demonstrated (Smith, 1985) that if the problem is symmetrical with respect to the origin, $\nabla^2 \rho_i$ in Eqs. A-1 can be replaced by:

$$\nabla^2 \alpha_i \Big|_{\rho=0} = 3 \cdot \frac{\partial^2 \alpha_i}{\partial \rho^2} \quad (\text{A-4})$$

In this model, symmetry only exists with respect to Φ direction. Therefore, for each time step, solution was first evaluated along the radial direction at $\theta = \pi/2$ and a finite value was found for $\rho \neq 0$. This value was then assigned to $\rho=0$ for every θ .

Several discretization strategies were tested to verify convergence of the results. A network with 21 grid points in the angular position and 111 in the radial position was finally selected.

The Fortran codes for solving the system in steady state (SS uniform catalyst partial wetting.for) and with liquid flow modulation (cycling uniform catalyst partial wetting.for) are included in the enclosed CD. They have filenames, which are self-referenced.

A.3- MODEL VERIFICATION

Steady state overall effectiveness factors for a spherical particle with complete wetting and with partial wetting were contrasted against generally accepted approximations for three-phase systems.

Steady state overall effectiveness factor for a gas limited, first order reaction that occurs in a completely wet particle can be easily estimated according to Ramachandran and Chaudhari, (1983) as:

$$\eta_{ss} = \frac{\eta_c}{1 + \frac{\eta_c \cdot k}{\left(\frac{1}{k l_A \cdot a_{gl}} + \frac{1}{k s_A \cdot a_p} \right)^{-1}}} = \frac{\eta_c}{1 + \frac{\eta_c \cdot \phi^2}{3 \cdot \text{Bi}_{gl,A}}} \quad (\text{A-5})$$

where η_c is the catalytic effectiveness factor.

For a particle with complete internal wetting and partial external wetting, the overall effectiveness factor can be evaluated as explained in section I.1.3.2. Taking into account Eq. A-5, it results in:

$$\eta_{ss} = f \cdot \frac{\eta_c}{1 + \frac{\eta_c \cdot \phi^2}{3 \cdot \text{Bi}_{gl,A}}} + (1-f) \cdot \eta_c \quad (\text{A-6})$$

Results obtained with the model are shown in Figure A.3 for different ratios of reactant concentration. Outcomes obtained from Eq. A-6 (indicated by the straight line) fully agree with those predicted by the model only when the liquid reactant is not completely consumed in any region of the particle. This situation arises at high values of C_B or small ξ . In fact, Eq. A-6 neither takes into account the liquid reactant depletion nor diffusion between the wet and the dry zones.

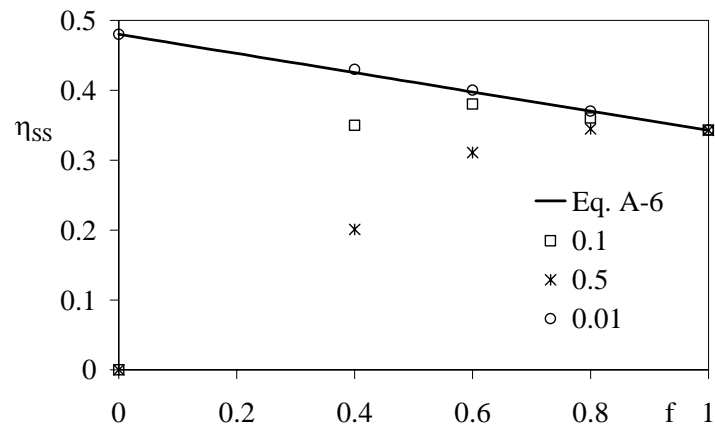


Figure A.3: Overall effectiveness factor as a function of the wetting efficiency for different values of ξ . $\phi=5$; $Bi_{glA,ss}=10$; $Bi_{lsB,ss}=100$; $\delta=0.5$.

APPENDIX B

Egg shell and uniform catalyst configuration performances are compared in a spherical particle with complete wetting. The discretization used was the one described by Eqs. A.3a-c. Resolution of the model presented in section III.1 is carried out with the procedure described in Appendix A. Computational time is considerably reduced since the analysis was done for $f = 1$.

For egg shell catalysts (in which the Thiele modulus is high), extreme care has to be taken with the discretization along the radial direction. Several discretization strategies were tested to verify convergence of the results. As an example, when the active layer corresponds to 10% of the particle radius, 301 grid points in the whole radial position were finally selected and 1001 for the egg shell, in which the active layer corresponds to 1% of the particle radius.

The Fortran codes for solving the system at steady state for a particle with a porous core (ES SS (1,1) P.for) and a non porous core (ES SS (1,1) NP.for), both with a (1,1) kinetic and for a particle with a porous core (ES SS (1,0) P.for) with a (1,0) kinetic are included in the enclosed CD.

Also, the Fortran codes for solving the system with liquid flow modulation for a particle with a porous core (ES cycling (1,1) P.for) and with a non porous core (ES cycling (1,1) NP.for), both with a (1,1) kinetic and for a particle with a porous core (ES cycling (1,0) P.for) with a (1,0) kinetic are also included in the CD.

APPENDIX C

The instantaneous conductances were measured through an 8-channel multiconductimeter. Table C.1 shows the correspondence between electrodes and channels. Channels 5 and 8 were not used in this work.

Table C.1: Channels used for measurements

ELECTRODE	#1	#2	#3	#4	#5	#6
CHANNEL	7	3	6	4	2	1

Data were collected with a frequency of 200 Hz. All the measurements were recorded in files listed in the following sections, which are included in the enclosed CD.

C.1. RTD EXPERIMENTS

Table C.2: Files with RTD experiments.

ul (cm/s)	ug (cm/s)	File name
0.07	1.4	ul1ug1.txt – ul1ug1b.txt
0.15	1.4	ul2ug1.txt – ul2ug1b.txt - ul2ug1c.txt
0.24	1.4	ul3ug1.txt – ul3ug1b.txt
0.38	1.4	ul4ug1.txt – ul4ug1b.txt
0.48	1.4	ul5ug1.txt – ul5ug1b.txt
0.66	1.4	ul7ug1.txt – ul7ug1b.txt
0.89	1.4	ul10ug1.txt – ul10ug1b.txt
0.07	3.0	ul1ug3.txt
0.15	3.0	ul2ug3.txt – ul2ug3b.txt
0.24	3.0	ul3ug3.txt – ul3ug3b.txt
0.38	3.0	ul4ug3.txt

0.48	3.0	ul5ug3.txt
0.58	3.0	ul6ug3.txt
0.75	3.0	ul8ug3.txt

C.2. STEADY STATE EXPERIMENTS

The value of κ is obtained as the ratio between the signal measured in the column working as a TBR and the signal measured when the column is flooded. Both measures are carried out the same day in order to avoid conductance variations mainly due to changes in dissolved salts concentration. An average value for the flooded column is used if measurements are repeated in the same day.

Table C.3: Files with steady state experiments.

ul (cm/s)	ug (cm/s)	File name (TBR)	File name (liquid full)
0.15	1.4	EE2ug1.txt	CI1.txt – CI1b.txt – CI1c.txt
		EE2ug1.txt	CI4.txt – CI4b.txt
0.24	1.4	EE3ug1.txt	CI1.txt – CI1b.txt – CI1c.txt
0.38	1.4	EE4ug1.txt – EE4ug1b.txt	CI1.txt – CI1b.txt – CI1c.txt
		EE4ug1c.txt	CI4.txt – CI4b.txt
0.48	1.4	EE5ug1.txt	CI1.txt – CI1b.txt – CI1c.txt
0.89	1.4	EE10ug1.txt	CI1.txt – CI1b.txt – CI1c.txt
0.15	3.0	EE2ug3.txt – EE2ug3b.txt	CI1.txt – CI1b.txt – CI1c.txt
		EE2ug3c.txt – EE2ug3d.txt	CI2.txt
0.24	3.0	EE3ug3.txt	CI1.txt – CI1b.txt – CI1c.txt
		EE3ug3b.txt	CI2.txt
0.38	3.0	EE4ug3.txt	CI2.txt
		EE4ug3b.txt	CI3.txt – CI3b.txt
0.48	3.0	EE5ug3.txt	CI2.txt
0.89	3.0	EE10ug3.txt	CI2.txt

C.3. CYCLING EXPERIMENTS

Cycling parameters are clearly indicated in the file name.

Table C.4: Files with cycling experiments.

$u_{l,mean}$ (cm/s)	u_g (cm/s)	File name (TBR)	File name (liquid full)
0.38	3.0	P=5_s=0,5_ulm4_ug3.txt	CI3.txt – CI3b.txt
0.15	3.0	P=5_s=0,65_ulm2-ug3.txt	CI4.txt – CI4b.txt
0.38	3.0	P=5_s=0,65_ulm4-ug3.txt	CI4.txt – CI4b.txt
0.15	3.0	P=10_s=0,17_ulm2_ug3.txt	CI2.txt
0.15	3.0	P=10_s=0,32_ulm2_ug3.txt	CI2.txt
0.15	3.0	P=10_s=0,65_ulm2_ug3.txt	CI2.txt
0.38	3.0	P=10_s=0,5_ulm4_ug3.txt	CI3.txt – CI3b.txt
0.38	3.0	P=10_s=0,65_ulm4_ug3.txt	CI3.txt – CI3b.txt
0.15	3.0	P=30_s=0,17_ulm2_ug3.txt	CI2.txt
0.15	3.0	P=30_s=0,32_ulm2_ug3.txt	CI2.txt
0.15	3.0	P=30_s=0,65_ulm2_ug3.txt	CI2.txt
0.15	3.0	P=30_s=0,65_ulm2_ug3b.txt	CI2.txt
0.15	3.0	P=60_s=0,17_ulm2_ug3.txt	CI2.txt
0.15	3.0	P=60_s=0,32_ulm2_ug3.txt	CI2.txt
0.15	3.0	P=60_s=0,65_ulm2_ug3.txt	CI2.txt
0.15	3.0	P=100_s=0,17_ulm2_ug3.txt	CI3.txt – CI3b.txt
0.15	3.0	P=100_s=0,32_ulm2_ug3.txt	CI3.txt – CI3b.txt
0.15	3.0	P=100_s=0,65_ulm2_ug3.txt	CI3.txt – CI3b.txt
0.38	3.0	P=100_s=0,5_ulm4_ug3.txt	CI3.txt – CI3b.txt
0.38	3.0	P=100_s=0,65_ulm4_ug3.txt	CI3.txt – CI3b.txt
0.15	3.0	P=180_s=0,17_ulm2_ug3.txt	CI2.txt
0.15	3.0	P=180_s=0,32_ulm2_ug3.txt	CI2.txt
0.15	3.0	P=180_s=0,65_ulm2_ug3.txt	CI2.txt
0.25	3.0	P=180_s=0,65_ulm0,25_ug3.txt	CI2.txt
0.38	3.0	P=180_s=0,65_ulm4_ug3.txt	CI2.txt

0.15	3.0	P=360_s=0,17_ulm2_ug3.txt	CI2.txt
0.15	3.0	P=360_s=0,32_ulm2_ug3.txt	CI2.txt
0.15	3.0	P=360_s=0,65_ulm2_ug3.txt	CI2.txt
0.15	3.0	P=900_s=0,65_ulm2_ug3.txt	CI2.txt
0.15	1.4	P=5_s=0,32_ulm2-ug120.txt	CI4.txt – CI4b.txt
0.15	1.4	P=5_s=0,65_ulm2-ug120.txt	CI4.txt – CI4b.txt
0.38	1.4	P=5_s=0,5_ulm4-ug120.txt	CI4.txt – CI4b.txt
0.38	1.4	P=5_s=0,65_ulm4-ug120.txt	CI4.txt – CI4b.txt
0.15	1.4	P=10_s=0,17_ulm2-ug120.txt	CI4.txt – CI4b.txt
0.15	1.4	P=10_s=0,32_ulm2-ug120.txt	CI4.txt – CI4b.txt
0.15	1.4	P=10_s=0,65_ulm2-ug120.txt	CI4.txt – CI4b.txt
0.38	1.4	P=10_s=0,5_ulm4-ug120.txt	CI4.txt – CI4b.txt
0.38	1.4	P=10_s=0,65_ulm4-ug120.txt	CI4.txt – CI4b.txt
0.15	1.4	P=30_s=0,17_ulm2-ug120.txt	CI4.txt – CI4b.txt
0.15	1.4	P=30_s=0,32_ulm2-ug120.txt	CI4.txt – CI4b.txt
0.15	1.4	P=30_s=0,65_ulm2-ug120.txt	CI4.txt – CI4b.txt
0.15	1.4	P=30_s=0,65_ulm4-ug120.txt	CI4.txt – CI4b.txt
0.15	1.4	P=60_s=0,17_ulm2-ug120.txt	CI4.txt – CI4b.txt
0.15	1.4	P=60_s=0,32_ulm2-ug120.txt	CI4.txt – CI4b.txt
0.15	1.4	P=60_s=0,65_ulm2-ug120.txt	CI4.txt – CI4b.txt
0.38	1.4	P=60_s=0,5_ulm4-ug120.txt	CI4.txt – CI4b.txt
0.38	1.4	P=60_s=0,65_ulm4-ug120.txt	CI4.txt – CI4b.txt
0.15	1.4	P=100_s=0,17_ulm2-ug120.txt	CI4.txt – CI4b.txt
0.15	1.4	P=100_s=0,32_ulm2-ug120.txt	CI4.txt – CI4b.txt
0.15	1.4	P=100_s=0,65_ulm2-ug120.txt	CI4.txt – CI4b.txt
0.38	1.4	P=100_s=0,5_ulm4-ug120.txt	CI4.txt – CI4b.txt
0.38	1.4	P=100_s=0,65_ulm4-ug120.txt	CI4.txt – CI4b.txt
0.42	1.4	P=100_s=0,73_ulm0,42-ug120.txt	CI4.txt – CI4b.txt
0.15	1.4	P=180_s=0,17_ulm2-ug120.txt	CI4.txt – CI4b.txt
0.15	1.4	P=180_s=0,32_ulm2-ug120.txt	CI4.txt – CI4b.txt
0.15	1.4	P=180_s=0,65_ulm2-ug120.txt	CI4.txt – CI4b.txt

0.38	1.4	P=180_s=0,5_ulm4-ug120.txt	CI4.txt – CI4b.txt
0.38	1.4	P=180_s=0,65_ulm4-ug120.txt	CI4.txt – CI4b.txt
0.15	1.4	P=360_s=0,17_ulm2-ug120.txt	CI4.txt – CI4b.txt
0.15	1.4	P=360_s=0,32_ulm2-ug120.txt	CI4.txt – CI4b.txt
0.15	1.4	P=360_s=0,65_ulm2-ug120.txt	CI4.txt – CI4b.txt
0.38	1.4	P=360_s=0,65_ulm4-ug120.txt	CI4.txt – CI4b.txt
0.15	0.0	P=5_s=0,65_ulm2-ug0.txt	CI2.txt
0.38	0.0	P=5_s=0,65_ulm4-ug0.txt	CI2.txt
0.15	0.0	P=10_s=0,65_ulm2-ug0.txt	CI2.txt
0.38	0.0	P=10_s=0,65_ulm4-ug0.txt	CI2.txt
0.15	0.0	P=60_s=0,65_ulm2-ug0.txt	CI2.txt
0.38	0.0	P=60_s=0,65_ulm4-ug0.txt	CI2.txt

APPENDIX D

A multivariate polynomial regression available as a package in MathCad 2001 is applied to establish the dependence between χ and the cycle period, the split, the mean superficial liquid velocity, the superficial gas velocity and the bed length.

The REGRESS function for high dimensional form takes three arguments:

- a real array, **M**: each column of which represents data corresponding to one of the independent variables;
- a real vector, **V**: representing the data for the dependent variable;
- a positive integer, **n**: specifying the degree of the polynomial function to which the data will be fit.

This function tends to fit the data to a single polynomial expression. The output of the REGRESS function gives the estimated values for the specific coefficients associated with individual monomial terms in the model function. The detailed program code is available in the help section of the software.

In this particular case, there are five variables, thus the fitting polynomial expression is:

$$p(a, b, c, d, e) := \sum_{i=0}^5 \text{coeffs}_i \cdot a^{I_{i,0}} \cdot b^{I_{i,1}} \cdot c^{I_{i,2}} \cdot d^{I_{i,3}} \cdot e^{I_{i,4}}$$

The parameter χ seems to follow a power law expression. Consequently, the variables a, b, c, d and e are expressed as the natural logarithms of the dimensionless cycle period, split, $u_{l,\text{mean}}$, u_g and bed length, respectively. In this way, the functionality for $\ln(\chi)$ is obtained and subsequently, χ is easily recovered.

NOTATION

a_{gl}	gas-liquid interfacial area per unit volume of catalyst particle (m^{-1})
a_p	external surface area per unit volume of catalyst particle (m^{-1})
A/L	effective cell constant in the electrode (m)
b	stoichiometric coefficient for B
Bi	Biot number
C	fluid phase concentration in the catalyst ($kmol/m^3$)
D_c	column diameter (m)
D	effective diffusivity ($m^2 \cdot s^{-1}$)
$E(t)$	residence time distribution function
$Eö$	Eötvös number ($=\zeta_1 \cdot g \cdot dp^2 / \sigma_l$)
f	wetting efficiency
F	fraction of dry period of the cycle (defined in section II.2.1)
Ga	Galileo number ($=8 \cdot R^3 \cdot \zeta^2 \cdot g / \mu^2$)
H	Heaviside function $H(\alpha_B) = \begin{cases} 0 & \text{if } \alpha_B \leq 0 \\ 1 & \text{if } \alpha_B > 0 \end{cases}$
k	reaction rate constant ($kmol \cdot m^{-3} \cdot s^{-1}$)
kl	overall gas liquid mass transfer coefficient (m/s)
ks	liquid to particle mass transfer coefficient (m/s)
l	distance between electrodes (m)
L	total bed length (m)
P	dimensional cycle period (s)
Q	volumetric flow rate ($m^3 \cdot s^{-1}$)
r	radial variable in the catalyst (m)
Re	Reynolds number ($=\zeta \cdot u \cdot 2 \cdot R / \mu$)
R	radius of the catalyst particle (m)
$R(t)$	signal response of the conductimetric probes (arbitrary units)
s	split
t	time (s)
u	velocity (m/s)

V	dimensionless active layer volume
z	bed length (m)
Z	dimensionless bed length ($=z/L$)

Greek letters

α	dimensionless reactant concentration
χ	parameter that characterize the liquid holdup decay (s)
δ	model parameter ($=D_B/D_A$)
ε	enhancement factor (defined in Eq. II-5)
ε_b	bed porosity
ε_l	total liquid holdup
ε_p	porosity in the catalyst particle
ε_s	static liquid holdup
ϕ	Thiele modulus
γ	parameter defined in Eq. I-4.
γ_l	conductivity ($S.cm^{-1}$)
κ	normalized conductivity
μ	viscosity (Pa.s)
η	overall effectiveness factor
Π	dimensionless cycle period ($=P.u_{l,mean}/L$)
θ	angular variable in the catalyst
θ_l	mean residence time (s)
ρ	dimensionless radial variable in the catalyst
σ	surface tension (Pa.s)
τ	dimensionless time ($=t.D_A/(R^2 \cdot \varepsilon_p)$)
ξ	model parameter ($=b.C_A^*/C_{B0}$)
ψ	instantaneous conductivity
ζ	density ($kg.m^{-3}$)

Subscripts

0	initial value
A	gaseous reactant

B	non volatile liquid reactant
c	dimensionless radius of the non-active core
cyc	cycling
es	egg shell catalyst
g	gas
l	liquid
mean	referred to the mean liquid velocity
nw	non wet cycle
ss	steady state
un	uniform active catalyst
w	wet cycle

Superscripts

*	saturation value
---	------------------

Acronyms

PBC	packed bubble column
RTB	reactores trickle-bed
RTD	residence time distribution
TBR	trickle bed reactor

REFERENCES

- Al-Dahhan, M.; Larachi, F.; Dudokovic, Laurent, M. (1997) A. High-pressure trickle-bed reactors: A Review, *Ind. Eng. Chem. Res.*, 36, 3292-3314
- An, W.; Zhang, Q.; Ma, Y.; Chuang, K. (2001) Pd-based catalysts for catalytic wet oxidation of combined Kraft pulp mill effluents in a trickle bed reactor. *Catalysis Today*, 64, 289-296.
- Aris, R. (1975) *The mathematical theory of diffusion and reaction in permeable catalysts*. V.1, Oxford University Press, London
- Banchero, M., Manna, L., Sicardi, S., Ferri, A. (2004) Experimental investigation of fast-mode liquid modulation in a trickle-bed reactor, *Chem. Eng. Science*, 59, 4149–4154.
- Basic, A., Dudukovic, M. P. (1995). Liquid hold-up in rotating packed beds: Examination of the film flow assumption. *AIChE J.*, 41, 301–316.
- Beaudry, E.G.; Duduković, M.P.; Mills, P.L. (1987) Trickle-bed reactors: liquid diffusional effects in a gas-limited reaction. *AIChE J.*, 33, 1435-1447.
- Boelhouwer, J.G. (2001) *Nonsteady operation of trickle-bed reactors: Hydrodynamics, mass and heat transfer*, PhD Thesis, Technische Universiteit Eindhoven, The Netherlands.
- Borremans et al. (2004) Liquid flow distribution and particle-fluid heat transfer in trickle bed reactors: the influence of periodic operation. *Chem. Eng. Science*, 43, 1403-1410
- Burghardt, A., Bartelmus, G., Gancarzyk, A. (1999) Hydrodynamics of pulsing flow in three-phase chemical reactors. *Chem. Eng. Process.*, 38, 411-426

-
- Burns, J.R., Jamil, J.N., Ramshaw, C. (2000) Process intensification: operating characteristics of rotating packed beds – determination of liquid hold-up for a high-voidage structured packing. *Chem. Eng. Science*, 55, 2401–2415.
 - Cassanello, M.C. (1992) *Caracterización Fluidodinámica de Reactores Trifásicos de Lecho Fijo*, Tesis de Doctorado, Universidad de Buenos Aires, Argentina.
 - Castellari, A.T., Haure, P.M. (1995) Experimental study of the periodic operation of a trickle-bed reactor. *AIChE Journal*, 41, 1593–1597.
 - Charpentier, J., Favier, M. (1975) Some liquid holdup experimental data in trickle bed reactors for foaming and non-foaming hydrocarbons. *AIChE J.*, 21, 1213.
 - Dietrich, W., Grunewald, M., Agar, D. (2005) Dynamic modelling of periodically wetted catalyst particles. *Chem. Eng. Science*, 60, 6254-6261
 - Dudukovic, M., Larachi, F., Mills, P. (2002) Multiphase catalytic reactors a perspective on current knowledge and future trends. *Catalysis Reviews*, 44, 123–246.
 - Dudukovic, M.P. (1977) Catalyst effectiveness factor and contacting efficiency in Trickle Bed reactors. *AIChE J.*, 23, 376.
 - Dudukovic, M.P., Larachi, F., Mills, P.L. (2002) Multiphase Catalytic Reactors: A Perspective on Current Knowledge and Future Trends. *Catalysis Reviews*, 44, 123–246.
 - Fogler, H. S., *Elements of Chemical Reaction Engineering*, Prentice Hall International, 1992, p. 628.
 - Fraguío, M.S., Muzen, A., Martínez, O., Bonelli, P., Cassanello, M. (2004) Catalytic wet oxidation of ethanol in an integral trickle-bed reactor operated with liquid flow modulation. *Latin American Applied Res.*, 34, 11–16.
 - Gabarain, L., Castellari, A., Cechini, J., Tobolski, A., Haure, P.M. (1997) Analysis of rate enhancement in a periodically operated trickle-bed reactor. *AIChE Journal*, 43, 166–172.

-
- Gavriilidis, A.; Varma A.; Morbidelli, M. (1993) Optimal distribution of catalyst in pellets. *Catalysis Reviews-Science and Engineering*, 35, 399-456.
 - Giakoumakis, D., Kostoglou, M., Karabelas, A.J. (2005) Induced pulsing in trickle beds-characteristics an attenuation pulses. *Chem. Eng. Science*, 60, 5185-5199
 - Gianetto, A., Silveston, P.L. (1986) *Multiphase Chemical Reactors*, Hemisphere Publ. Corp., Washington D.C.
 - Gianetto, A., Specchia, V. (1992) Trickle Bed reactors: state of the art and perspectives. *Chem. Eng. Science*, 47, 3197-3213.
 - Goto, S. and Smith, J.M., (1975) Trickle bed reactor performance: 1.Hold-up and mass transfer effects. *AIChE J.* 21, 6, 706-713.
 - Gupta R. (1985) Pulsed flow vapour-liquid reactor. *US Pat.* 4, 526, 757
 - Hanika, J., Kucharová, M., Kolena, J., Smejkal, Q. (2003) Multi-functional trickle bed reactor for butylacetate synthesis. *Catalysis Today*, 79–80, 83–87.
 - Harold, M.P., Ng K.M. (1987) Effectiveness enhancement and reactant depletion in a partially wetted catalyst. *AIChE J.*, 33 (9), 1448-1465
 - Haure P, Hudgins RR, Silveston PL (1989) Periodic operation of a trickle bed. *AIChE J.* 35: 1437-1444
 - Herskowitz, M. (1981) Wetting efficiency in trickle-bed reactors: its effect on the reactor performance. *Chem. Eng. J.*, 22, 167-175
 - Herskowitz, M. (2001) *Trickle-Bed Reactors and Hydrotreating Processes. Design, Analysis and Applications. Lecture Series given in YPF/Repsol, Buenos Aires, Argentina.*
 - Horowitz, G.I., Martínez, O.M., Cukierman, A.L., Cassanello, M.C. (1999) Effect of the catalyst wettability on the performance of a trickle-bed reactor for ethanol oxidation as a case study. *Chem. Eng. Science*, 54, 4811.

-
- Houserová, P.; Hanika, J. Experiments with periodically operated liquid feed stream. Proc. of CHISA 2002 - 15th Int. Congress of Chemical and Process Eng., Praga, Zchech Republic, 2002.
 - Iliuta, I., Larachi F., Bernard P., Grandjean, A., Wild, G. (1999a) Gas-liquid interfacial mass transfer in trickle-bed reactors: state-of-the-art correlations. Chem. Eng. Science, 54 5633-5645.
 - Iliuta, I., Larachi, F., Grandjean, B. (1999b) Catalyst wetting in trickle-flow reactors. Trans. IChemE, 77, part A. The neural network based correlation, developed using NNFit software is available at the web site address: <http://www.gch.ulaval.ca/~nnfit>
 - Iliuta, I., Ortiz-Arroyo, A., Larachi, F., Grandjean, B., Wild, G. (1999c) Hydrodynamics and mass transfer in trickle-bed reactors: an overview. Chem. Eng. Science, 54, 5329-5337. The neural network based correlation, developed using NNFit software is available at the web site address: <http://www.gch.ulaval.ca/~nnfit>
 - Khadilkar, M., Al-Dahhan, M.H., Dudukovic, M.P. (1999) Parametric study of unsteady-state flow modulation in trickle-bed reactors. Chem. Eng. Science, 54, 2585–2595.
 - Khadilkar, M.R., Al-Dahhan, M.H., Dudukovic, M.P. (2005) Multicomponent flow-transport-reaction modeling of trickle bed reactors: application to unsteady state liquid flow modulation. Ind. Eng. Chem. Res., 44, 6354–6370.
 - Khadilkar, M.R., Wu, Y. X., Al-Dahhan, M. H., Dudukovic, M. P. (1996) Evaluation of trickle bed reactor models for a liquid limited reaction. Chem. Eng. Science, 51, 2139-2148.
 - Kluytmans, J.H.J., Markusse, A.P., Kuster, B.F.M., Marin, G.B., Schouten, J.C. (2000) Engineering aspects of the aqueous noble metal catalysed alcohol oxidation. Catalysis Today, 57, 143–155.

-
- Kolaczowski, S., Plucinski, P., Beltran, F., Rivas, F., Mc Lurgh, D. (1999) Wet air oxidation: a review of process technologies and aspects in reactor design. *Chem. Eng. J.*, 73, 143-160.
 - Kouris, Ch., Neophytides, St., Vayenas, C. G., Tsamopoulos, J. (1998) Unsteady state operation of catalytic particles with constant and periodically changing degree of external wetting. *Chem. Eng. Science*, 53, 3129–3142.
 - Lange, R. (1978) Beitrag zur experimentellen Untersuchung und modellierung von teilprozessen für katalytische dreiphasenreaktionen im rieselbettreaktor. PhD. Thesis, Technical university of Leuna-Merseburg, Germany
 - Lange, R., Gutsche, R., Hanika, J. (1999). Forced periodic operation of a trickle-bed reactor. *Chem. Eng. Science*, 54, 2569–2573.
 - Lange, R., Hanika, J., Stradiotto, D., Hudgins, R.R., Silveston, P.L. (1994) Investigations of periodically operated trickle-bed reactors. *Chem. Eng. Science*, 49, 5615–5622.
 - Lange, R.; Schubert, M.; Dietrich, W.; Grunewald, M. (2004) Unsteady-state operation of trickle-bed reactors. *Chem. Eng. Science.*, 59, 5355–5361.
 - Larachi, F., Belfares, L., Grandjean, B. (2001) Prediction of liquid-solid wetting efficiency in trickle flow reactors. *Int. Comm. Heat mass transfer*, 28, 5, 595-603
 - Larachi, F., Belfares, L., Iliuta, I., Grandjean, B. (2003) Heat and Mass Transfer in Cocurrent Gas-Liquid Packed Beds. Analysis, Recommendations, and New Correlations. *Ind. Eng. Chem. Res.*, 42, 222-242.
 - Larachi, F., Laurent, A., Midoux, N., Wild, G. (1991). Experimental study of a trickle-bed reactor operating at high pressure: Two-phase pressure drop and liquid saturation. *Chem. Eng. Science*, 46, 1233-1246.
 - Lee, C.K., Bailey J.E. (1974) Diffusion waves and selectivity modifications in cyclic operation of porous catalyst, *Chem. Eng. Science*, 29, 1157-1163

-
- Lee, J., Hudgins, R., Silveston, P. (1995) A cycled trickle-bed reactor for SO₂ oxidation, *Chem. Eng. Science*, 50, 2523-2530.
 - Lekhal, A., Glasser, J., Khinast, J. (2001) Impact of drying on the catalyst profile in supported impregnation catalysts. *Chem. Eng. Science*, 56, 4473-4487.
 - Lemcoff, N.O., Cukierman, A.L., Martínez, O.M. (1988) Effectiveness factor of partially wetted catalyst particles: evaluation and application to the modeling of trickle-bed reactors. *Cat. Rev. Sci. Eng.*, 30, 393.
 - Levine, I., *Physical Chemistry*, McGraw-Hill, 5th Edition, 1995.
 - Liu G., Duan, Y., Wang, Y., Wang L., Mi, Z. (2005) Periodically operated trickle-bed reactor for EAQs hydrogenation: Experiments and modeling. *Chem. Eng. Science*, 60, 6270-6278
 - Lutran, P.G., Ng, K.M., Delikat, E.P. (1991) Liquid distribution in trickle beds. An experimental study using computer-assisted tomography. *Ind. Eng. Chem. Res.*, 30, 1270-1280.
 - Marchot, P., Toye, D., Crine, M., Pelsser, A.-M., L'Homme, G. (1999) Investigation of liquid maldistribution in packed columns by X-ray tomography. *Trans. IChemE*, 77, 511-518.
 - Martinez, O., Cassanello, M., Cukierman, A. (1994) Three phase fixed bed catalytic reactors: Application to hydrotreatment processes. *Trends Chem. Eng.*, 2, 393-453.
 - Massa, P., Ayude, M.A., Ivorra, F., Fenoglio, R., Haure, P. (2005) Phenol oxidation in a periodically operated trickle bed reactor. *Catalysis Today*, 107-108, 630-636.
 - Maucci, A., Briens, C., Martinuzzi, R., Wild, G. (2001) Modeling of transient particle-liquid mass transfer in liquid and liquid-solid systems. *Chem. Eng. Sc.* 56, 4555-4570.
 - Mears, D. (1974) The role of liquid holdup and effective wetting in Trickle Bed Reactors. 3rd. Int. Symp. Chem. React. Eng., Adv. Chem. Ser., 133, 218

-
- Mills, P. L. and Dudukovic, M. P. (1984) A comparison of current models for isothermal trickle-bed reactors: Application to a model reaction system, in chemical and reacting reactor modeling. ACS Symposium Series, 185th Meeting, pp. 37-59.
 - Mills, P.L., Chaudhari, R.V. (1997) Multiphase catalytic reactor engineering and design for pharmaceuticals and fine chemicals. *Catalysis Today*, 37, 367–404.
 - Morbidelli, M; Varma, A. (1983) On shape normalization for non-uniformly active catalyst pellets-II. *Chem. Eng. Science*, 38, 297.
 - Murugesan, T., Sivakumar, V. (2005) Liquid holdup and interfacial area in cocurrent gas-liquid upflow through packed beds. *J. Chem. Eng. Japan*, 38, 229-242.
 - Muzen, A. (2005) Estudio de reactores trickle-bed: aplicación a la oxidación limpia de compuestos orgánicos, PhD thesis, Universidad de Buenos Aires, Argentina.
 - Muzen, A., Cassanello, M. (2005) Liquid Holdup in Columns Packed with Structured Packings: Countercurrent vs. Cocurrent Operation, *Chem. Eng. Science*, 60, 6226–6234.
 - Nauman, E., Buffham, B. (1983) *Mixing in Continuous Flow System*, J. Wiley & Sons Inc., New York.
 - Nemeč, D. (2002) Pressure drop and liquid holdups in packed beds with cocurrent two phase flow at high pressures. Doctoral thesis. Ljubljana, Slovenia.
 - Nigam, K., Larachi, F. (2005) Process intensification in trickle-bed reactors. *Chem. Eng. Science*, 60, 5880-5894.
 - Nigam, K. D. P. Kundu, A. (2005) Trickle bed reactor. In *Encyclopedia of Chemical Processing (ECHP)*, Marcel Dekker, New York, U.S.A., in press.
 - Pironti, F., Mizrahi, D., Acosta, A., Gonzalez-Mendizabal, D. (1999) Liquid-solid wetting factor in trickle bed reactors: its determination by a physical method. *Chem. Eng. Science*, 54, 3793-3800

-
- Prost, C., Le Goff, P. (1964). Étude, par conductivité électrique, de filets liquides coulant dans une colonne à garnissage avec contre-courant ou co-courant de gaz. *Genie Chimique*, 91, 6–11.
 - Ramachandran, P., Smith, J. (1979) Effectiveness factors in trickle bed reactors. *AIChE J.*, 25, 538.
 - Ramachandran, P.A., Chaudhari, R.V. (1983) *Three Phase Catalytic Reactors*, Gordon & Breach Science Publ., Londres, Inglaterra.
 - Rao, V., Drinkenburg, A. (1985) Solid-liquid mass transfer in packed beds with cocurrent gas-liquid downflow. *AIChE J.*, 31, 7, 1059-1067.
 - Sáez, A., Carbonell, R. (1985) Hydrodynamic parameters for gas-liquid cocurrent flow in packed beds. *AIChE J.*, 31, 1, 52-62.
 - Saroha, A., Nigam, K. (1996) Trickle Bed Reactors Reviews. *Rev. Chem. Eng.*, 12, 207.
 - Satterfield C. (1975) Trickle-bed reactors. *AIChE J.*, 21, 2, 209-228.
 - Shah, Y.T. (1979) *Gas-Liquid-Solid Reactor Design*, McGraw-Hill, New York.
 - Silveston, P.L., Hanika, J. (2002) Challenges for the periodic operation of trickle-bed catalytic reactors, *Chem. Eng. Science*, 57, 3373–3385.
 - Smith, G. (1985) *Numerical Solution of P.D.E.: Finite difference methods*. Oxford University Press, London.
 - Skala, D., Hanika, J., (2002) Periodic operations of trickle-bed reactor, in *Proc. of CHISA 2002 - 15th Int. Congress of Chemical and Process Eng.*, Praga, Zchec Republic, August 2002.
 - Stegasov, A.N., Kirillov, V.A., Silveston, P.L. (1994) Modeling of catalytic SO₂ oxidation for continuous and periodic liquid flow through a trickle bed. *Chem. Engng Sci.*, 49, 3699–3710.

-
- Stegmüller, R. (1986) Caracterización hidrodinámica de reactores de lecho mojado. Doctoral Thesis, Universidad Nacional de Buenos Aires, Argentina.
 - Stitt, E.H. (2002) Alternative multiphase reactors for fine chemicals. A world beyond stirred tanks? *Chem. Eng. J.*, 90, 47–60.
 - Stradiotto, D., Hudgins, R., Silveston, P. (1999) Hydrogenation of crotonaldehyde under periodic flow interruption in a trickle bed. *Chem. Eng. Science*, 54, 2561-2568.
 - Sylvester N, Kulkarni A Carberry J. (1975) Slurry and trickle bed reactor effectiveness factor. *Can. J. Chem. Eng.*, 53, 313.
 - Tan C. and Smith, J. (1980) Catalyst particle effectiveness with unsymmetrical boundary conditions. *Chem. Eng. Sc.*, 35, 1601.
 - Tan C. and Smith, J. (1981) Mass transfer in trickle bed reactors. *Lat. Am. J. Chem. Eng. Appl. Chem.*, 11, 59-69.
 - Taylor, R., Krishna, R. (1993) *Multicomponent Mass-Transfer*, Wiley, USA.
 - Trivizadakis M., Giakoumakis D. and Karabelas A. J. (2004) The effect of packing particle type on fluid mechanical characteristics of trickle bed reactors. Workshop of CPERI.
 - Tsochatzidis, N. A., Karabelas, A. J. (1995). Properties of pulsing flow in a trickle bed. *AIChE J.*, 41, 2371–2382.
 - Tsochatzidis, N., Karapantsios, T. D., Kostoglou, M., & Karabelas, A. J. (1992). A conductance probe for measuring liquid fraction in pipes and packed beds. *Int. J. of Multiphase Flow*, 18, 653–667.
 - Tukac, V., Hanika, J., Chyba, V. (2003) Periodic state of wet oxidation in trickle-bed reactor. *Catalysis Today*, 79–80, 427–431.

- Turco, F., Hudgins, R.R., Silveston, P.L., Sicardi, S., Manna, L., Banchemo, M. (2001) Investigation of periodic operation of a trickle-bed reactor, *Chem. Eng. Science*, 56, 1429
- Urrutia, G. Bonelli, P. Cassanello, M., Cukierman, A. (1996) On dynamic liquid holdup determination by the drainage method. *Chem. Eng. Science*, 51, 3721-3726.
- Urseanu, M., Boelhouwer, J., Bosman, H., Schroijen, J., Kwant, G. (2005) Induced pulse operation of high-pressure trickle bed reactors with organic liquids: hydrodynamics and reaction study. *Chem. Eng. and Proc.*, 43, 1411-1416.
- Wen, C.Y., Fan, L.T. (1975) *Models for Flow Systems and Chemical Reactors*, M. Deccker Inc., New York.
- Westertep, K., Van Swaaj, W., Beenackers, A. (1984) *Chemical reactor design and operation*. Copyright John Wiley & Sons, p. 191-194.
- Xiao, Q., Cheng, Z. M., Jiang, Z. X., Anter, A. M., Yuan, W. K. (2001) Hydrodynamic behavior of a trickle bed reactor under forced pulsing flow. *Chem. Eng. Science*, 56, 1189-1195.

CURRICULUM VITAE

Name: AYUDE, María Alejandra

Date of birth: June 26, 1977

Place of birth: Mar del Plata, Argentina

Degrees

- Chemical Engineer, December 1999, Universidad Nacional de Mar del Plata, Argentina.
- MS in Chemical Engineering, October 2003, Universidad Nacional de Mar del Plata, Argentina.

Publications

- "Phenol Oxidation in a Periodically Operated Trickle Bed Reactor." (2005) P. Massa, M. A. Ayude, F. Ivorra, R. Fenoglio, and P. Haure. *Catalysis Today*, ISSN: 0920-5861. 107-108, 630-636.
- "Periodic Operation of Trickle Bed Reactors: An approach to catalyst design through modeling at the particle scale." (2005) M.A. Ayude, M.C. Cassanello, P.M. Haure, O.M. Martinez. *Industrial Engineering & Chemistry Research*, ISSN: 0888-5885. 44 (25) 9594-9600.
- "Phenomenological approach to interpret the effect of liquid flow modulation in trickle-bed reactors at the particle scale." (2005) M. A. Ayude, M. C. Cassanello, O. M. Martínez, P. M. Haure. *Chemical Engineering Science*, ISSN: 0009-2509. 60 (22) 6262-6269.
- "Clean Oxidation of Alcohols in a Trickle-Bed Reactor with Liquid Flow Modulation." (2005) A. Muzen, M. S. Fraguío, M. C. Cassanello, M. A. Ayude, P. M. Haure, and O. M. Martínez. *Industrial Engineering & Chemistry Research*, ISSN: 0888-5885. 44 (14) 5275 - 5284.
- "Catalyst systems for the oxidation of phenol in water." (2004) P. Massa, A. Ayude, R. Fenoglio, J. F. Gonzalez, P. Haure. *Latinoamerican Applied Research*, ISSN: 0327-0793. 34, 133-140.

Proceedings and presentations

- "Periodic Operation of Trickle Bed reactors: Towards the development of a systematic design strategy", M.A. Ayude, M.C. Cassanello, O.M. Martinez, P.M. Haure. *Indian Chemical Engineering Congress (CHEMCON)*, Nueva Delhi, India, 2005.

- “Experimental trends observed with liquid flow modulation of Trickle Bed reactors”, M.A. Ayude, P.M. Haure, O.M. Martinez, M.C. Cassanello. Indian Chemical Engineering Congress (CHEMCON), Nueva Delhi, India, 2005.
- “Phenomenological approach to interpret the effect of liquid flow modulation in trickle bed reactors at the particle scale”, M.A. Ayude, M.C. Cassanello, O.M. Martinez, P.M. Haure. 7th Conference on Gas Liquid and Gas Liquid Solid Reactor Engineering. Strasbourg, France, 2005.
- “Reactant depletion in periodic operation of trickle bed reactors” M.A. Ayude, M.C. Cassanello, O.M. Martinez, P.M. Haure. 2nd Mercosur Congress on Chemical Engineering & 4th Mercosur Congress on Process Systems Engineering, Rio de Janeiro, Brasil, 2005.
- "Periodic Operation of Trickle Bed Reactors: An Approach to Catalyst Design." M.A. Ayude, M.C. Cassanello, P.M. Haure, O.M. Martinez. Aceptado para ser presentado en CAMURE-5 / ISMR-4 Symposium, Portoroz - Portorose, Slovenia, 2005. Oral presentation.
- “Phenomenological approach to understand the behavior of trickle bed reactors with liquid flow modulation.”, M. A. Ayude, M. C. Cassanello, O. M. Martínez, P. M. Haure. 16th. International Congress of Chemical and Process Engineering (CHISA), Praga, Rep. Checa, 2004.
- “Catalytic wet oxidation of alcohols in trickle bed reactors with liquid flow modulation.”, A. Muzen, M.S. Fraguío, M.A. Ayude, O. Martínez, M. Cassanello. 16th. International Congress of Chemical and Process Engineering (CHISA), Praga, Rep. Checa, 2004.
- “Selectivity Analysis in a Cycled Trickle Bed Reactor for Catalytic Wet Air Oxidation”, V. Mignaqui, M.A. Ayude and P.M. Haure. 16th. International Congress of Chemical and Process Engineering (CHISA), Praga, Rep. Checa, 2004.
- “Estudio de la oxidación de fenol en un reactor Trickle Bed operado en forma periódica”, Paola Massa, Alejandra Ayude, Fernando Ivorra, Rosa Fenoglio y Patricia Haure. XIX Simposio Iberoamericano de Catálisis Mérida, México, 2004.
- “Degradación de pentaclorofenol con células inmovilizadas: un modelo cinético”, M. Alejandra Ayude, Erica Wolski, Patricia M. Haure, Jorge F. Gonzalez. XIII Congreso

Argentino de Catálisis (JAC 2003) y 2º Congreso de Catálisis (2º MercoCat), Córdoba, Argentina, 2003.

- “Catalyst systems for the oxidation of phenol in water”, P. Massa, A. Ayude, R. Fenoglio, J. F. Gonzalez, P. Haure. 3rd Congress on process systems engineering and 1st Mercosur Congress on Chemical Engineering, Santa Fe, Argentina, 2001. Oral presentation.